

EXPLORING THE REACTIVITY OF ELECTROPHILIC
TRISPHOSPHINE PLATINUM(II) COMPLEXES IN THE
CYCLOISOMERIZATION OF DIENES

Jeremiah A. Feducia

A dissertation submitted to the faculty of the University of North Carolina at Chapel Hill
in partial fulfillment of the requirements for the degree of Doctor of Philosophy in the
Department of Chemistry.

Chapel Hill
2007

Approved by

Advisor: Professor Michel R. Gagné

Reader: Professor Maurice Brookhart

Reader: Professor Cynthia Schauer

ABSTRACT

JEREMIAH A. FEDUCIA: Exploring the Reactivity of Electrophilic Trisphosphine Platinum(II) Complexes in the Cycloisomerization of Dienes
(Under the Direction of Michel R. Gagné)

The cycloisomerization of 1,5-dienes bearing nucleophilic traps with electrophilic trisphosphine Pt(II) complexes generates a cationic Pt-alkyl species which is stable to protonolysis by bulky diaryl ammonium acids. An investigation of tridentate pincer ligand effects in a model system where the alkyl group was –Me revealed that small electron donating substituents at phosphorus enhanced the rate of protonolysis by almost two orders of magnitude. Mechanistic experiments suggested that protonation at Pt generated a 5-coordinate intermediate which eliminated methane by reductive coupling and rapid associative ligand substitution. The large difference in protonolysis rates between pincer and non-pincer systems was attributed to torsional strain inherent to square planar pincer systems.

Polyene cyclizations with dicationic Pt complexes typically resulted in a large forward rate constant for cyclization with diastereoselectivity of the polycyclic products governed by the Stork-Eschenmoser postulate. Ligand effects, more specifically electronics, were observed to affect the mode of cyclization (concerted or stepwise). The first direct observation of the equilibrating species in a polycyclization reaction ($\text{Pt}(\eta^2\text{-alkene})$ and Pt-alkyl) was made using the electron donating bis(2-diethylphosphinoethyl)ethylphosphine (EtPPPEt) ligand and a 1,5-dienyl sulfonamide. Cyclization was determined to be stepwise in nature, generating the more

thermodynamically favored *cis* ring junction in the 6,5-bicyclic Pt-alkyl product. The variables which affect the cyclization equilibrium were investigated and included: solvent polarity, metal electrophilicity, acid/base strength, and ring strain. These factors were used as a guideline to control stereoselectivity in polyene cascade cyclizations. Medium range stereocontrol was observed using a 1,5-dienol substrate but such control was not present in the cyclization of trienol substrates.

The effects of ligand design on Pt(II) catalyzed cyclopropanation reactions was also investigated. Deconstructing the PPP ligand framework into a combination of mono- and bidentate phosphine ligands allowed for a modular approach to catalyst optimization. The optimal achiral catalyst for the cyclopropanation of 1,6- and 1,7-dienes was found to be (dppm)(PMe₃)Pt²⁺. This catalyst was extremely electrophilic and carbophilic; increasing rates by a factor of 20 and allowing for more functional group tolerance. An asymmetric ligand with a similar bite angle to dppm was also synthesized and tested for enantioselective catalysis.

To Heather and Will

ACKNOWLEDGEMENTS

As expected, I have to thank Mike for this first and foremost. Although I didn't spend too much time in his office, his door and brain were always open. I've never met someone so enthusiastic about chemistry and I was always encouraged by his unending optimism. While Mike was the mastermind of the last four and a half years, I never would have kept my little bit of sanity without the cast of supporting characters in the trenches with me. Out of all the characters I have worked with, I have to thank Charles. It was great to have someone to bounce ideas off of, talk about things other than chemistry, complain, and in general just be someone who I knew was also suffering. I also have to thank Will Kerber for not only showing me the ropes but also keeping me in check in lab. I couldn't have asked for someone better to work beside for the two years we overlapped. To Jeff Anthis and Jen Becker, I appreciate the advice on chemistry and engagement rings. Mike and Mike (Tarselli and Nailz), it has been great working with two of the smartest younger grad students to come into the group. Please use the wisdom I've passed on to you to make Mike G. famous. To the rest, it's been real, it's been fun, it has not been real fun.

After I got out of lab, I could have never asked for more love or support than what I got from my wife, Heather. I have finished this because of you. In writing this dissertation I must also thank my son, William Anthony whose late night outbursts have kept me out of synch and with little sleep but I love you for it. I also have to thank my parents, grandparents, and in-laws; you have no idea what I actually do but you guys

have been more than supportive. To wrap up I have to thank my closest friends. Kirby and Danny, thank you for getting me off of Mount Marcy. Lee, I don't make Styrofoam. Seth, I will vote for you in 2020. To those I have left out of this, I apologize but know that I am grateful for your support.

TABLE OF CONTENTS

LIST OF TABLES.....	ix
LIST OF FIGURES.....	xi
LIST OF ABBREVIATIONS AND SYMBOLS.....	xiii
Chapter 1. Cation-Olefin Polycyclizations with Platinum(II).....	1
1.1 Enzymatic and Biomimetic Polyolefin Cyclizations.....	1
1.2 Pt(II)-Initiated Polyolefin Cyclizations.....	3
1.3 Research Objectives.....	7
Chapter 2. Protonolysis of Cationic Pt-C Bonds Using Mild Acids.....	9
2.1 Introduction.....	9
2.2 Results and Discussion.....	12
A. Synthesis of Model Compounds.....	12
B. Protonation of $[(RPPPR')PtMe][BF_4]$ and $[(P_2)(PR_3)PtMe][BF_4]$	14
C. Results of Mechanistic Experiments.....	20
D. Analysis of Mechanistic Experiments.....	28
E. Hypothesis for Rate Enhancement.....	32
2.3 Conclusions.....	34
2.4 Experimental.....	36
Chapter 3. Reversibility in Pt(II)-Mediated Polycyclizations.....	48
3.1 Introduction.....	48
3.2 Results and Discussion.....	53

A. Factors Governing Reversibility.....	53
B. Stereocontrol in Reversible Polycyclizations.....	61
3.3 Conclusions.....	74
3.4 Experimental.....	75
Chapter 4. Designing Modular Catalysts to Improve Diene Cycloisomerization.....	80
4.1 Introduction.....	80
4.2 Results and Discussion.....	83
A. First Generation PPP Catalysts.....	83
B. Modular Catalyst Development.....	86
C. Asymmetric Catalysis.....	95
4.3 Conclusions.....	100
4.4 Experimental.....	101
APPENDIX A. X-Ray Structure of [(CyPPP)PtMe][Cl] (Chapter 2).....	110
APPENDIX B. X-Ray Structure of 3 (Chapter 3).....	114
APPENDIX C. X-Ray Structure of 5 (Chapter 3).....	118
APPENDIX D. X-Ray Structure of 6 (Chapter 3).....	122
APPENDIX E. X-Ray Structure of [(dppm)(PMe ₃)PtI][I] (Chapter 4).....	130
REFERENCES	135

LIST OF TABLES

Table 2.1	Ligand effects on the rate of protonation of [(RPPPR')PtMe][BF ₄]	17
Table 3.1	Solvent effects on the cyclization of 1 with (EtPPEt)Pt ²⁺	56
Table 3.2	Ligand effects on the cyclization of 1 with (RPPPR')Pt ²⁺	58
Table 3.3	Acid or base additive effects on the cyclization of 1	60
Table 4.1	Cycloisomerization of dienes with [(PPP)PtMe][BF ₄]	84
Table 4.2	The effect of bidentate ligand on the cycloisomerization of 1	89
Table 4.3	The effect of monodentate ligand on the cycloisomerization of 1 to 2	90
Table 4.4	Cycloisomerization of dienes with (dppm)(PMe ₃)Pt ²⁺	92
Table 4.5	Cycloisomerization reactions with ((<i>R</i>)-xylyl-BINAP)(PMe ₃)Pt ²⁺	96
Table 4.6	Cycloisomerization reactions with ((<i>R,R</i>)- <i>t</i> Bu-MiniPHOS)PtI ₂	100
Table A.1	Bond distances (Å) for [(CyPPP)PtMe][Cl]	111
Table A.2	Bond angles (°) for [(CyPPP)PtMe][Cl]	112
Table B.1	Bond distances (Å) for 3	115
Table B.2	Bond angles (°) for 3	116
Table C.1	Bond distances (Å) for 5	119
Table C.2	Bond angles (°) for 5	119
Table C.3	Torsion angles (°) for 5	120
Table D.1	Bond distances (Å) for 6	123
Table D.2	Bond angles (°) for 6	124
Table D.3	Torsion angles (°) for 6	126
Table E.1	Bond distances (Å) for [(dppm)(PMe ₃)PtI][I]	131
Table E.2	Bond angles (°) for [(dppm)(PMe ₃)PtI][I]	132

Table E.3 Torsion angles ($^{\circ}$) for [(dppm)(PMe ₃)PtI][I].....	133
--	-----

LIST OF FIGURES

Figure 1.1 Cyclization of squalene to hopene by SHC.....	2
Figure 1.2 Competing transition states during cyclization with (PPP)Pt ²⁺	6
Figure 2.1 PPP ligands used in protonation studies.....	14
Figure 2.2 ¹ H NMR of the Pt-Me region of [(PPPEt)PtMe][BF ₄].....	15
Figure 2.3 ³¹ P NMR of [(PPPEt)PtMe][BF ₄].....	16
Figure 2.4 ³¹ P NMR of [(PPPEt)PtMe][BF ₄] under protonolysis conditions.....	16
Figure 2.5 ORTEP representation of [(CyPPP)PtMe][Cl].....	19
Figure 2.6 Diphosphine ligands used in protonation studies.....	20
Figure 2.7 <i>k</i> _{obs} (from initial rates) vs. [Ph ₂ NH ₂][BF ₄] for the protonolysis of 1 (10 equiv. NCC ₆ F ₅ , 0.01 M in 1).....	21
Figure 2.8 <i>k</i> _{obs} (from initial rates) vs. NCC ₆ F ₅ for the protonolysis of 1 (10 equiv. [Ph ₂ NH ₂][BF ₄], 0.01 M in 1).....	22
Figure 2.9 Plot of ln [1] versus time (10 eq. [Ph ₂ NH ₂][BF ₄], 10 eq. NCC ₆ F ₅): with 0 (◆), 1 (■), 2.5 (▲), 5 (●), and 10 (×) eq. Ph ₂ NH.....	23
Figure 2.10 (a) Averaged NH chemical shift of Ph ₂ NH and Ph ₂ NH ₂ ⁺ (δ) versus mole fraction (<i>X</i>) of Ph ₂ NH; [Ph ₂ NH ₂][BF ₄] = 0.08 M. (b) NH chemical shift of equimolar solution of Ph ₂ NH and Ph ₂ NH ₂ ⁺ (δ) versus [Ph ₂ NH + Ph ₂ NH ₂ ⁺].....	25
Figure 2.11 Typical plot of ln [1] vs. time (10 equiv. [Ph ₂ NH ₂][BF ₄], 10 equiv. 2); initial concentration = 0.01 M; [(EtPPP)PtMe][BF ₄] (1).....	26
Figure 2.12 ¹ H NMR (500 MHz) spectrum of CD ₃ H.....	27
Figure 2.13 ¹ H NMR spectrum of methane isotopologs.....	27
Figure 2.14 Plot of ln [Pt-Me] vs. time (10 equiv. [Ph ₂ NH ₂][BF ₄], 10 equiv. NCC ₆ F ₅) for 1 (●) and 1 -d ₃ (▲); <i>k</i> _H / <i>k</i> _D = 1.2.....	28
Figure 2.15 Typical C-P-C and P-Pt-P bond angles in square planar (PPP)Pt complexes	33
Figure 3.1 Stereorelationships defined by polyolefin cyclization.....	50

Figure 3.2 ^{31}P NMR of cyclization of 1 with $(\text{EtPPP}(\text{Et})\text{Pt})^{2+}$ in CH_2Cl_2	55
Figure 3.3 ^{31}P NMR of cyclization of 1 with $(\text{EtPPP}(\text{Et})\text{Pt})^{2+}$ in MeNO_2	57
Figure 3.4 ^{31}P NMR of cyclization of 1 with $(\text{EtPPP})\text{Pt}^{2+}$ in MeNO_2	59
Figure 3.5 ORTEP representation of 3	63
Figure 3.6 ^{31}P NMR stack plot of cyclization of 4 with $(\text{EtPPP})\text{Pt}^{2+}$	66
Figure 3.7 ORTEP representation of 5	67
Figure 3.8 ORTEP representation of 6	68
Figure 3.9 Models of Pt-alkyls for AM1 calculations.....	71
Figure 4.1 Examples of [3.1.0] bicyclic natural products.....	82
Figure 4.2 Non-phosphine monodentate ligands tested for modular catalysts.....	91
Figure 4.3 ORTEP representation of $[(\text{dppm})(\text{PMe}_3)\text{PtI}][\text{I}]$	95
Figure A.1 ORTEP representation of $[(\text{CyPPP})\text{PtMe}][\text{Cl}]$	110
Figure B.1 ORTEP representation of 3	114
Figure C.1 ORTEP representation of 5	118
Figure D.1 ORTEP representation of 6	122
Figure E.1 ORTEP representation of $[(\text{dppm})(\text{PMe}_3)\text{PtI}][\text{I}]$	130

LIST OF ABBREVIATIONS AND SYMBOLS

\angle	bite angle
2°	secondary
3°	tertiary
Å	angstrom
AIBN	azobisisobutyronitrile
BINAP	2,2'-bis(diphenylphosphino)-1,1'-binaphthyl
BINOL	1,1'-bi-2-naphthol
BLA	Brønsted-Lewis acid
Bn	benzyl
BQ	1,4-benzoquinone
Bu	butyl
χ	Tolman constant
°C	Celsius
COD	1,5-cyclooctadiene
Cy	cyclohexyl
δ	chemical shift
dd	doublet of doublets
dfepe	1,2-bis-(bispentafluoroethyl)ethane
dfmp	methyl(bispentafluoroethyl)phosphine
DFT	density functional theory
ΔG	free energy

DMF	N,N-dimethylformamide
dmpe	1,2-bis(dimethylphosphino)ethane
dmpm	1,2-bis(dimethylphosphino)methane
DPEN	1,2-diphenylethylenediamine
DPEphos	bis(2-diphenylphosphinophenyl)ether
dppb	1,2-bis(diphenylphosphino)butane
dppbz	1,2-bis(diphenylphosphino)benzene
dppe	1,2-bis(diphenylphosphino)ethane
dppf	1,2-bis(diphenylphosphino)ferrocene
dppm	1,2-bis(diphenylphosphino)methane
dppp	1,2-bis(diphenylphosphino)propane
dr	diastereomeric ratio
ee	enantiomeric excess
<i>endo</i>	endocyclic
eq	equation
equiv	equivalent
ESI	electrospray ionization
Et	ethyl
<i>exo</i>	exocyclic
g	gram
GC	gas chromatography
h	hour
HNTf ₂	bis-trifluoromethanesulfonamide

HRMS	high resolution mass spectrometry
Hz	hertz
J	three-bond H-H coupling constant
$J_{\text{Pt-P}}$	one-bond Pt-P coupling constant
k	rate constant
kcal	kilocalorie
K_{eq}	equilibrium constant
KIE	kinetic isotope effect
L	liter
m	multiplet
M	molarity
M ⁺	molecular ion
Me	methyl
mg	milligram
MHz	megahertz
min	minute
mL	milliliter
μL	microliter
mm	millimeter
μM	micromolar
mmol	millimole
mol%	molar percentage
MS	mass spectrometry

ν_{CO}	infrared stretching frequency of carbon monoxide
NMR	nuclear magnetic resonance
OAc	acetate
ORTEP	Oak Ridge thermal ellipsoid plot
OTf	trifluoromethanesulfonate
<i>p</i> -TsOH	<i>para</i> -toluenesulfonic acid
P ₂	diphosphine
Ph	phenyl
PNP	2,6-bis((diphenylphosphino)methyl)pyridine
ppm	parts per million
PPP	bis(2-diphenylphosphinoethyl)phenylphosphine
PR ₃	trisubstituted phosphine
s	singlet
<i>rac</i>	racemic
S _E (ox)	oxidative electrophilic substitution
S _E 2	bimolecular electrophilic substitution
<i>sec</i> Bu	1-methylpropyl
SEGPPOS	5,5'-bis(diphenylphosphino)-4,4'-bi-1,3-benzodioxole
SHC	squalene-hopene cyclase
t	triplet
t _{50%}	time to 50% completion

<i>t</i> Bu	1,1-dimethylethyl
<i>t</i> Bu-MiniPHOS	1,2-bis(<i>tert</i> -butylmethylphosphino)methane
TFA	trifluoroacetic acid
THF	tetrahydrofuran
TIPS	triisopropylsilyl
TMS	trimethylsilyl
tolyl	4-methylphenyl
<i>t</i> _R	retention time
Ts	(4-methylphenyl)sulfonamide
TS	transition state
w/w	weight-to-weight ratio
<i>X</i>	mole fraction
X	halide
xylyl	3,5-dimethylphenyl

Chapter 1

Cation-Olefin Polycyclizations With Platinum(II)

1.1 Enzymatic and Biomimetic Polyolefin Cyclizations

Of interest to many synthetic chemists is the ability to control polyene cascade cyclizations with similar efficiency and selectivity as enzymes.¹ One enzyme class in particular is the family of cyclase enzymes that converts squalene (and squalene derivatives) to hopene (and other polycyclic products).² The transformation of polyene substrates to stereoselective cyclic products is achieved by preorganization within the enzyme followed by a series of cation-olefin reactions to selectively form new C-C bonds as shown in Figure 1.1 for squalene-hopene cyclase.³ In this example, the acyclic squalene is converted to a polycyclic product with five new rings and ten set stereocenters.

¹ Yoder, R. A.; Johnston, J. N. *Chem. Rev.* **2005**, *105*, 4730-4756 and references within.

² (a) Wendt, K. U.; Poralla, K.; Schulz, G. E. *Science* **1997**, *277*, 1811-1815. (b) Reinert, D. J.; Balliano, G.; Schulz, G. E. *Chem. Biol.* **2004**, *11*, 121-125.

³ (a) See reference 1. (b) Gao, D.; Pan, Y. K.; Byun, K.; Gao, J. *J. Am. Chem. Soc.* **1998**, *120*, 4045-4046. (c) Kannenberg, E. L.; Poralla, K. *Naturwissenschaften* **1999**, *86*, 168-176.

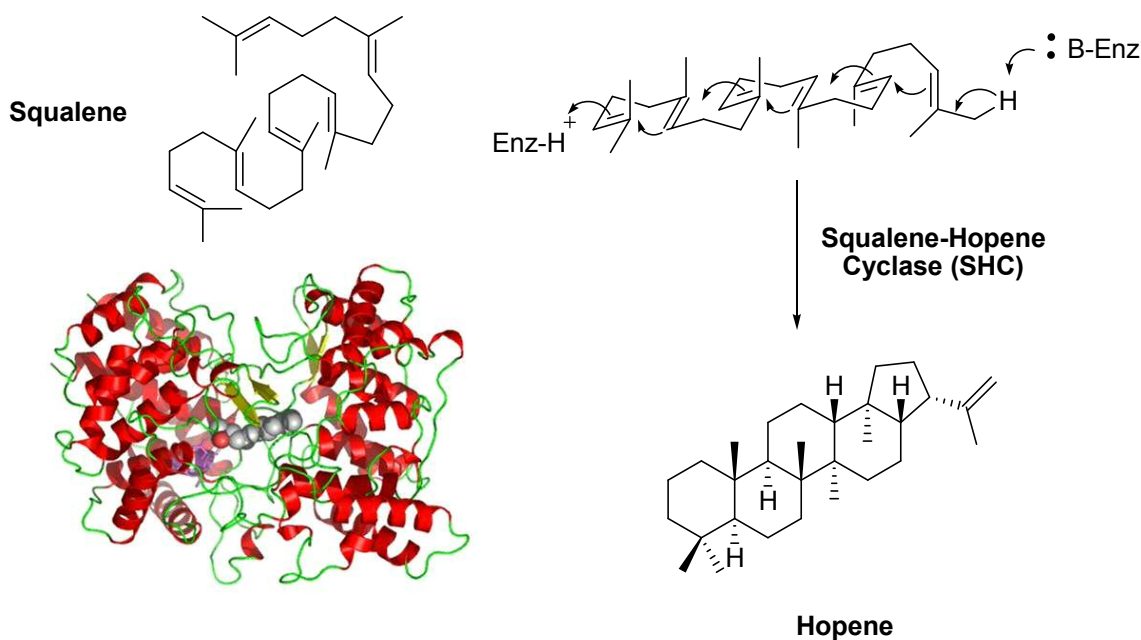
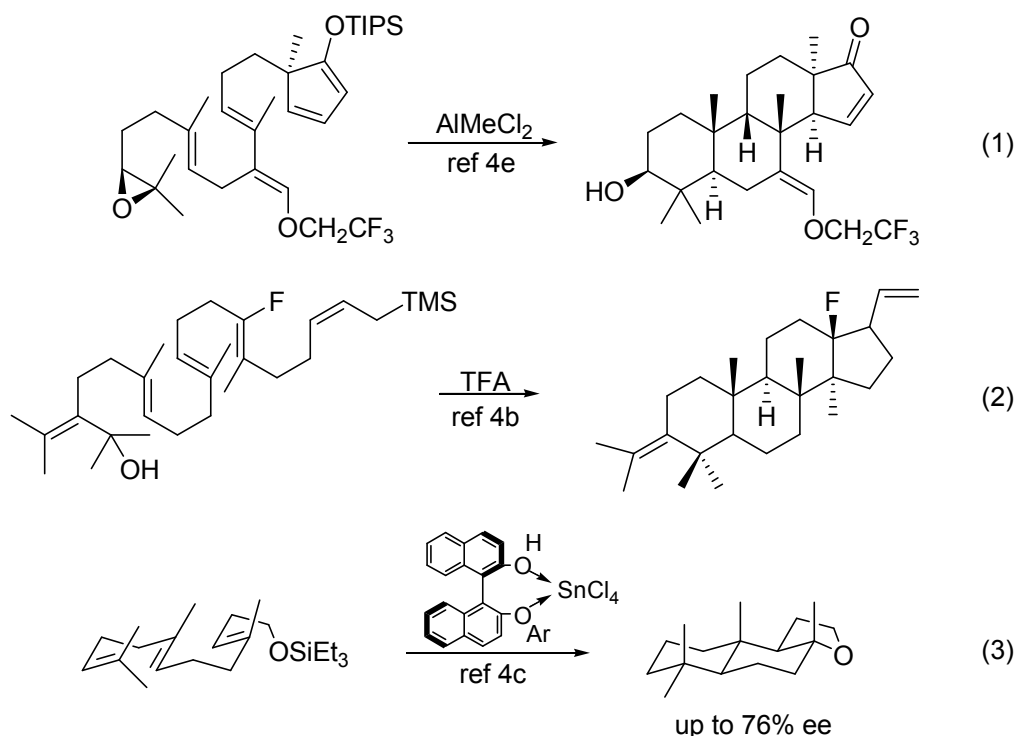


Figure 1.1. Cyclization of squalene to hopene by SHC.

The work to develop a nonenzymatic process for stereoselective polycyclizations has been an ongoing challenge for several decades. Attempts at achieving the selectivity unique to enzymes have focused on protonation with Brønsted acids, ionization with Lewis acids, and even addition of Hg^{2+} to achiral polyolefin starting materials.⁴ More recently, Yamamoto has developed a chiral Brønsted-Lewis acid using a Sn(IV) /BINOL combination to perform polycyclizations with good enantioselectivity.^{4c} Examples of some nonenzymatic systems are highlighted in equations 1-3.⁴ The greatest challenge to overcome with nonenzymatic polycyclizations is controlling the diastereo- and enantioselectivity of the products of cyclization. Few examples, including the chiral BLA by Yamamoto, exist where highly selective reactions are achieved and these

⁴ (a) Bartlett, P. A. In *Asymmetric Synthesis*; Morrison, J. D., Ed.; Academic Press: New York, 1984; Vol. 3, p 341-409. (b) Johnson, W. S.; Bartlett, W. R.; Czeskis, B. A.; Gautier, A.; Lee, C. H.; Lemoine, R.; Leopold, E. J.; Luedtke, G. R.; Bancroft, K. J. *J. Org. Chem.* **1999**, *64*, 9587-9595. (c) Ishihara, K.; Ishibashi, H.; Yamamoto, H. *J. Am. Chem. Soc.* **2002**, *124*, 3647-3655. (d) Nishizawa, M.; Takenaka, H.; Hayashi, Y. *J. Org. Chem.* **1986**, *51*, 806-813. (e) Corey, E. J.; Wood, H. B. *J. Am. Chem. Soc.* **1996**, *118*, 11982-11983.

reactions are typically plagued by low product yields. While enzymes enjoy the ability to direct the cyclization of polyolefins, nonenzymatic processes have struggled to achieve stereocontrol in similar reactions even though many of these cyclizations are concerted and thereby quite stereoselective.⁵



1.2 Pt(II)-Initiated Polyolefin Cyclizations

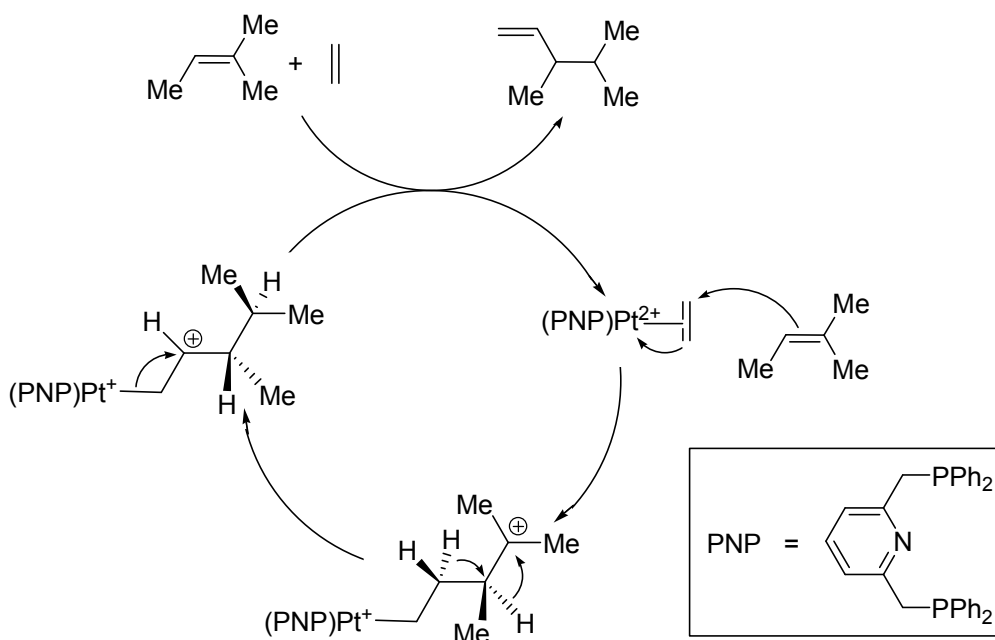
Electrophilic transition metal complexes have been shown to initiate polyunsaturated starting materials to form C-C bonds, typically by cyclization.⁶ Unique to group 10 metal complexes is the ability to preferentially coordinate to the least substituted olefin in

⁵ Further explanation of this phenomenon is found in the discussion and references in Chapter 3.

⁶ (a) Aubert, C.; Buisine, O.; Malacria, M. *Chem. Rev.* **2002**, *102*, 813-834. (b) Trost, B. M. *Acc. Chem. Res.* **1990**, *23*, 34-42. (c) Trost, B. M.; Krische, M. J. *Synlett*, **1998**, 1-16. (d) Widenhoefer, R. A. *Acc. Chem. Res.* **2002**, *35*, 905-913. (e) Echavarren, A. M.; Nevado, C. *Chem. Soc. Rev.* **2004**, *33*, 431-436. (f) Diver, S. T.; Giessert, A. J. *Chem. Rev.* **2004**, *104*, 1317-1382. (g) Lloyd-Jones, G. C. *Org. Biomol. Chem.* **2003**, *1*, 215-236.

polyolefin substrates.⁷ Of particular interest was a case reported in 2002 by Vitagliano and coworkers in which a dicationic Pt catalyst supported by a tridentate pincer ligand (PNP) catalyzed the dimerization of ethylene and 2-methyl-2-butene, as depicted in Scheme 1.1.⁸ This system not only allowed for nucleophilic attack on coordinated ethylene by a mild carbon nucleophile but also inhibited β -H elimination from the Pt-alkyl formed by dimerization and thereby permitted the reaction pathway observed (1,2-H shifts followed by expulsion of Pt^{2+}).

Scheme 1.1

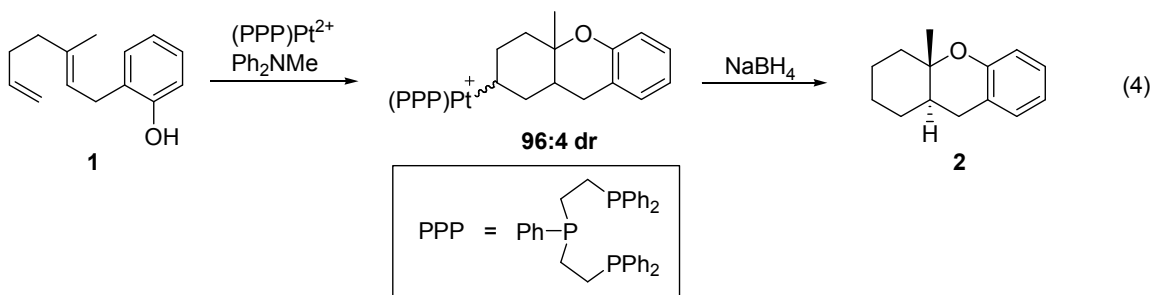


Following the same approach to inhibit β -H elimination, an intramolecular polycyclization was attempted by using a tridentate phosphine pincer ligand coordinated

⁷ (a) Hegedus, L. S. In *Comprehensive Organic Synthesis*; Trost, B. M., Ed.; Pergamon Press: Elmsford, NY, 1991; Vol. 4, pp 551-569. (b) Hegedus, L. S. in *Transition Metals in the Synthesis of Complex Organic Molecules*; University Science Books: Mill Valley, California, 1994; pp 199-236.

⁸ Hahn, C.; Cucciolito, M. E.; Vitagliano, A. *J. Am. Chem. Soc.* **2002**, *124*, 9038-9039.

to Pt(II) and a dienyl phenol substrate (**1**, eq. 4).⁹ In this system, Pt coordinated to the terminal olefin followed by C-C bond formation between the internal olefin and the coordinated monosubstituted olefin. At this point a tertiary carbocation was generated and subsequently quenched by an intramolecular phenol trap. A weak base was added to the system to quench H⁺ generated from cyclization and protonate the putative monocationic Pt-alkyl. Unfortunately, protonolysis to give the fully saturated product was unsuccessful leaving a stable Pt-alkyl which required reductive cleavage with NaBH₄ to obtain the organic product.



Characterization of **2** determined that the tricyclic compound had a *trans* ring juncture. This stereochemistry was expected from the cyclization of **1** according to the Stork-Eschenmoser (S-E) postulate which states that the ring junction is determined by the geometry of the starting alkene (*E* → *trans*; *Z* → *cis*).¹⁰ While the *trans* product was the exclusive product isolated from reductive cleavage, the Pt-alkyl observed prior to cleavage¹¹ was in a 96:4 diastereomeric ratio indicating that epimers existed at the Pt-containing stereocenter. This observation was consistent with the presence of competing

⁹ Koh, J. H.; Gagné, M. R. *Angew. Chem. Int. Ed.* **2004**, 43, 3459-3461.

¹⁰ (a) Stork, G.; Burgstahler, A. W. *J. Am. Chem. Soc.* **1955**, 77, 5068-5077. (b) Eschenmoser, A.; Ruzika, L.; Jeger, O.; Arigoni, D. *Helv. Chim. Acta.* **1955**, 38, 1890-1904.

¹¹ Diastereomeric ratio of Pt-alkyls was determined by *in situ* ³¹P NMR analysis.

transition states during cyclization having the chair-chair and boat-chair conformations shown in Figure 1.2.

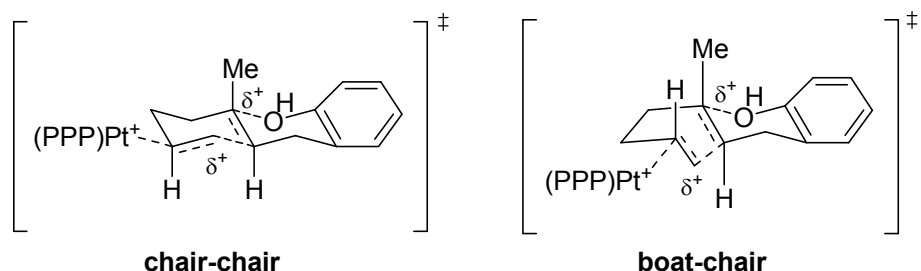
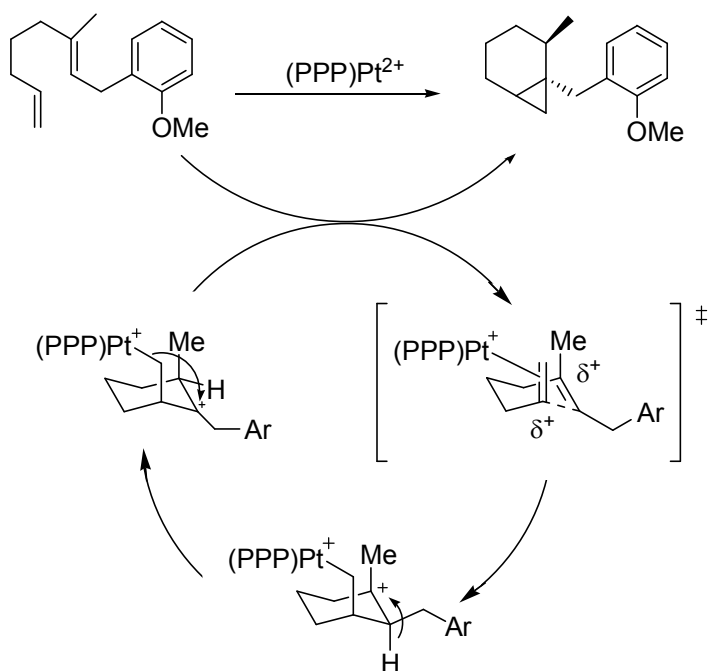


Figure 1.2. Competing transition states during cyclization with $(\text{PPP})\text{Pt}^{2+}$.

While systems in which an intramolecular trap was present in the diene substrate (-OH, -NHTs, etc.) formed stable Pt-alkyls, removal of the trap in 1,6- and 1,7-dienes resulted in the catalytic formation of cyclopropanes (Scheme 1.2). In these cases, the mechanism, as determined by deuterium labeling, followed a similar pathway as before: initiation at the terminal olefin with subsequent C-C bond formation and concurrent carbocation generation. When the carbocation was formed in the absence of a trap, a 1,2-hydride shift followed by cyclopropane ring formation occurred to regenerate the active $(\text{PPP})\text{Pt}^{2+}$ catalyst. Using $[(\text{PPP})\text{PtMe}][\text{BF}_4]$ as an achiral catalyst precursor, various 1,6- and 1,7-dienes were converted to [3.1.0] and [4.1.0] bicyclopropanes in moderate yields at elevated temperatures.

Scheme 1.2

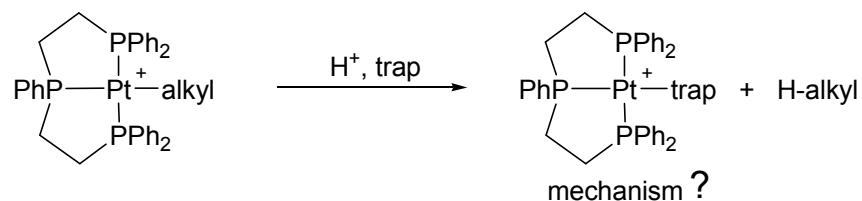


1.3 Research Objectives

Previous work demonstrated the ability of $\text{Pt}(\text{II})$ to initiate cascade cyclizations with polyolefin substrates. It was observed that systems with a heteroatom nucleophile as an intermediate carbocation trap were arrested at the stable $\text{Pt}-\text{alkyl}$ while 1,6- and 1,7-dienes lacking this feature produced bicyclopropanes catalytically. What was unclear in these studies was the role of the tridentate pincer ligand PPP on the observed reactivity. Central to this investigation would be the modification of the ligand structure supporting the $\text{Pt}(\text{II})$ metal center.

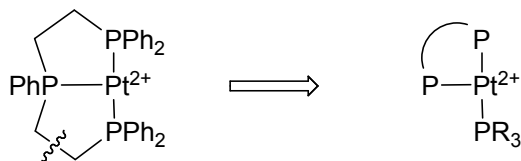
The first body of work discussed involves an examination of the turnover limiting step (protonolysis of $\text{Pt}-\text{C}$) in cyclizations with substrates bearing heteroatom carbocation traps. Stoichiometric cyclizations only involved the electron withdrawing PPP ligand which generated a very electrophilic metal center stable to protonolysis. Protonolysis

studies were used to investigate steric and electronic effects of the ligand surrounding Pt(II). A unique role of the ligand structure in this oxidative process was also discussed.



Following these studies is a discussion on the nature of cyclization using substrates similar to **1**. Previous work pointed to a concerted mechanism of polycyclization, with diastereoselectivity controlled by the S-E postulate. Studies with less electrophilic dicationic Pt complexes resulted in reversible cyclizations with a 1,5-dienyl sulfonamide substrate in which both equilibrating species were observed. Reversibility was used to affect the stereochemical outcome of bicyclizations.

The need for a pincer ligand for successful olefin activation/cyclization was also of interest and studies involving modular $(P_2)(PR_3)Pt^{2+}$ complexes were developed and applied to various cyclization systems. The reactivity of these compounds with H^+ was used to help construct a mechanism for protonolysis in $(PPP)Pt^{2+}$ systems. Modular catalysts were also optimized for the catalytic synthesis of bicyclopropanes and showed enhanced reactivity over first generation $(PPP)Pt^{2+}$ catalysts.



Chapter 2

Protonolysis of Cationic Pt-C Bonds Using Mild Acids

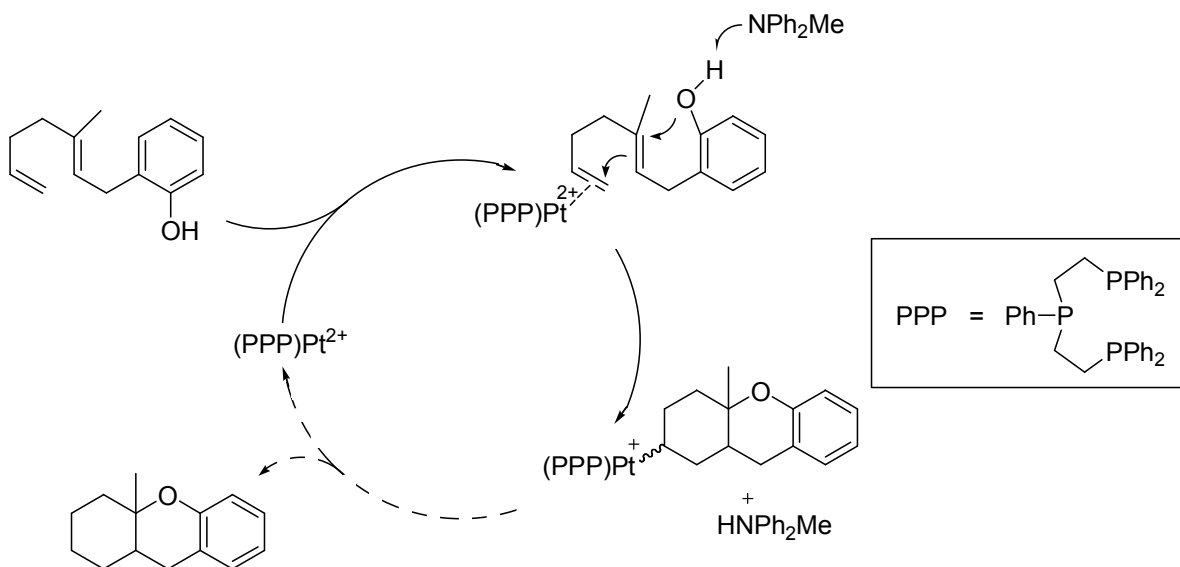
2.1 Introduction

The use of electrophilic Pt/Pd complexes to initiate the cyclization of linear polyolefins has been previously reported.¹ One particular system involved the cyclization of a 1,6-dienyl phenol mediated by a tridentate Pt(II) pincer complex as shown in Scheme 2.1. It was envisioned that catalytic turnover by protonolysis would generate a fully saturated bicyclic product. Unfortunately, the Pt-alkyl formed from this cyclization was stable to protonolysis by an external ammonium acid rendering these reactions stoichiometric.²

¹ (a) Kerber, W. D.; Gagné, M. R. *Org. Lett.* **2005**, *7*, 3379-3381. (b) Kerber, W. D.; Koh, J. H.; Gagné, M. R. *Org. Lett.* **2004**, *6*, 3013-3015. (c) Koh, J. H.; Mascarenhas, C.; Gagné, M. R. *Tetrahedron* **2004**, *60*, 7405-7410. (d) Koh, J. H.; Gagné, M. R. *Angew. Chem. Int. Ed.* **2004**, *43*, 3459-3461.

² The Pt-alkyl generated is stable up to 100 °C without decomposition. The saturated bicyclic product was cleaved by NaBH₄. See reference 1d.

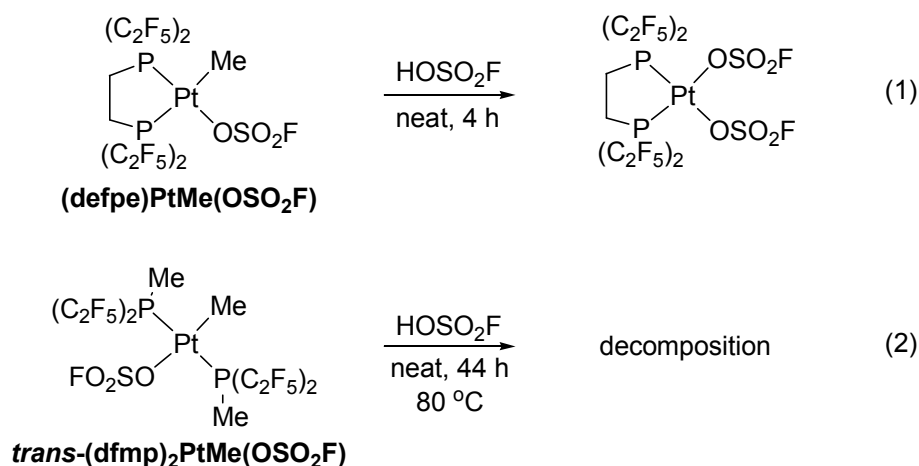
Scheme 2.1



Resistance towards protonation was not surprising for this system considering the stability of other cationic Pt-alkyl systems towards protonolysis. The overall charge of the Pt complex is very important with regards to reactivity towards protonolysis. Protonation of Pt-C bonds in neutral complexes has been shown to be relatively facile and serves as a useful turnover step in catalytic cycles.³ Widenhoefer and coworkers reported PtCl_2 catalyzed cyclization reactions initiated by activating a terminal olefin and were terminated by protonolysis of a putative Pt-C bond (ethers,^{3b} indoles,^{3c} etc.). The proton in these systems was generated during cyclization or was added as HCl. In contrast, the Pt-C bonds of cationic complexes are much more difficult to cleave with H^+ . Although these systems had been shown to be susceptible to protonolysis under much more rigorous conditions, some cases had even been reported where the Pt-C bond of the

³ (a) Fanizzi, F. P.; Intini, F. P.; Maresca, L.; Natile, G. *J. Chem. Soc.; Dalton Trans.* **1992**, 309-312. (b) Qian, H.; Han, X.; Widenhoefer, R. A. *J. Am. Chem. Soc.* **2004**, 126, 9536-9537. (c) Liu, C.; Han, X.; Wang, X.; Widenhoefer, R. A. *J. Am. Chem. Soc.* **2004**, 126, 3700-3701. (d) Helfer, D. S.; Atwood, J. D. *Organometallics* **2004**, 23, 2412-2420.

complexes were completely resistant to superacid conditions.⁴ Platinum complexes bearing electron withdrawing phosphine ligands provide the best examples of the stability of cationic Pt-alkyls to protonolysis. One illustrative case was reported by Roddick wherein it took 4 h for (dfep)PtMe(OSO₂F) to undergo complete protonolysis to (dfep)Pt(OSO₂F)₂ at ambient temperature in neat fluorosulfonic acid (eq. 1). The *trans*-(dfmp)₂PtMe(OSO₂F) isomer was stable under these conditions up to 80 °C after which decomposition occurred (eq. 2).⁵



Although protonation of cationic Pt(II) alkyls had been reported to be difficult, systems in which the Pt center was supported by a tridentate phosphine ligand showed that protonation was possible with strong acids like HOTf. The enhanced reactivity under acidic conditions observed with (PPP)Pt²⁺ systems implied that protonation could be a plausible mechanism for turnover in catalytic cycles similar to that described by

⁴ (a) Heyduk, A. F.; Labinger, J. A.; Bercaw, J. E. *J. Am. Chem. Soc.* **2003**, *125*, 6366-6367. (b) Thorn, D. L. *Organometallics* **1998**, *17*, 348-352. (c) Annibale, G.; Bergamini, P.; Cattabriga, M. *Inorg. Chim. Acta* **2001**, *316*, 25-32. (d) Butikofer, J. L.; Hoerter, J. M.; Peters, R. G.; Roddick, D. M. *Organometallics* **2004**, *23*, 400-408. (e) Peters, R. G.; White, S.; Roddick, D. M. *Organometallics* **1998**, *17*, 4493-4499, and references therein. (f) Lucey, D. W.; Helfer, D. S.; Atwood, J. D. *Organometallics* **2003**, *22*, 826-833.

⁵ Decomposition products such as metal free phosphines were common by-products of these reactions, see references 4d and 4e.

Scheme 2.1. Unfortunately, strong acids like triflic acid were incompatible with polyene substrates because of their susceptibility to Brønsted catalysis. Therefore, reactivity studies with weaker acids were initiated, with the hope that more compatible acid sources could be identified to mediate the problematic step of Scheme 2.1, the protonolysis of cationic (PPP)Pt-alkyl complexes.

To determine what factors governed protonation, a model system was developed in which the cyclized alkyl fragment was substituted with $-\text{CH}_3$. By modifying the substituents on the phosphorus atoms of the PPP ligand architecture, the electrophilicity and the sterics surrounding the Pt center were systematically tuned. Subsequent studies showed that simple Pt-alkyl models could be protonated under mild conditions using diaryl ammonium acids, namely $[\text{Ph}_2\text{NH}_2][\text{BF}_4]$.

Surprisingly, modular analogs (combination of a bidentate and monodentate phosphine; abbreviated as P_2P) of the (PPP)Pt-Me models were unreactive towards the protonolysis conditions. To explain these results, a hypothesis was constructed wherein inherent ring strain present in the square planar complexes with triphos was responsible for the enhanced reactivity observed. This chapter discusses the synthesis and reactivity of these model compounds as well as an in depth mechanistic analysis of protonation.

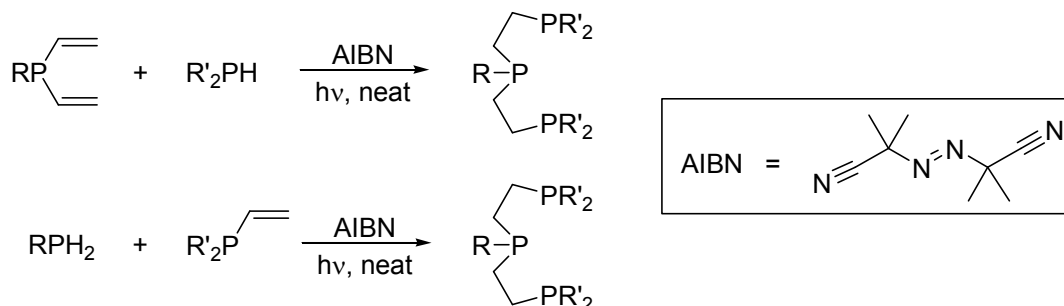
2.2 Results and Discussion

A. Synthesis of Model Compounds. Analogs of the commercially available tridentate PPP ligand⁶ were synthesized by two photolytic methods developed by

⁶ This ligand is commercially available from Strem Chemicals.

DuBois.⁷ First, $\text{RP}(\text{CH}=\text{CH}_2)_2$ (R = alkyl or aryl) was coupled with two equivalents of a secondary phosphine in the presence of a radical initiator (AIBN). The other pathway involved the reaction of a primary phosphine with two equivalents of $\text{R}_2\text{P}(\text{CH}=\text{CH}_2)$ (R = alkyl or aryl) again with a catalytic amount of initiator. As previously described by DuBois, reaction times and product purity were primarily dependent on the steric bulk of the phosphine's substituents. For instance, the smallest ligand, EtPPPEt (abbreviations defined by Figure 2.1) had faster reaction times and higher yields (4 h, 82%) than the most sterically demanding ligand, PPPCy (48 h, 66%). Impurities generated during photolysis were either removed *in vacuo* at elevated temperatures (120 °C) or were eliminated upon complexation to Pt. The ligands used in this study are shown in Figure 2.1.

Scheme 2.2



⁷ DuBois, D. L.; Miedaner, A.; Haltiwanger, R. C. *J. Am. Chem. Soc.* **1991**, *113*, 8753-8764.

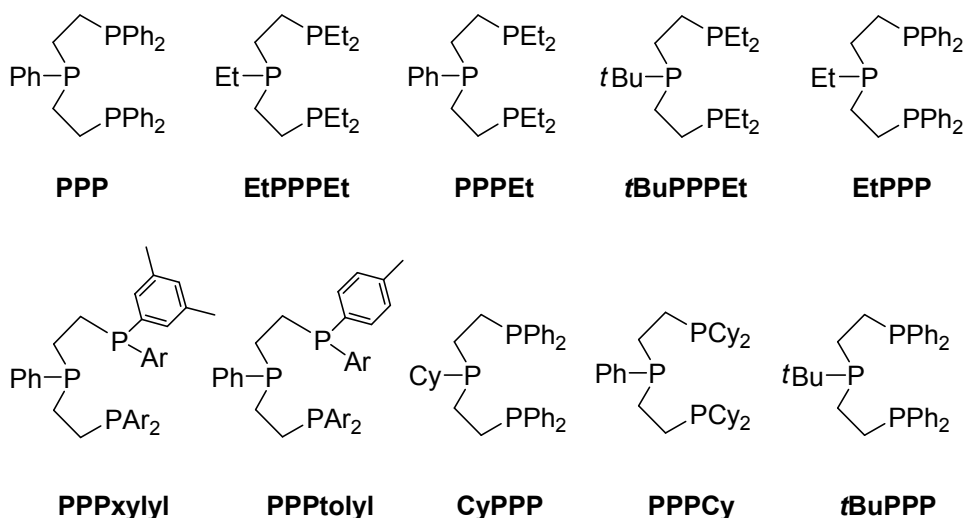


Figure 2.1. PPP ligands used in protonation studies.

Synthesis of the Pt(II) model compounds was achieved by addition of the corresponding tridentate ligand to (COD)Pt(Me)Cl⁸ to give the cationic [(RPPPR')PtMe][Cl] compound. Counter ion exchange with NaBF₄ gave the desired model compounds. It is important to note that while this route gave clean model compounds, a one-pot synthesis using ligand, (COD)Pt(Me)Cl and AgBF₄ consistently gave brown compounds (presumably with trace amounts of Ag⁺) that could not be obtained in analytically pure form even after several recrystallization attempts. Modular analogs which combined a bidentate and monodentate phosphine, [(P₂)(PMe₃)PtMe][BF₄] (P₂ = dppe, dppp, dppf, dppb, DPEphos, BINAP) and [(dppe)(PR₃)PtMe][BF₄] (R₃ = Ph₃, Ph₂Me, PhMe₂, Me₃) were synthesized by addition of the monophosphine to (P₂)Pt(Me)Cl followed by counter ion exchange with NaBF₄.⁹

B. Protonation of [(RPPPR')PtMe][BF₄] and [(P₂)(PR₃)PtMe][BF₄]. While it was already reported that strong acids protonated cationic Pt(II) alkyls, the purposes of this

⁸ Clark, H. C.; Manzer, L. E. *J. Organomet. Chem.* **1973**, 59, 411-428.

⁹ Synthesis and protonation studies of modular [(P₂)(PR₃)PtMe][BF₄] compounds were performed with the help of Alison Campbell and Dr. Jeff Anthis.

study were twofold. The first objective was to show if cationic Pt-Me bonds could be protonated by a mild acid (similar to those generated in a cyclization reaction; Scheme 2.1) and secondly to determine what effects ligand basicity and steric bulk had on the rates of protonation. Initial protonation studies were performed under pseudo first order conditions using 10 equivalents of $[\text{Ph}_2\text{NH}_2][\text{BF}_4]$ and 10 equivalents of NCC_6F_5 which served to trap the open coordination site generated by protonolysis of Pt-Me. Since amine bases were potent ligands (and poisons) under catalytic conditions, the scope of acids utilized for these studies was limited to those which generated poor ligands for Pt(II). The diarylammonium acids $[\text{Ph}_2\text{NH}_2][\text{BF}_4]$ and $[\text{Ph}_2\text{NMeH}][\text{BF}_4]$ possessed these properties. Protonation experiments were performed in dichloromethane in sealed NMR tubes and monitored by ^{31}P NMR observing the disappearance of Pt-Me ($J_{\text{Pt-Pcentral}} \sim 1500$ Hz) and formation of Pt-NCC₆F₅ ($J_{\text{Pt-Pcentral}} \sim 3300$ Hz). Figures 2.2 and 2.3 are representative NMR spectra (^1H and ^{31}P respectively) of the starting Pt-Me compounds, Figure 2.4 depicts a protonolysis reaction in progress.

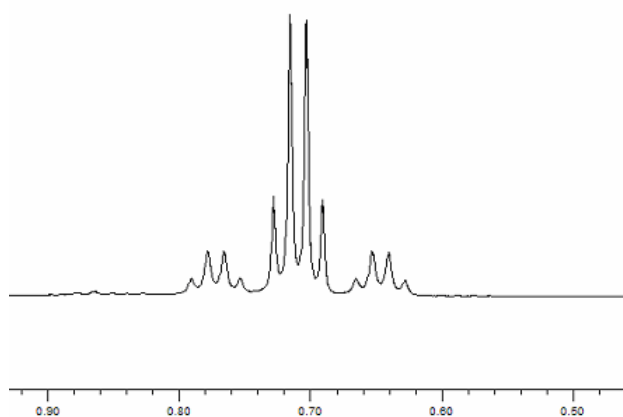


Figure 2.2. ^1H NMR of the Pt-Me region of $[(\text{PPPEt})\text{PtMe}][\text{BF}_4]$.

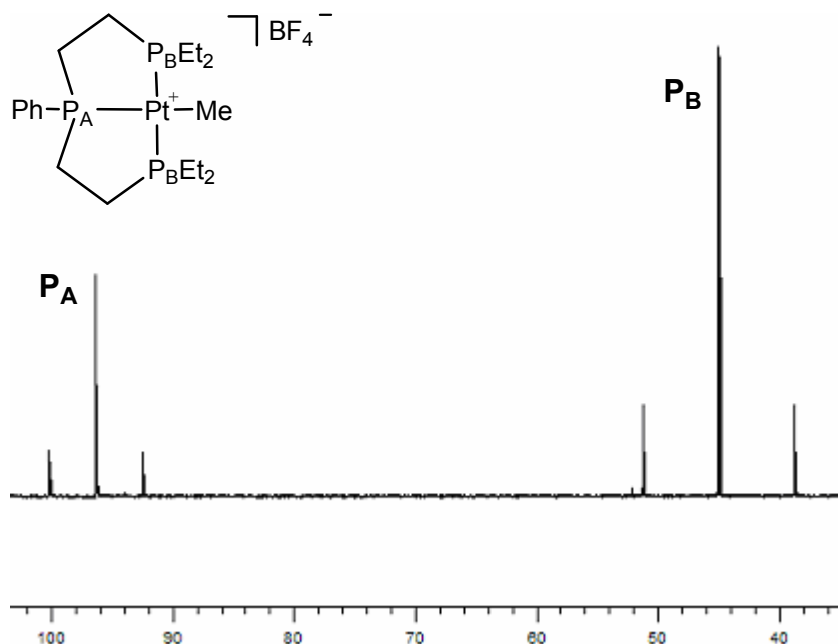


Figure 2.3. ^{31}P NMR of $[(PPPEt)PtMe][BF_4]$.

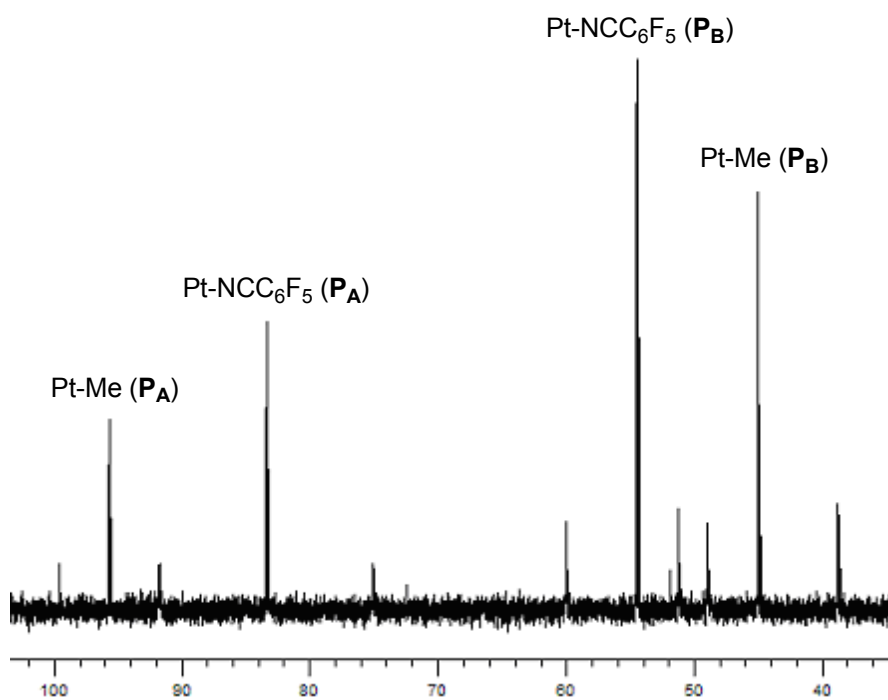


Figure 2.4. ^{31}P NMR of $[(PPPEt)PtMe][BF_4]$ under protonolysis conditions (15 min).

Under a set of standard conditions¹⁰ [(PPP)PtMe][BF₄] was observed to undergo protonolysis, generating methane and the Pt-nitrile adduct with a 50% conversion time of approximately 8 hours. Table 2.1 shows the rate improvements observed when the ligands from Figure 2.1 were tested under the same conditions. The trends from this table clearly show that *smaller and more basic ligands enhance the rate of protonolysis*. Most notable was the ligand structure EtPPPEt where the smaller more electron donating –Et substituents increased the rate of protonolysis by almost two orders of magnitude from the original PPP model compound (< 5 min versus 445 min).

Table 2.1. Ligand effects on the rate of protonation of [(RPPPR')PtMe][BF₄].



R	R'	t _{50%} (min)
Et	Et	<5
Ph	Et	10
<i>t</i> Bu	Et	50
Et	Ph	185
Ph	tolyl	220
Ph	xylyl	250
Cy	Ph	345
Ph	Cy	435
Ph	Ph	445
<i>t</i> Bu	Ph	610

The proper balance of sterics and electronics was important for faster protonation rates.

For example, while the –Cy substituent ($\chi = 0.1$)¹¹ is more electron donating than –Et (χ

¹⁰ [Pt]₀ = 0.01 M; 10 equiv. [Ph₂NH₂][BF₄]; 10 equiv. NCC₆F₅ in CH₂Cl₂; 25(1) °C.

¹¹ This value corresponds to the contribution which specific substituents on P donate towards the overall electron releasing ability of PR₃ as measured by IR stretching frequencies (ν_{CO}) in Ni(CO)₃L complexes. More electron donating substituents have smaller χ values; see Tolman, C. A. *Chem. Rev.* **1977**, 77, 313-348.

= 1.8), PPPCy was 40 times slower than PPPEt, presumably due to the fact that the –Cy group demanded more space and thus blocked the Pt center for protonation by the hindered acid $[\text{Ph}_2\text{NH}_2][\text{BF}_4]$. When comparing the –Cy group to the less bulky phenyl substituent, PPPCy was a slightly better ligand for protonation than PPP due to the greater electron donating ability of –Cy.

Replacing the –Et substituent in the central position of EtPPPEt for the much larger –*t*Bu group reduced the rate of protonation by a factor of 10. However, changing the ethyl substituent in the central position of EtPPPEt to the more electron donating cyclohexyl group reduced the rate by a factor of 70 suggesting that the rates of protonation were more sensitive to steric rather than electronic changes in the central P position. A better understanding of this effect was depicted in an X-ray structure of $[(\text{CyPPP})\text{PtMe}][\text{Cl}]$ which showed that the cyclohexyl group on the central P was forced into a position that hindered access to the Pt center (Figure 2.5). While it was not evident by low temperature studies (*vide infra*) which face (top or bottom) of the Pt(II) center was protonated, the results from Table 2.1 would predict that protonation occurred at the top face since sterics at the central P would not greatly affect protonation on the bottom face.

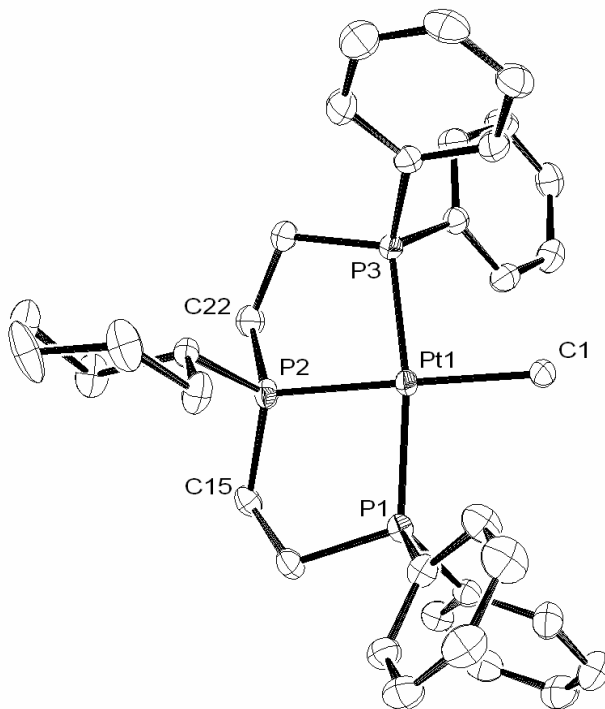


Figure 2.5. ORTEP representation of $[(\text{CyPPP})\text{PtMe}][\text{Cl}]$. Hydrogen atoms and Cl^- counter ion omitted for clarity. Selected bond lengths (\AA): $\text{Pt-P}_1 = 2.2907(6)$, $\text{Pt-P}_2 = 2.2674(6)$, $\text{Pt-P}_3 = 2.2949(6)$, $\text{Pt-C}_1 = 2.144(2)$. Selected bond angles (deg): $\text{P}_1\text{-Pt-P}_2 = 85.25(2)$, $\text{P}_2\text{-Pt-P}_3 = 84.80(2)$, $\text{P}_1\text{-Pt-C}_1 = 94.69(6)$, $\text{P}_3\text{-Pt-C}_1 = 94.97(6)$, $\text{C}_{15}\text{-P}_2\text{-C}_{22} = 111.57(7)$.

At this point, a modular approach to study ligand sterics and basicity was undertaken. This was accomplished by subjecting $[(\text{P}_2)(\text{PR}_3)\text{PtMe}][\text{BF}_4]$ compounds to standard protonolysis conditions. Commercially available diphosphine ligands (Figure 2.6) spanning a wide range of ligand basicity, steric bulk and diphosphine bite angles were tested. Virtually no protonation was observed with any modular compounds even at elevated temperatures and over long periods of time (eq. 3).¹² The only reactivity observed during these experiments was small amounts of dissociation and protonation of the monodentate phosphine when PMe_3 was used.

¹² No reaction (<5% conversion by ^{31}P NMR) was observed at 40°C over a period of 4-5 days. Reactions with HOTf were also slow, giving ~40% conversion over this same time period.

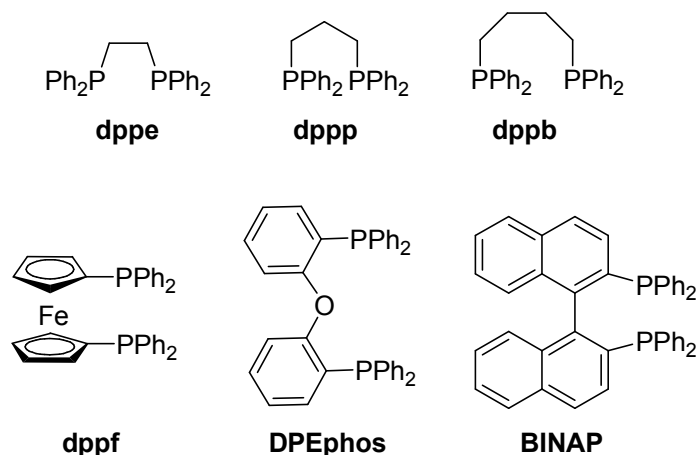
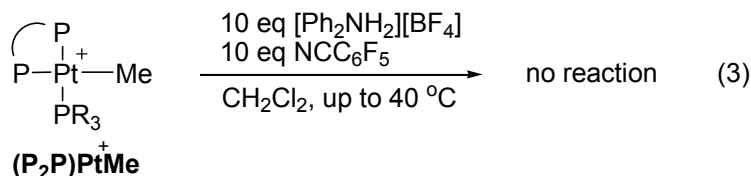


Figure 2.6. Diphosphine ligands used in protonation studies.



C. Results of Mechanistic Experiments. To explain the observed reactivity, more detailed kinetic experiments were performed. Kinetic experiments (eq. 4) to determine the order in acid and trapping ligand were carried out using $[(\text{EtPPP})\text{PtMe}][\text{BF}_4]$ (**1**) since the time to 50% conversion (~ 3 h; Table 2.1) was convenient for monitoring initial rates by ^{31}P NMR. By measuring initial rates using pseudo first order conditions (10 equivalents of reagent), the reaction was determined to be first order in acid (Figure 2.7) and zero order in trapping ligand (Figure 2.8). As previously mentioned, initial rates were measured with ^{31}P NMR by monitoring the disappearance of Pt-Me ($J_{\text{Pt-Pcentral}} \sim 1500$ Hz) and formation of Pt-NCC₆F₅ ($J_{\text{Pt-Pcentral}} \sim 3300$ Hz) as shown in Figure 2.4. These signals were diagnostic of the species present in solution (due to the large differences in $J_{\text{Pt-Pcentral}}$, Figure 2.4) and convenient to observe since the chemical shift of

the central phosphorus in PPP pincer Pt complexes appears further downfield than the terminal phosphines ($\Delta\delta \sim 40\text{-}50$ ppm). Also, the signal for the Pt-Me complex was around 10 ppm further downfield than the signal for the Pt-nitrile complex, thereby simplifying analysis by ^{31}P NMR.

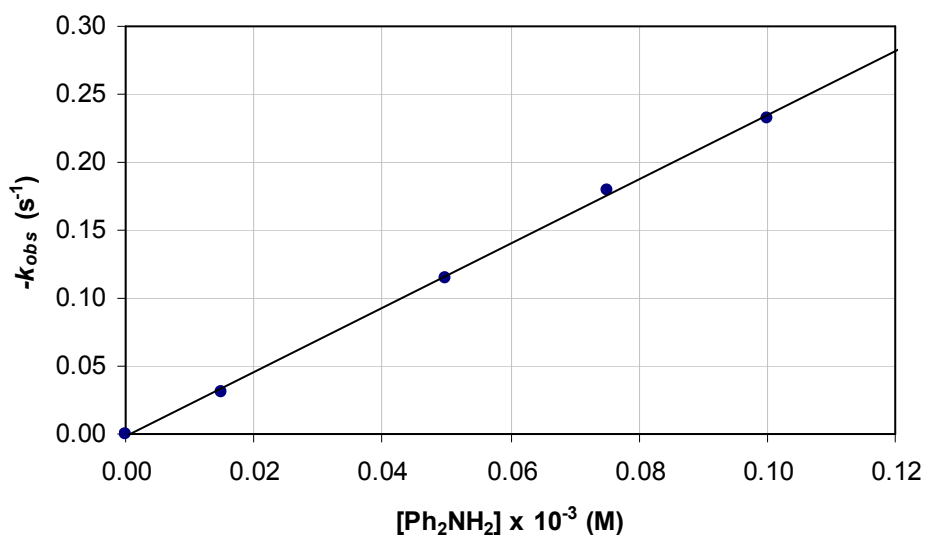
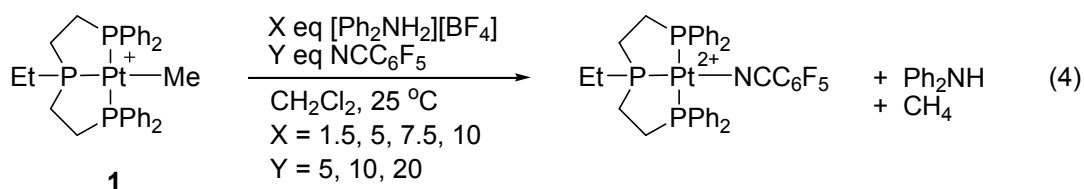


Figure 2.7. k_{obs} (from initial rates) vs. $[\text{Ph}_2\text{NH}_2][\text{BF}_4]$ for the protonolysis of **1** (10 equiv. NCC_6F_5 , 0.01 M in **1**). The order in acid is 1.

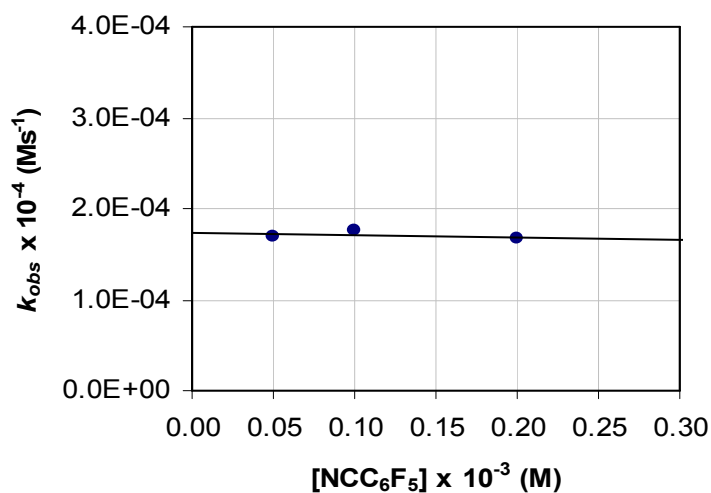


Figure 2.8. k_{obs} (from initial rates) vs. NCC_6F_5 for the protonolysis of **1** (10 equiv. $[\text{Ph}_2\text{NH}_2][\text{BF}_4]$, 0.01 M in **1**). The order in nitrile is zero.

In a plot of $\ln [\mathbf{1}]$ versus time, the rate of consumption of **1** at initial times appeared linear although over longer periods of time, a gradual decrease in rate was observed (inset plot, Figure 2.9). A decrease in the rate of protonolysis could be due to several reasons. Decomposition of the metal complex was immediately ruled out as no spectroscopic evidence of ligand dissociation from the metal center was observed (either off-arm dissociation or complete ligand cleavage). Since the metal complex was not the source of rate retardation, the role of the ammonium acid was questioned. As protonolysis occurred under conditions utilizing a nitrile trap, Ph_2NH was produced and could behave in various manners.

First, if protonation was reversible, then an increase in the concentration of base could explain the observed rate reduction since competitive deprotonation of a five-coordinate Pt-H intermediate would drive the protonation equilibrium (Scheme 2.4) towards the Pt-Me starting complex and therefore decrease the overall rate of protonolysis. To test this

hypothesis, the order in base was determined by studying protonolysis rates with added amine. These results are shown in Figure 2.9 and the order in base was determined to be -0.8. Since this reaction was not simply inverse first order in base it was believed that the base must be participating in another reaction which retarded the rate of protonation by either attenuating the acidity of the reaction mixture or by consuming $[\text{Ph}_2\text{NH}_2][\text{BF}_4]$ such that it could not react with Pt-Me. One such possibility was homoconjugation which is defined as the association between a base and its conjugate acid through a hydrogen bond (eq. 5).

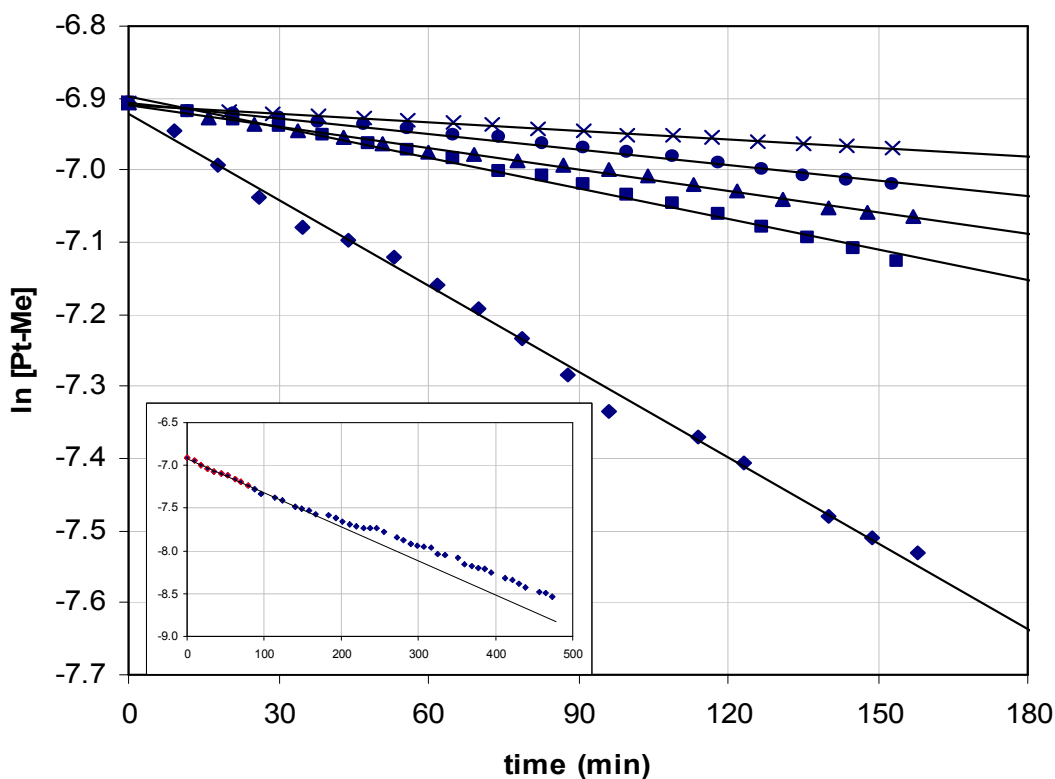
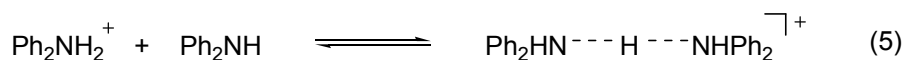


Figure 2.9. Plot of $\ln [1]$ versus time (10 eq. $[\text{Ph}_2\text{NH}_2][\text{BF}_4]$, 10 eq. NCC_6F_5): with 0 (\blacklozenge), 1 (\blacksquare), 2.5 (\blacktriangle), 5 (\bullet), and 10 (\times) eq. Ph_2NH .



The presence of a homoconjugate pair was spectroscopically tested by monitoring the chemical shift of acid (Ph_2NH_2^+) while titrating base (Ph_2NH) into the system. For this test, a linear relationship between the averaged NH chemical shift and X_{base} would indicate a simple fast exchange of protons occurs between Ph_2NH and its conjugate acid, not homoconjugate pairing of the two. A deviation from linearity (“bowing” effect) however, would be a positive test for homoconjugation.¹³ Figure 2.10a depicts a large deviation from linearity for this test. This indicated that association between $[\text{Ph}_2\text{NH}_2][\text{BF}_4]$ and Ph_2NH existed under these conditions. If hydrogen bond association occurred as shown in equation 5, then diluting a solution with this complex should perturb the equilibrium enough to observe a change in the chemical shift of the homoconjugate pair (Figure 2.10b). This experiment showed a downfield shift as concentration increased which again suggested that homoconjugation occurred between $[\text{Ph}_2\text{NH}_2][\text{BF}_4]$ and Ph_2NH . These results supported the possibility that homoconjugation may be present in the protonation reaction. This phenomenon may explain why inhibition studies did not result in an inverse first order dependence on added amine. From these studies it was not clear if homoconjugation was the cause of rate retardation at longer reaction times. There was however a direct correlation between concentration of base and protonation rates regardless of the exact role of Ph_2NH in these reactions.

¹³ Papish, E. T.; Rix, F. C.; Spetseris, N.; Norton, J. R.; Williams, R. D. *J. Am. Chem. Soc.* **2000**, *122*, 12235-12242.

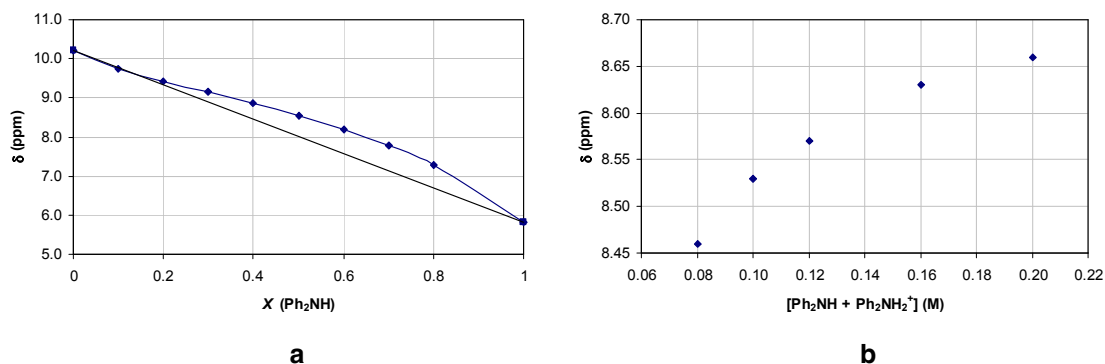


Figure 2.10. (a) Averaged NH chemical shift of Ph₂NH and Ph₂NH₂⁺ (δ) versus mole fraction (X) of Ph₂NH; [Ph₂NH₂][BF₄] = 0.08 M. (b) NH chemical shift of equimolar solution of Ph₂NH and Ph₂NH₂⁺ (δ) versus [Ph₂NH + Ph₂NH₂⁺].

To obtain linear kinetic plots for mechanistic analysis, the source of inhibition had to be eliminated. This was achieved by changing the trap from pentafluorobenzonitrile to a 1,5-dienyl sulfonamide (**2**) as shown in equation 6. This substrate was chosen since cyclization was known to be rapid and irreversible and upon cyclization, a proton capable of reprotonating Ph₂NH was generated thus removing Ph₂NH from solution and eliminating the formation of a homoconjugate pair. This substrate was also known to only slowly undergo background Brønsted monocyclization (catalyzed by [Ph₂NH₂][BF₄]) in contrast to the 1,5-dienyl phenol substrates mentioned previously. Protonation experiments using this trapping ligand were observed to give well behaved kinetics and linear ln [**1**] versus time plots even at long reaction times as shown in Figure 2.11. Similar to the systems involving a nitrile trap, protonolysis followed by trapping with **2** was shown to be first order in acid and zero order in trapping ligand resulting in a rate that was $\propto [\text{Pt}]^1[\text{acid}]^1[\text{trap}]^0$.

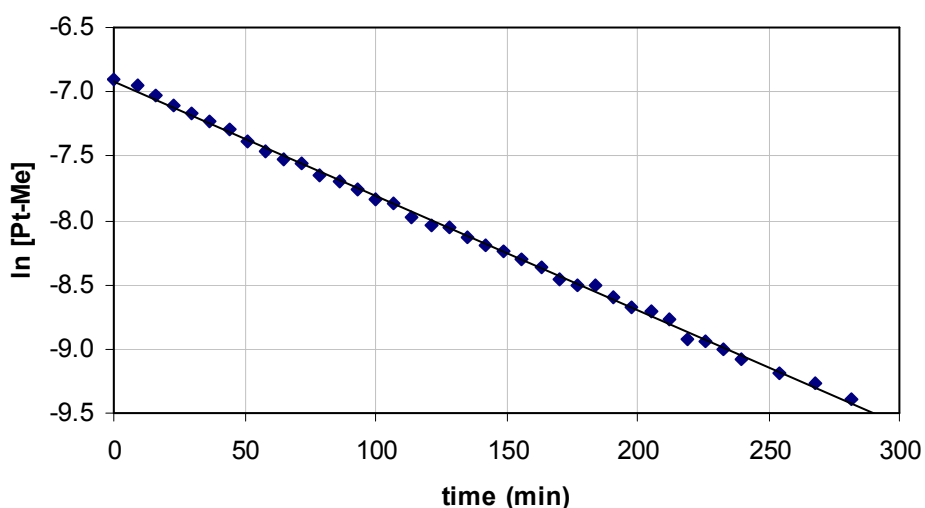
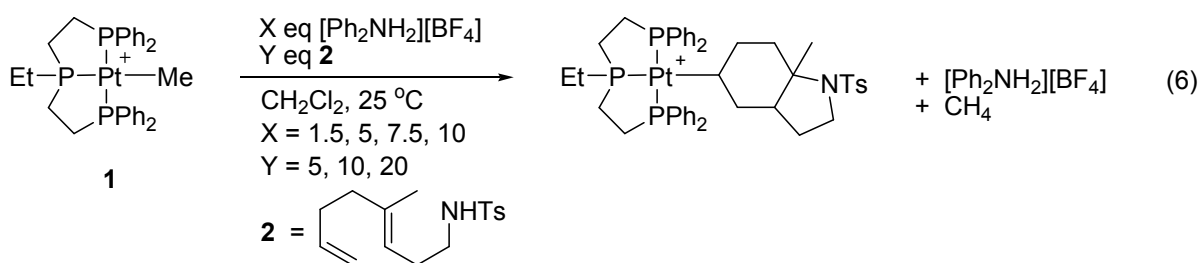


Figure 2.11. Typical plot of $\ln [1]$ vs. time (10 equiv. $[\text{Ph}_2\text{NH}_2][\text{BF}_4]$, 10 equiv. **2**); initial concentration = 0.01 M; $[(\text{EtPPP})\text{PtMe}][\text{BF}_4]$ (**1**).

Deuterium labeling was performed to determine if H/D scrambling occurred between Pt-Me and the external ammonium acid. By using the d_3 -analog of **1** and monitoring the ^1H NMR spectrum in the methane region, no isotopologs other than CD_3H were observed (Figure 2.12). The full range of methane isotopologs is shown in Figure 2.13.¹⁴ Also, no scrambling was observed in the Pt- CD_3 region at any point during the reaction. The implication of this data on the mechanism of protonation is further detailed in the following section. By comparing the rates of protonation between **1** and **1-d**₃ a kinetic isotope effect (KIE) was calculated to be 1.2 as shown by Figure 2.14.

¹⁴ Stahl, S. S.; Labinger, J. A.; Bercaw, J. E. *J. Am. Chem. Soc.* **1996**, *118*, 5961-5976.

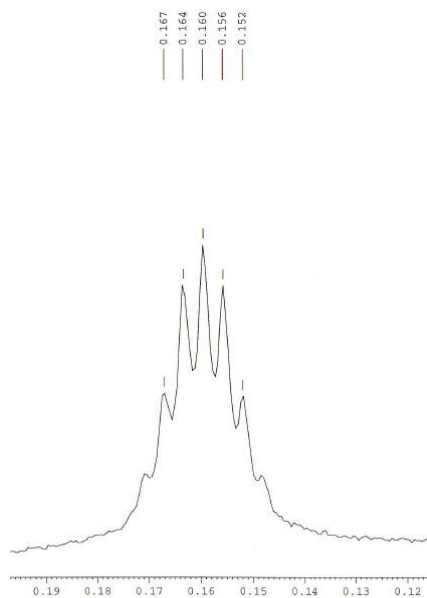


Figure 2.12. ^1H NMR (500 MHz) spectrum of CD_3H .

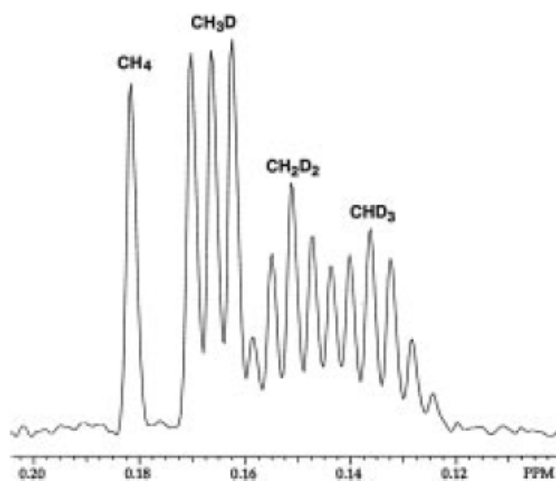


Figure 2.13. ^1H NMR spectrum of methane isotopologs.¹⁴

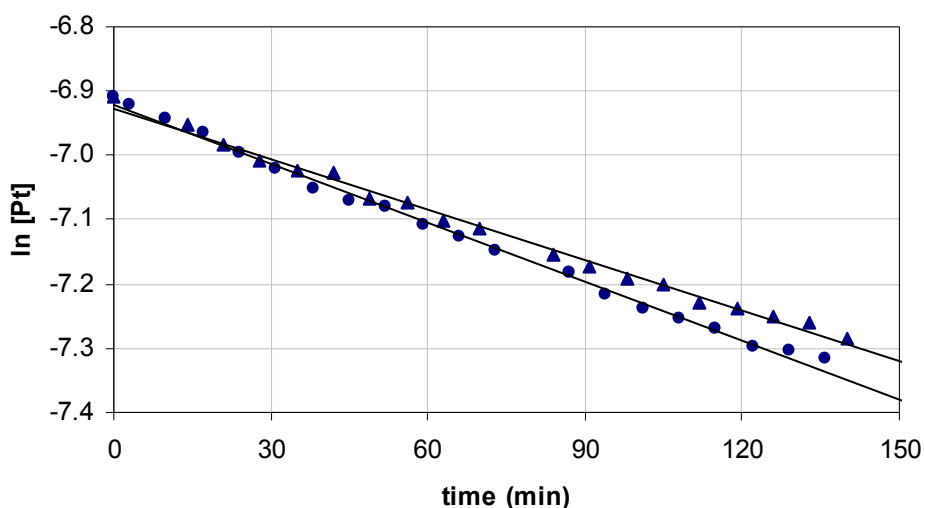


Figure 2.14. Plot of $\ln [\text{Pt-Me}]$ vs. time (10 equiv. $[\text{Ph}_2\text{NH}_2][\text{BF}_4]$, 10 equiv. NCC_6F_5) for **1** (●) and **1-d₃** (▲); $k_{\text{H}}/k_{\text{D}} = 1.2$.

D. Analysis of Mechanistic Experiments. All research to date proposed two mechanistic pathways for the protonation of Pt-alkyl or -aryl complexes.¹⁵ The first mechanism involved direct electrophilic attack at the Pt-C bond while the second was an oxidative addition of HX to Pt followed by reductive elimination to give the free alkyl or aryl product (Scheme 2.3). Evidence for both mechanisms were abundant including cases where similar $(\text{L})_2\text{Pt}(\text{R})(\text{X})$ systems behaved differently.¹⁶ A standard test to distinguish between the two mechanisms was proposed by Puddephatt and involved examining the rate differences between isostructural Pt-Me and Pt-Ph systems.¹⁷ Unfortunately, the data presented above did not differentiate between these two

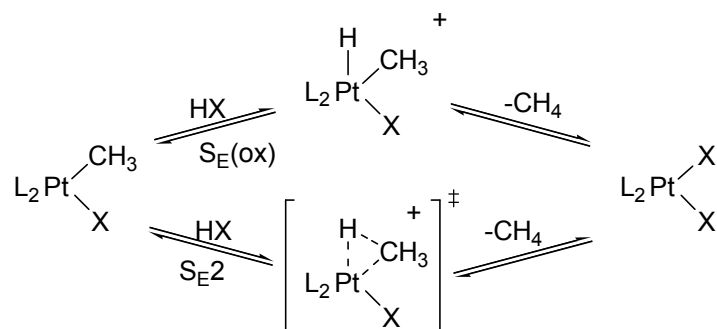
¹⁵ For reviews on this topic see: (a) Lersch, M.; Tilset, M. *Chem. Rev.* **2005**, *105*, 2471-2526. (b) Puddephatt, R. J. *Coord. Chem. Rev.* **2001**, *219-221*, 157-185.

¹⁶ (a) Kalberer, E. W.; Houllis, J. F.; Roddick, D. M. *Organometallics* **2004**, *23*, 4112-4115 and references 2-4 within. (b) Bennett, B. L.; Hoerter, J. M.; Houllis, J. F.; Roddick, D. M. *Organometallics* **2000**, *19*, 615-621. (c) Hill, G. S.; Rendina, L. M.; Puddephatt, R. J. *Organometallics* **1995**, *14*, 4966-4968.

¹⁷ Results suggested that when $k(\text{Me})/k(\text{Ph}) \gg 1$, then $\text{S}_{\text{E}}(\text{ox})$ was operative and $k(\text{Ph})/k(\text{Me}) \gg 1$, implied an $\text{S}_{\text{E}}2$ mechanism, see: Jawad, J. K.; Puddephatt, R. J.; Stalteri, M. A. *Inorg. Chem.* **1982**, *21*, 332-337.

mechanisms although the hypothesis for rate enhancement favored an $S_E(\text{ox})$ type mechanism (*vide infra*).

Scheme 2.3

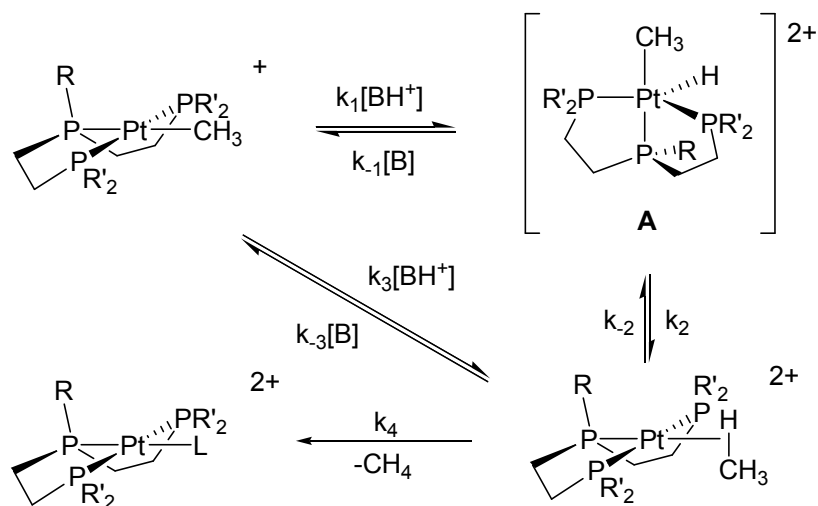


Several key mechanistic observations were determined from the data obtained during this study. First, protonolysis of Pt-Me was determined to be first order in acid and zero order in trapping ligand (nitrile or **2**) resulting in a rate that was $\propto [\text{Pt}]^1[\text{acid}]^1[\text{trap}]^0$. Along with this information, isotope labeling studies showed no kinetic isotope effect ($k_H/k_D = 1.2$) and only one isotopolog from protonolysis, CD_3H . Finally, in what may be the most important observation, protonolysis occurred only in systems with an RPPPR' ligand architecture, not in P_2P modular systems.

Scheme 2.4 depicts the possible mechanistic pathways that could be operative in the protonolysis of $[(\text{RPPPR}')\text{PtMe}][\text{BF}_4]$ by diaryl ammonium acids. The initial protonation by $[\text{Ph}_2\text{NH}_2][\text{BF}_4]$ could follow two different routes. The first possibility is stepwise reversible protonation at the metal center (k_1) to give a five coordinate intermediate **A**. Protonation can also occur at the methyl group or at the Pt-C bond as shown in the S_E2 mechanism in Scheme 2.3. The first order dependence on acid (Figure 2.7) and the inhibition by added amine (Figure 2.9) was consistent with either protonation mechanism. The large retardation of rate upon addition of amine was suggestive of a

protonation equilibrium that favored the Pt-CH₃ starting complex. Neither k_1 nor k_3 could be excluded by this data, however the small KIE (1.2) determined from deuterium labeling studies did not support direct protonation at the Pt-C bond (or at methyl).^{15b} In order to propose k_1 as the initial protonation pathway, attempts were made to characterize intermediate **A**.

Scheme 2.4



Attempts to observe the 5-coordinate Pt(IV) dication **A** by low temperature ¹H NMR experiments were unsuccessful. Reaction of **1** with HOTf at -78 °C gave complete conversion to the Pt-OTf within 10 minutes with no signs of a Pt-H by ¹H NMR. Protonation of [(PPP)PtMe][BF₄] with HNTf₂ at -65 °C over 2 hours in the presence of a nitrile trap gave complete conversion to the Pt-nitrile complex with no observed intermediates. A positive identification (by ¹H NMR) of a Pt-H would have provided evidence of a Pt(IV) intermediate (**A**) and therefore indicated a stepwise S_E(ox) mechanism. These types of intermediates had been previously observed in Pt(diimine) systems using HX (X = Cl, Br, I) except when the acid had a weakly coordinating counter ion (triflic or trifluoroacetic acid).^{15c}

Deuterium labeling studies were employed to investigate the reversibility of σ methane adduct formation (k_2). Previous reports involving this type of investigation with Pt-CH₃ showed that the formation of a σ methane adduct was reversible since protonolysis with deuterated acid resulted in methane isotopologs with more than one deuterium incorporated into the molecule.¹⁴ If reductive coupling was reversible in the triphos systems, performing protonolysis on a Pt-CD₃ complex would result in methane products of the form CD_{3-n}H_{1+n} or mixtures of Pt-CD_{3-n}H_n during the reaction. No isotopologs other than CD₃H were observed during the protonation of **1-d₃** with [Ph₂NH₂][BF₄] by ¹H NMR. Therefore, one of two assumptions could be made: 1) formation of a σ methane adduct was irreversible or 2) the rate of associative ligand substitution (k_4) was much greater than the reverse pathway of reductive coupling (k_2).

The final step of the protonolysis reaction was believed to be an associative displacement of the σ methane adduct by the weakly coordinating ligand NCC₆F₅.¹⁸ The zero order behavior in trapping ligand (nitrile or alkene) was indicative of a fast methane displacement step. Associative ligand substitution is common in Pt/Pd triphos systems¹⁹ as well as in protonolysis reactions with Pt(II).^{18b} The mechanistic data presented here was consistent with oxidative reversible protonation at the metal center to generate a 5-coordinate Pt(IV) intermediate which then underwent irreversible reductive coupling followed by rapid associative ligand substitution.

¹⁸ (a) Wik, B. J.; Lersch, M.; Tilset, M. *J. Am. Chem. Soc.* **2002**, *124*, 12116-12117. (b) Johansson, L.; Tilset, M. *J. Am. Chem. Soc.* **2001**, *123*, 739-740. (c) Procelewska, J.; Zahl, A.; van Eldik, R.; Zhong, H. A.; Labinger, J. A.; Bercaw, J. E. *Inorg. Chem.* **2002**, *41*, 2808-2810.

¹⁹ (a) Aizawa, S.; Sone, Y.; Kawamoto, T.; Yamada, G. I.; Joe, M.; Nakamura, M.; *Inorg. Chim. Acta* **2002**, *338*, 235-239. (b) Dockter, D. W.; Fanwick, P. E.; Kubiak, C. P. *J. Am. Chem. Soc.* **1996**, *118*, 4846-4852.

E. Hypothesis for Rate Enhancement. While this study showed that mild acids could be used to protonate cationic (PPP)Pt-Me bonds, what was most interesting about this study was the fact that protonolysis occurred in the tridentate PPP system and not in modular analogs. This fact led to the hypothesis that the rate enhancement was a result of some inherent factor in the ground state energy of the starting cationic (PPP)Pt-Me complexes.

Following a concerted protonolysis mechanism (S_E2), there should be no discrete differences between the PPP complexes and the non-pincer modular analogs. This led to the belief that these reactions followed a stepwise $S_E(ox)$ type mechanism as outlined by k_1 and k_2 in Scheme 2.4. Unique to *square planar* (RPPPR')Pt²⁺ complexes is an inherent torsional strain in the phosphine pincer ligand.²⁰ The coordination of PPP to Pt creates strain by forcing the ligand to adopt a bicyclic structure. This places Pt and the three phosphorus atoms into a single plane thereby creating torsional strain in the square planar complex. Torsional strain was proposed to be the source of the large downfield chemical shift of the coordinated central phosphine in PPP ligands²¹ and had been used to explain the enhanced rates of phosphine arm dissociation with (PPP)PdCl.²²

X-ray structures supply ample evidence in the solid state for these structural distortions. At the central P, the C-P-C bond angles were expanded far from the normal sp^3 angle (112-117°). This large angle was a result of the enforced “planarity” by the

²⁰ Garrou, P. E. *Chem. Rev.* **1981**, *81*, 229-266.

²¹ (a) See references 4c and 7. (b) Annibale, G.; Bergamini, P.; Bertolasi, V.; Besco, E.; Cattabriga, M.; Rossi, R. *Inorg. Chim. Acta* **2002**, *333*, 116-123. (c) Fernández, D.; Sevillano, P.; García-Seijo, M. I.; Castiñeiras, A.; János, L.; Berente, Z.; Kollár, L.; García-Fernández, M. E. *Inorg. Chim. Acta* **2001**, *312*, 40-52. (d) Tau, K. D.; Uriarte, R.; Mazanec, T. J.; Meek, D. W. *J. Am. Chem. Soc.* **1979**, *101*, 6614-6619. (e) DuBois, D. L.; Miedaner, A. *J. Am. Chem. Soc.* **1987**, *109*, 113-117.

²² Sevillano, P.; Habtemariam, A.; Parsons, S.; Castiñeiras, A.; García, M. E.; Sadler, P. J. *J. Chem. Soc., Dalton Trans.* **1999**, 2861-2870.

tridentate coordination in the square plane. More normal C-P-C bond angles ($104\text{--}108^\circ$) were observed for the two terminal phosphines. Another obvious solid state distortion occurs in the transoid P-Pt-P bond angle which typically is found to be around 180° in square planar systems. In an attempt to reduce torsional strain at the central P, transoid P-Pt-P angles are compressed to $162\text{--}168^\circ$. These distortions are shown more clearly in Figure 2.15.

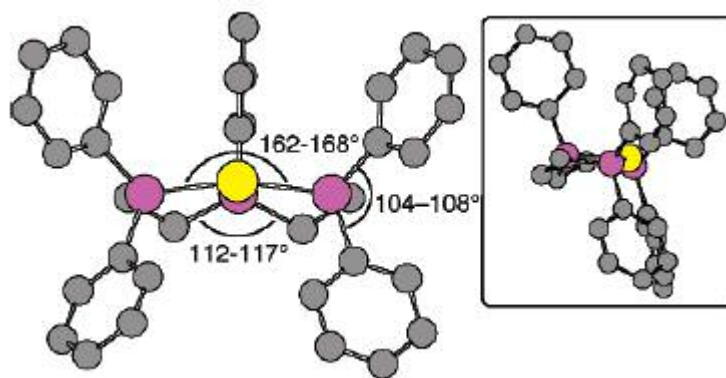


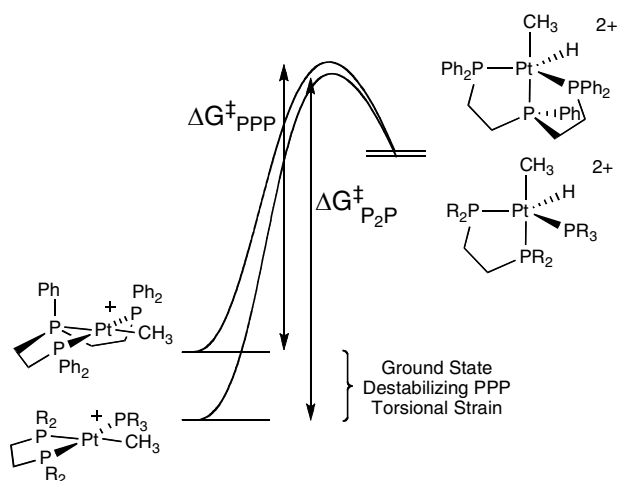
Figure 2.15. Typical C-P-C and P-Pt-P bond angles in square planar (PPP)Pt complexes.²³ Boxed in structure is a side view of (PPP)Pt complex.

Upon conversion from a square planar to a trigonal bipyramidal complex, the central phosphine of the ligand can occupy an axial position thus projecting the ligand arms into more natural directions (Scheme 2.5). Repositioning by the ligand in a trigonal bipyramidal structure relieves the torsional strain inherent in the square planar configuration. Evidence for this is manifested again in the ^{31}P NMR chemical shifts as well as C-P-C and P-M-P bond angles.²⁴

²³ Bond angles shown are from a compilation of (PPP)Pt X-ray structures, see: (a) reference 21 (b) Annibale, G.; Bergamini, P.; Bertolasi, V.; Cattabriga, M.; Ferretti, V. *Inorg. Chem. Commun.* **2000**, 3, 303-306. (c) Ferguson, G.; *et. al. J. Organomet. Chem.* **2001**, 617-618, 671-680.

²⁴ (a) DuBois, D. L.; Meek, D. W. *Inorg. Chem.* **1976**, 15, 3076-3083. (b) Siedle, A. R.; Newmark, R. A.; Pignolet, L. H. *J. Am. Chem. Soc.* **1981**, 103, 4947-4948. (c) DuBois, D. L.; Miedaner, A. *Inorg. Chem.* **1986**, 25, 4642-4650. (d) Petöcz, G.; Jánosi, L.; Wissensteiner, W.; Csók, H. E.; Man, Z.; Kollár, L. *Inorg. Chim. Acta* **2000**, 303, 300-305. (e) López-Torres, M.; Fernández, A.; Fernández, J. J.; Suárez, A.; Pereira, M. T.; Ortigueira, J. M.; Vila, J. M.; Adams, H. *Inorg. Chem.* **2001**, 40, 4583-4587.

Scheme 2.5



Directly comparing the PPP complexes to the P₂P complexes using a torsional strain analysis would suggest that the starting (PPP)Pt-Me complex had a higher ground state energy relative to the (P₂P)Pt-Me compounds since no such strain would exist in the modular P₂P analogs. Assuming that a stepwise S_E(ox) mechanism was operative, the release of ground state torsional strain upon protonation to a five-coordinate Pt-H structure would result in an overall lowering of activation energy ($\Delta G^\ddagger_{\text{PPP}}$) for protonation as depicted in Scheme 2.5. As a result of this, a 4-5-4 coordination number change would be greatly accelerated in a PPP pincer system relative to a P₂P ligand structure. The results described in this study agreed with this hypothesis as protonolysis in the PPP pincer systems was much more facile than modular P₂P complexes.

2.3 Conclusions

These results showed that Pt(II) tridentate PPP compounds were protonated much more readily than modular analogs of similar size and basicity using a buffered ammonium acid as the proton source. These conditions were some of the most mild reported for the protonation of cationic Pt(II) alkyl bonds. The hypothesis for this

enhanced reactivity involved the release of inherent ring strain in the ground state square planar Pt-Me complex upon protonation to a 5-coordinate intermediate. Mechanistic studies provided evidence for initial reversible protonation to a 5-coordinate Pt(IV) intermediate followed by irreversible reductive coupling and subsequent associative ligand substitution.

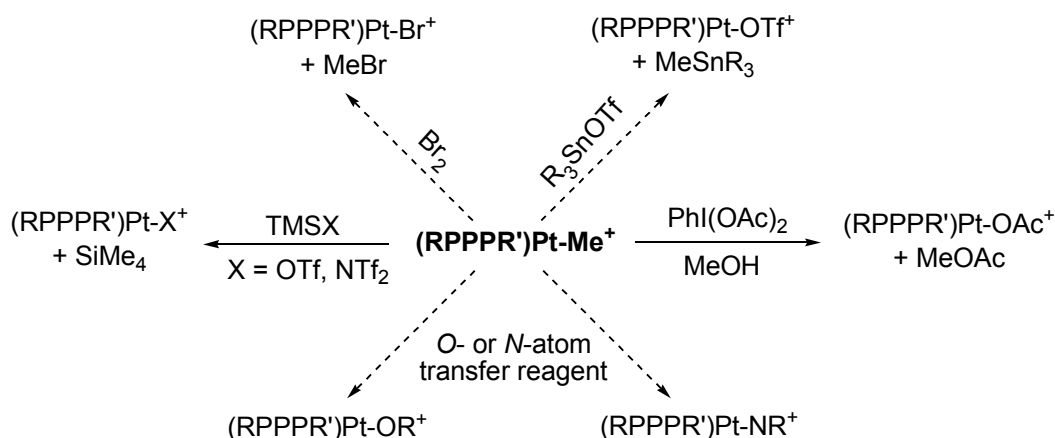
The enhanced associative reactivity reported may be of greater importance as a general phenomenon which could be applied to other systems involving inherent ground state strain. Scheme 2.6 depicts methods of electrophilic Pt-C cleavage that were successfully performed on pincer Pt-Me model complexes. Test experiments indicated that [(PPP)PtMe][SbF₆] reacted quickly with TMSOTf and TMSNTf₂ at room temperature to generate tetramethylsilane.²⁵ Also, [(EtPPPEt)PtMe][BF₄] reacted with PhI(OAc)₂ in 5 hours in MeOH at room temperature to give MeOAc and Pt-OAc, presumably through a Pt(IV) intermediate similar to the cases shown by Sanford.²⁶ Similar to protonation attempts, this reactivity was not observed with more complex cyclized Pt-alkyl compounds. Studies are ongoing into electrophilic turnover possibilities as well as the use of *O*- and *N*-atom transfer reagents to generate Pt-alkoxo or -amido species which should be more prone to protonation under mild conditions.²⁷

²⁵ Unpublished results.

²⁶ (a) Desai, L. V.; Hull, K. L.; Sanford, M. S. *J. Am. Chem. Soc.* **2004**, *126*, 9542-9543. (b) Dick, A. R.; Hull, K. L.; Sanford, M. S. *J. Am. Chem. Soc.* **2004**, *126*, 2300-2301.

²⁷ (a) Matsunaga, P. T.; Mavropoulos, J. C.; Hillhouse, G. L. *Polyhedron* **1995**, *14*, 175-185. (b) Matsunaga, P. T.; Hillhouse, G. L.; Rheingold, A. L. *J. Am. Chem. Soc.* **1993**, *115*, 2075-2077.

Scheme 2.6



2.4 Experimental

General Synthetic Procedures:

Bis(2-diphenylphosphinoethyl)phenylphosphine (**PPP**), bis(2-bis(3,5-dimethylphenyl)phosphinoethyl)phenylphosphine (**PPPxylyl**), bis(2-bis(*p*-tolyl)phosphinoethyl)phenylphosphine (**PPPtoly**), bis(2-cyclohexylphosphinoethyl)phenylphosphine (**PPPCy**), bis(2-diethylphosphinoethyl)phenylphosphine (**PPPEt**), bis(2-diphenylphosphinoethyl)ethylphosphine (**EtPPP**), bis(2-diethylphosphinoethyl)ethylphosphine (**EtPPPEt**), bis(2-diphenylphosphinoethyl)cyclohexylphosphine (**CyPPP**), bis(2-diphenylphosphinoethyl)*tert*-butylphosphine (***t*BuPPP**), and bis(2-diethylphosphinoethyl)*tert*-butylphosphine (***t*BuPPPEt**) were prepared using the methods reported by DuBois (Scheme 2.2).⁷ Some ligands had traces of impurities which were easily removed after metal coordination. Divinylethylphosphine and divinyl*tert*-butylphosphine were prepared using a modified procedure by Weiner.²⁸

²⁸ Weiner, M. A.; Pasternack, G. J. *Org. Chem.* **1967**, 32, 3707-3709.

(COD)Pt(Me)Cl⁸, [Ph₂NH₂][BF₄]²⁹, and **2**^{1c} were synthesized following published procedures. AIBN (2,2'-azobisisobutyronitrile) was recrystallized from methanol prior to use. Pentafluorobenzonitrile, divinylphenylphosphine, dichloroethylphosphine, diphenylamine, tetrafluoroboric acid, and vinylmagnesium bromide were purchased from Aldrich and used as received. Vinyldiphenylphosphine, dicyclohexylphosphine, diethylphosphine, cyclohexylphosphine, diphenylphosphine, *t*-butyldichlorophosphine, and sodium tetrafluoroborate were purchased from Strem Chemicals and used as received. CD₂Cl₂ and CDCl₃ were passed through a plug of activated alumina and stored in a glovebox. Dichloromethane used for kinetic experiments was dried by passage through a column of activated alumina and degassed by several successive freeze-pump-thaw cycles and stored in a glovebox. All other solvents were dried by passage through a column of activated alumina.

All reactions were performed under an inert atmosphere of N₂ using standard Schlenk techniques or using an MBraun Lab-Master 100 glove box. Photochemistry was performed using an Oriel 350W Hg Arc Lamp. NMR spectra were recorded on a Bruker AMX300 MHz or a Bruker Avance 400 MHz spectrometer. Protonation kinetic experiments were performed on a Bruker Avance 500 MHz spectrometer. Chemical shifts are reported in ppm and referenced to residual solvent peaks (¹H and ¹³C NMR) or to an external standard (85% H₃PO₄, ³¹P NMR). Elemental microanalyses were performed by Complete Analysis Laboratories, Parsippany, NJ and Robertson Microlit Laboratories, Madison, NJ.

²⁹ Forschner, T. C.; Cutler, A. R. *Organometallics* **1985**, 4, 1247-1257.

General Synthesis of PPP Ligands:

In a glove box, the dialkyl- or diaryl-phosphine was added to the corresponding divinylphosphine neat with 3 mol% AIBN in a sealable Kontes tube.⁷ The mixture was irradiated at 350 nm at room temperature for 4 - 48 hours. Any volatile unreacted materials were removed under vacuum with heat. Figure 2.1 depicts the PPP ligands synthesized by this manner.

PPPtoly: The resulting white solid was rinsed with pentane to remove excess phosphine starting material to yield 1.2207 g (89%); ¹H NMR (400 MHz, CD₂Cl₂): δ 7.1-7.4 (m, 21H, Ph); 2.3 (s, 12H, CH₃); 1.6-2.0 (m, 8H, CH₂CH₂). ³¹P{¹H} NMR (161.8 MHz, CD₂Cl₂): δ -12.7 (d, ³J_{P-P} = 27.8 Hz, 2P); -14.0 (t, ³J_{P-P} = 27.8 Hz, 1P).

PPPxyl: The resulting white solid was rinsed with pentane to remove excess phosphine starting material to yield 560.4 mg (84%); ¹H NMR (400 MHz, CD₂Cl₂): δ 6.9-7.4 (m, 17H, Ph); 2.2 (s, 24H, CH₃); 1.7-2.1 (m, 8H, CH₂CH₂). ³¹P{¹H} NMR (161.8 MHz, CD₂Cl₂): δ -11.1 (d, ³J_{P-P} = 29.6 Hz, 2P); -13.7 (t, ³J_{P-P} = 29.6 Hz, 1P).

EtPPP: Volatile phosphine starting materials were removed in vacuo at 130 °C to yield 2.1011 g (85%) of colorless oil; ¹H NMR (400 MHz, CD₂Cl₂): δ 7.3-7.6 (m, 20H, Ph); 1.0-2.2 (m, 13H, C₂H₅ and CH₂CH₂). ³¹P{¹H} NMR (161.8 MHz, CD₂Cl₂): δ -12.9 (d, ³J_{P-P} = 25.9 Hz, 2P); -17.4 (t, ³J_{P-P} = 25.9 Hz, 1P).

EtPPPEt: Volatile phosphine starting materials were removed in vacuo at 120 °C to yield 816.3 mg (82%) of orange oil; ¹H NMR (400 MHz, CD₂Cl₂): δ 1.0-1.5 (m, 33H, C₂H₅ and CH₂CH₂). ³¹P{¹H} NMR (161.8 MHz, CD₂Cl₂): δ -18.0 (m, 3P).

***t*BuPPP:** Volatile phosphine starting materials were removed in vacuo at 130 °C to yield 1.3462 g (80%) of colorless oil; ¹H NMR (400 MHz, CD₂Cl₂): δ 7.3-7.5 (m, 20H,

Ph); 1.2-2.2 (m, 8H, CH₂CH₂); 0.92 (s, 9H, C(CH₃)₃). ³¹P{¹H} NMR (161.8 MHz, CD₂Cl₂): δ 11.6 (t, ³J_{P-P} = 31.6 Hz, 1P); -10.5 (d, ³J_{P-P} = 31.6 Hz, 2P).

General Synthesis of [(RPPPR')Pt-CH₃][BF₄]:

In a glovebox, a solution of the phosphine ligand in CH₂Cl₂ (~0.1 M) was added dropwise to a solution of (COD)Pt(Me)Cl in CH₂Cl₂ (~0.1 M). After 4 h of stirring, the solvent was removed and the resulting white solid was washed with pentane to yield [(RPPPR')Pt-CH₃][Cl]. NaBF₄ was added to [(RPPPR')Pt-CH₃][Cl] in CH₂Cl₂ (~0.1 M) and stirred 18-20 h. The resulting suspension was filtered through a 0.45 μm syringe filter and the solvent was removed to give [(RPPPR')Pt-CH₃][BF₄] as a white or pale brown powder. [(RPPPR')Pt-CH₃][Cl] was characterized by ¹H and ³¹P NMR. The BF₄⁻ salts of these compounds, [(RPPPR')Pt-CH₃][BF₄], were characterized by ¹H and ³¹P{¹H} NMR in addition to elemental analysis.

[(EtPPPEt)Pt-CH₃][Cl]: 421.6 mg (72%); ¹H NMR (400 MHz, CDCl₃): δ 1.0-2.9 (m, 33H, C₂H₅ and CH₂CH₂); 0.59 (q, ²J_{Pt-H} = 61.4 Hz, ³J_{P-H} = 6.1 Hz, 3H, CH₃). ³¹P{¹H} NMR (161.8 MHz, CDCl₃): δ 99.1 (s, ³J_{Pt-P} = 1499 Hz, 1P); 45.4 (s, ³J_{Pt-P} = 2573 Hz, 2P).

[(PPPEt)Pt-CH₃][Cl]: 120.0 mg (72%); ¹H NMR (400 MHz, CDCl₃): δ 7.4-7.9 (m, 5H, Ph); 1.1-3.1 (m, 28H, C₂H₅ and CH₂CH₂); 0.71 (q, ²J_{Pt-H} = 62.4 Hz, ³J_{P-H} = 6.3 Hz, 3H, CH₃). ³¹P{¹H} NMR (161.8 MHz, CDCl₃): δ 97.9 (s, ³J_{Pt-P} = 1562 Hz, 1P); 46.5 (s, ³J_{Pt-P} = 2544, 2P).

[(*t*BuPPPEt)Pt-CH₃][Cl]: 67.6 mg (59%); ¹H NMR (400 MHz, CDCl₃): δ 1.1-3.0 (m, 37H, C₂H₅, C(CH₃)₃ and CH₂CH₂); 0.67 (q, ²J_{Pt-H} = 60.5 Hz, ³J_{P-H} = 6.2 Hz, 3H, CH₃).

$^{31}\text{P}\{^1\text{H}\}$ NMR (161.8 MHz, CDCl_3): δ 120.7 (s, $^3J_{\text{Pt-P}} = 1530$ Hz, 1P); 44.1 (s, $^3J_{\text{Pt-P}} = 2600$ Hz, 2P).

[(EtPPP)Pt-CH₃][Cl]: 78.4 mg (63%); ^1H NMR (400 MHz, CDCl_3): δ 7.3-7.8 (m, 20H, Ph); 2.3-3.6 (m, 8H, CH_2CH_2); 1.0-2.1 (m, 5H, C_2H_5); 0.61 (q, $^2J_{\text{Pt-H}} = 61.6$ Hz, $^3J_{\text{P-H}} = 6.0$ Hz, 3H, CH_3). $^{31}\text{P}\{^1\text{H}\}$ NMR (161.8 MHz, CDCl_3): δ 97.6 (s, $^3J_{\text{Pt-P}} = 1457$ Hz, 1P); 44.3 (s, $^3J_{\text{Pt-P}} = 2780$ Hz, 2P).

[(PPPxylyl)Pt-CH₃][Cl]: 82.6 mg (75%); ^1H NMR (400 MHz, CDCl_3): δ 8.1 and 7.5 (m, 5H, Ph); 7.1 (m, 12H, *ArH*); 2.2-3.7 (m, 8H, CH_2CH_2); 2.3 and 2.28 (s, 24H, *ArCH*₃); 0.81 (q, $^2J_{\text{Pt-H}} = 61.6$ Hz, $^3J_{\text{P-H}} = 6.0$ Hz, 3H, *Pt-CH*₃). $^{31}\text{P}\{^1\text{H}\}$ NMR (161.8 MHz, CDCl_3): δ 96.0 (s, $^3J_{\text{Pt-P}} = 1529$ Hz, 1P); 42.3 (s, $^3J_{\text{Pt-P}} = 2733$ Hz, 2P).

[(PPPtoly)Pt-CH₃][Cl]: 94.2 mg (83%); ^1H NMR (400 MHz, CDCl_3): δ 7.2–8.1 (m, 25H, *ArH*); 2.2-3.6 (m, 8H, CH_2CH_2); 2.4 (s, 12H, *ArCH*₃); 0.77 (q, $^2J_{\text{Pt-H}} = 61.2$ Hz, $^3J_{\text{P-H}} = 6.0$ Hz, 3H, *Pt-CH*₃). $^{31}\text{P}\{^1\text{H}\}$ NMR (161.8 MHz, CDCl_3): δ 96.2 (s, $^3J_{\text{Pt-P}} = 1527$ Hz, 1P); 41.7 (s, $^3J_{\text{Pt-P}} = 2731$ Hz, 2P).

[(CyPPP)Pt-CH₃][Cl]: 113.6 mg (83%); ^1H NMR (400 MHz, CDCl_3): δ 7.3-7.8 (m, 20H, Ph); 0.8-3.6 (m, 19H, C_6H_{11} and CH_2CH_2); 0.55 (q, $^2J_{\text{Pt-H}} = 61.2$ Hz, $^3J_{\text{P-H}} = 6.0$ Hz, 3H, CH_3). $^{31}\text{P}\{^1\text{H}\}$ NMR (161.8 MHz, CDCl_3): δ 102.6 (s, $^3J_{\text{Pt-P}} = 1473$ Hz, 1P); 45.7 (s, $^3J_{\text{Pt-P}} = 2789$ Hz, 2P).

[(PPPCy)Pt-CH₃][Cl]: 207.5 mg (91%); ^1H NMR (400 MHz, CDCl_3): δ 7.4 and 7.9 (m, 5H, Ph); 2.1-3.4 (m, 8H, CH_2CH_2); 0.9-2.0 (m, 44H, C_6H_{11}); 0.82 (q, $^2J_{\text{Pt-H}} = 62.4$ Hz, $^3J_{\text{P-H}} = 6.0$ Hz, 3H, CH_3). $^{31}\text{P}\{^1\text{H}\}$ NMR (161.8 MHz, CDCl_3): δ 97.1 (s, $^3J_{\text{Pt-P}} = 1600$ Hz, 1P); 53.3 (s, $^3J_{\text{Pt-P}} = 2553$ Hz, 2P).

[(*t*BuPPP)Pt-CH₃][Cl]: 200.4 mg (93%); ¹H NMR (400 MHz, CDCl₃): δ 7.3-7.8 (m, 20H, Ph); 2.6-3.7 (m, 8H, CH₂CH₂); 0.95 and 0.98 (s, 9H, C(CH₃)₃); 0.48 (q, ²J_{Pt-H} = 60.8 Hz, ³J_{P-H} = 6.0 Hz, 3H, CH₃). ³¹P{¹H} NMR (161.8 MHz, CDCl₃): δ 121.7 (s, ³J_{Pt-P} = 1497 Hz, 1P); 49.2 (s, ³J_{Pt-P} = 2801 Hz, 2P).

[(EtPPPEt)Pt-CH₃][BF₄]: Obtained as a white powder, 89.7 mg (76%);³⁰ ¹H NMR (400 MHz, CDCl₃): δ 1.0-2.9 (m, 33H, C₂H₅ and CH₂CH₂); 0.59 (q, ²J_{Pt-H} = 61.6 Hz, ³J_{P-H} = 6.4 Hz, 3H, CH₃). ³¹P{¹H} NMR (161.8 MHz, CDCl₃): δ 99.2 (s, ³J_{Pt-P} = 1501 Hz, 1P); 45.5 (s, ³J_{Pt-P} = 2565 Hz, 2P). Anal. Calcd for C₁₅H₃₆BF₄P₃Pt: C, 30.47; H, 6.14. Found: C, 30.76; H, 6.03.

[(PPPEt)Pt-CH₃][BF₄]: Obtained as a sticky pale yellow solid, 125.4 mg (98%);³⁰ ¹H NMR (400 MHz, CDCl₃): δ 7.4-7.7 (m, 5H, Ph); 1.1-2.9 (m, 28H, C₂H₅ and CH₂CH₂); 0.71 (q, ²J_{Pt-H} = 62.8 Hz, ³J_{P-H} = 6.2 Hz, 3H, CH₃). ³¹P{¹H} NMR (161.8 MHz, CDCl₃): δ 96.2 (s, ³J_{Pt-P} = 1562 Hz, 1P); 44.8 (s, ³J_{Pt-P} = 2535 Hz, 2P). Anal. Calcd for C₁₉H₃₆BF₄P₃Pt: C, 35.70; H, 5.68. Found: C, 35.79; H, 5.73.

[(*t*BuPPPEt)Pt-CH₃][BF₄]: Obtained as a pale brown solid, 57.1 mg (79%);³⁰ ¹H NMR (400 MHz, CDCl₃): δ 1.1-2.9 (m, 37H, C₂H₅, C(CH₃)₃ and CH₂CH₂); 0.67 (q, ²J_{Pt-H} = 60.6 Hz, ³J_{P-H} = 6.1 Hz, 3H, CH₃). ³¹P{¹H} NMR (161.8 MHz, CDCl₃): δ 120.8 (s, ³J_{Pt-P} = 1529 Hz, 1P); 44.1 (s, ³J_{Pt-P} = 2598 Hz, 2P). Anal. Calcd for C₁₇H₄₀BF₄P₃Pt: C, 32.97; H, 6.51. Found: C, 33.18; H, 6.36.

[(EtPPP)Pt-CH₃][BF₄]: Obtained as a white solid, 71.3 mg (85%);³⁰ ¹H NMR (400 MHz, CDCl₃): δ 7.4-7.8 (m, 20H, Ph); 2.1-3.5 (m, 8H, CH₂CH₂); 1.0-2.0 (m, 5H, C₂H₅); 0.63 (q, ²J_{Pt-H} = 61.2 Hz, ³J_{P-H} = 6.0 Hz, 3H, CH₃). ³¹P{¹H} NMR (161.8 MHz, CDCl₃):

³⁰ Yields are for the conversion of chloride to BF₄⁻ salts.

δ 97.6 (s, $^3J_{\text{Pt-P}} = 1462$ Hz, 1P); 43.8 (s, $^3J_{\text{Pt-P}} = 2775$ Hz, 2P). Anal. Calcd for $\text{C}_{31}\text{H}_{36}\text{BF}_4\text{P}_3\text{Pt}$: C, 47.53; H, 4.63. Found: C, 47.87; H, 4.77.

[(PPPxylyl)Pt-CH₃][BF₄]: Obtained as a white solid, 40.2 mg (76%),³⁰ ^1H NMR (400 MHz, CDCl_3): δ 7.9 and 7.5 (m, 5H, Ph); 7.1 (m, 12H, ArH); 2.2-3.4 (m, 8H, CH_2CH_2); 2.3 (s, 24H, ArCH₃); 0.82 (q, $^2J_{\text{Pt-H}} = 61.8$ Hz, $^3J_{\text{P-H}} = 6.0$ Hz, 3H, Pt-CH₃). $^{31}\text{P}\{^1\text{H}\}$ NMR (161.8 MHz, CDCl_3): δ 94.9 (s, $^3J_{\text{Pt-P}} = 1538$ Hz, 1P); 40.5 (s, $^3J_{\text{Pt-P}} = 2726$ Hz, 2P). Anal. Calcd for $\text{C}_{43}\text{H}_{52}\text{BF}_4\text{P}_3\text{Pt}$: C, 54.73; H, 5.55. Found: C, 54.53; H, 5.62.

[(PPPtoly)Pt-CH₃][BF₄]: Obtained as a white solid, 15.7 mg (81%),³⁰ ^1H NMR (400 MHz, CDCl_3): δ 7.2–7.9 (m, 25H, ArH); 2.1-3.4 (m, 8H, CH_2CH_2); 2.4 (s, 12H, ArCH₃); 0.78 (q, $^2J_{\text{Pt-H}} = 61.8$ Hz, $^3J_{\text{P-H}} = 6.0$ Hz, 3H, Pt-CH₃). $^{31}\text{P}\{^1\text{H}\}$ NMR (161.8 MHz, CDCl_3): δ 95.1 (s, $^3J_{\text{Pt-P}} = 1535$ Hz, 1P); 39.7 (s, $^3J_{\text{Pt-P}} = 2723$ Hz, 2P). Anal. Calcd for $\text{C}_{39}\text{H}_{44}\text{BF}_4\text{P}_3\text{Pt}$: C, 52.78; H, 5.00. Found: C, 52.52; H, 4.82.

[(CyPPP)Pt-CH₃][BF₄]: Obtained as a white solid, 87.4 mg (72%),³⁰ ^1H NMR (400 MHz, CDCl_3): δ 7.3-7.8 (m, 20H, Ph); 0.9-3.5 (m, 19 H, C_6H_{11} and CH_2CH_2); 0.57 (q, $^2J_{\text{Pt-H}} = 61.0$ Hz, $^3J_{\text{P-H}} = 5.9$ Hz, 3H, CH₃). $^{31}\text{P}\{^1\text{H}\}$ NMR (161.8 MHz, CDCl_3): δ 103.1 (s, $^3J_{\text{Pt-P}} = 1473$ Hz, 1P); 45.1 (s, $^3J_{\text{Pt-P}} = 2786$ Hz, 2P). Anal. Calcd for $\text{C}_{35}\text{H}_{42}\text{BF}_4\text{P}_3\text{Pt}$: C, 50.19; H, 5.05. Found: C, 50.22; H, 5.06.

[(PPPCy)Pt-CH₃][BF₄]: Obtained as a white solid, 187.9 mg (86%),³⁰ ^1H NMR (400 MHz, CDCl_3): δ 7.45 and 7.75 (m, 5H, Ph); 1.1-3.1 (m, 52H, C_6H_{11} and CH_2CH_2); 0.84 (q, $^2J_{\text{Pt-H}} = 62.6$ Hz, $^3J_{\text{P-H}} = 5.9$ Hz, 3H, CH₃). $^{31}\text{P}\{^1\text{H}\}$ NMR (161.8 MHz, CDCl_3): δ 95.8 (s, $^3J_{\text{Pt-P}} = 1607$ Hz, 1P); 51.5 (s, $^3J_{\text{Pt-P}} = 2545$ Hz, 2P). Anal. Calcd for $\text{C}_{35}\text{H}_{60}\text{BF}_4\text{P}_3\text{Pt}$: C, 49.13; H, 7.07. Found: C, 48.90; H, 7.19.

[(*t*BuPPP)Pt-CH₃][BF₄]: Obtained as a white solid, 167.4 mg (82%);³⁰ ¹H NMR (400 MHz, CDCl₃): δ 7.2-7.8 (m, 20H, Ph); 2.4-3.5 (m, 8H, CH₂CH₂); 0.95 and 0.99 (s, 9H, C(CH₃)₃); 0.51 (q, ²J_{Pt-H} = 60.8 Hz, ³J_{P-H} = 6.0 Hz, 3H, CH₃). ³¹P{¹H} NMR (161.8 MHz, CDCl₃): δ 119.9 (s, ³J_{Pt-P} = 1495 Hz, 1P); 46.7 (s, ³J_{Pt-P} = 2797 Hz, 2P). Anal. Calcd for C₃₃H₄₀BF₄P₃Pt: C, 48.84; H, 4.97. Found: C, 48.84; H, 5.06.

General Procedure for Preparation of Isolated Products:

[(RPPP)Pt(NCC₆F₅)] [BF₄]₂: In a glovebox, (RPPP)PtI₂ (0.10 mmol) and AgBF₄ (0.25 mmol) were weighed out into a glass vial. In a separate vial, pentafluorobenzonitrile (0.40 mmol) was dissolved in 10 mL of dichloromethane. This mixture was shielded from light and stirred for 4 hours. The suspension was filtered through celite to remove AgI, concentrated *in vacuo* and washed with 250 mL of hexanes to remove excess NCC₆F₅.

[(PPP)Pt(NCC₆F₅)] [BF₄]₂: Obtained 95.1 mg (85%) of white solid; ¹H NMR (400 MHz, CDCl₃): δ 7.88 (m, 4 H); 7.77 (m, 2 H); 7.67 (m, 4 H); 7.56 (m, 12 H); 7.42 (m, 3 H); 3.47 (m, 4 H); 3.00 (m, 2 H); 2.46 (m, 2 H). ³¹P{¹H} NMR (161.8 MHz, CDCl₃): δ 85.5 (s, ³J_{Pt-P} = 3363 Hz, 1P); 49.2 (s, ³J_{Pt-P} = 2360 Hz, 2P). ¹⁹F NMR (376 MHz, CDCl₃): δ -127.6, -135.1, -151.8, -156.8. Anal. Calcd for C₄₁H₃₃B₂F₁₃NP₃Pt: C, 44.92; N, 1.28; H, 3.03. Found: C, 45.27; N, 1.20; H, 2.92.

[(EtPPP)Pt(NCC₆F₅)] [BF₄]₂: Obtained 87.0 mg (83%) of a white solid; ¹H NMR (400 MHz, CDCl₃): δ 7.96 (m, 4 H); 7.75 (m, 4 H); 7.68 (m, 2 H); 7.48 (m, 10 H); 3.48 (m, 2 H); 3.13 (m, 2 H); 2.85 (m, 2 H); 2.58 (m, 2 H); 1.81 (m, 2 H); 0.79 (m, 3H). ³¹P{¹H} NMR (161.8 MHz, CDCl₃): δ 89.5 (s, ³J_{Pt-P} = 3231 Hz, 1P); 51.6 (s, ³J_{Pt-P} =

2397 Hz, 2P). ^{19}F NMR (376 MHz, CDCl_3): δ -127.7, -135.6, -151.5, -157.0. Anal. Calcd for $\text{C}_{37}\text{H}_{33}\text{B}_2\text{F}_{13}\text{NP}_3\text{Pt}$: C, 42.39; N, 1.34; H, 3.17. Found: C, 42.16; N, 1.11; H, 3.27.

[(EtPPP)Pt(NTs-alkyl)][BF₄]: In a glovebox, (EtPPP)PtI₂ (0.10 mmol) and AgBF₄ (0.23 mmol) were weighed out into a glass vial. Dichloromethane was added to this and the solution was stirred for 10 minutes upon which **2** (0.11 mmol) was added to the solution dropwise. After an additional 10 minutes of stirring, AgI began to precipitate and diphenylmethylaniline (0.11 mmol) was added to the suspension. This mixture was shielded from light and stirred for 2 hours. The suspension was filtered through celite to remove AgI, washed three times with a saturated NaHCO₃ solution, dried over MgSO₄ and concentrated *in vacuo*. The product was precipitated three times from dichloromethane and Et₂O and dried to give 81.6 mg (72%) of a white solid; ^1H NMR (500 MHz, CDCl_3): δ 7.63 (m, 4 H); 7.58 (m, 6 H); 7.52 (d, 2 H, $J = 8.5$ Hz); 7.40 (m, 10 H); 7.15 (d, 2 H, $J = 8.5$ Hz); 3.38 (m, 2 H); 3.24 (m, 1 H); 2.82 (m, 1 H); 2.63 (m, 2 H); 2.44 (m, 2 H); 2.35 (s, 3 H); 2.25 (m, 2 H); 2.10 (m, 1 H); 1.68 (d, 1 H, $J = 10.0$ Hz); 1.51 (m, 2 H); 1.28 (m, 1 H); 1.15 (m, 3 H); 0.97 (m, 2 H); 0.80 (m, 5 H); 0.65 (s, 3 H). $^{31}\text{P}\{^1\text{H}\}$ NMR (161.8 MHz, CDCl_3): δ 90.2 (s, $^3J_{\text{Pt-P}} = 1242$ Hz, 1P); 44.6 (s, $^3J_{\text{Pt-P}} = 2999$ Hz, 2P). Anal. Calcd for $\text{C}_{46}\text{H}_{55}\text{BF}_4\text{NO}_2\text{P}_3\text{PtS}$: C, 52.08; N, 1.32; H, 5.23. Found: C, 51.81; N, 1.23; H, 5.28.

General Procedure for Protonation Experiments to Determine Ligand Effects

(Table 2.1):

In a glovebox, [(RPPPR')PtMe][BF₄] (0.006 mmol) and [Ph₂NH₂][BF₄] (0.06 mmol) were weighed out and placed into a glass scintillation vial. In a separate vial, NCC₆F₅ (0.06 mmol) was dissolved in dichloromethane (0.01 M in [(RPPPR')PtMe][BF₄]). [(RPPPR')PtMe][BF₄] and [Ph₂NH₂][BF₄] were dissolved in the nitrile solution and transferred to a sealed NMR tube which was immediately immersed in liquid nitrogen (the reaction was frozen from the time of addition until placement inside the probe, ~10 minutes). Upon warming to room temperature, the reaction was placed inside the NMR probe and monitored at 25(1) °C by ³¹P-NMR (observing the disappearance of Pt-Me and formation of Pt-NCC₆F₅) until completion.

General Procedure for Kinetic Experiments to Determine Order in [Ph₂NH₂][BF₄], NCC₆F₅ and **2**:

In a glovebox, [(EtPPP)PtMe][BF₄] (0.006 mmol) and [Ph₂NH₂][BF₄] (1.5, 5, 7.5, or 10 equivalents) were weighed out and placed into a glass scintillation vial. More than 10 equivalents of [Ph₂NH₂][BF₄] could not be used due to solubility problems of [Ph₂NH₂][BF₄] in dichloromethane. In a separate vial, NCC₆F₅ or **2** (5, 10, or 20 equivalents) was dissolved in 600 µL of dichloromethane. Pseudo first order conditions (10 equivalents of reagent not in question) were used to determine the order in [Ph₂NH₂][BF₄], NCC₆F₅ and **2**. The solution of nitrile or **2** (0.01 M in [(EtPPP)PtMe][BF₄]) was added to [(EtPPP)PtMe][BF₄] and [Ph₂NH₂][BF₄] and transferred to a sealed NMR tube which was immediately immersed in liquid nitrogen.

Upon warming to room temperature, the reaction was placed inside the NMR probe at 25.0(5) °C and monitored by ^{31}P -NMR for the formation of $[(\text{EtPPP})\text{Pt-NCC}_6\text{F}_5][\text{BF}_4]_2$ or **3**.³¹

General Procedure for Base Inhibition Experiments:

For Ph_2NH inhibition experiments, the desired amount of base (0, 1, 2.5, 5, or 10 equivalents) was weighed and added to a vial containing $[(\text{EtPPP})\text{PtMe}][\text{BF}_4]$ (0.006 mmol) and $[\text{Ph}_2\text{NH}_2][\text{BF}_4]$ (0.06 mmol). Base inhibition experiments were performed using 10 equivalents of $[\text{Ph}_2\text{NH}_2][\text{BF}_4]$ and nitrile (0.06 mmol). $[(\text{EtPPP})\text{PtMe}][\text{BF}_4]$, base, and $[\text{Ph}_2\text{NH}_2][\text{BF}_4]$ were dissolved in the nitrile solution (0.01 M in $[(\text{EtPPP})\text{PtMe}][\text{BF}_4]$) and transferred to a sealed NMR tube which was immediately immersed in liquid nitrogen. Upon warming to room temperature, the reaction was placed inside the NMR probe at 25.0(5) °C and monitored by ^{31}P -NMR for approximately 2.5 hours for the formation of $[(\text{EtPPP})\text{Pt-NCC}_6\text{F}_5][\text{BF}_4]_2$.

Procedures for Deuterium and Low Temperature Studies:

Preparation of $[(\text{EtPPP})\text{Pt}(\text{CD}_3)][\text{BF}_4]$, (1- d_3**):** Prepared in a manner similar to $[(\text{EtPPP})\text{PtMe}][\text{BF}_4]$ described above only using methyl- d_3 -lithium to synthesize the precursor (COD) $\text{Pt}(\text{Me-}d_3)\text{Cl}$ compound. Isolated as a white solid 195.3 mg (89%); ^1H NMR (400 MHz, CDCl_3): δ 7.65 (m, 4 H); 7.54 (m, 6 H); 7.40 (m, 10 H); 3.36 (m, 2 H); 2.67 (m, 4 H); 2.14 (m, 2 H); 1.89 (m, 2 H); 0.98 (m, 3 H). $^{31}\text{P}\{^1\text{H}\}$ NMR (161.8 MHz, CDCl_3): δ 97.8 (s, $^3J_{\text{Pt-P}} = 1465$ Hz, 1P); 43.8 (s, $^3J_{\text{Pt-P}} = 2775$ Hz, 2P).

³¹ Reactions to determine order in NCC_6F_5 and $[\text{Ph}_2\text{NH}_2][\text{BF}_4]$ were only monitored for approximately two hours to avoid the observed rate decrease (at later times) due to buildup of Ph_2NH upon protonation of $[(\text{EtPPP})\text{PtMe}][\text{BF}_4]$ by $[\text{Ph}_2\text{NH}_2][\text{BF}_4]$.

Protonation of 1-*d*₃ with [Ph₂NH₂][BF₄]: In a glovebox, 1-*d*₃ (0.013 mmol) and [Ph₂NH₂][BF₄] (0.13 mmol) were weighed out and placed into a glass scintillation vial. In a separate vial, pentafluorobenzonitrile (0.13 mmol) was dissolved in dichloromethane (0.01 M in 1-*d*₃). Compound 1-*d*₃ and [Ph₂NH₂][BF₄] were dissolved in the nitrile solution and transferred to a sealed NMR tube (almost no headspace so to avoid loss of CD₃H) which was immediately immersed in liquid nitrogen (the reaction was frozen from the time of addition until placement inside the probe, ~10 minutes). Upon warming to room temperature, the reaction was placed inside the NMR probe and monitored at 25(1) °C by ¹H-NMR for the exclusive formation of CD₃H.

General Procedures for Low Temperature Studies:

In a glovebox, [(PPP)PtMe][BF₄] or [(EtPPP)PtMe][BF₄] (0.006 mmol) was weighed out and placed into a glass scintillation vial. In a separate vial, pentafluorobenzonitrile (0.06 mmol) was dissolved in 450 μL of dichloromethane. The corresponding Pt-Me compound was dissolved in the nitrile solution and transferred to an NMR tube sealed with a rubber septum, removed from the glovebox and cooled to -78 °C. A separate solution of 0.012 mmol acid (HOTf or HNTf₂) in 150 μL of dichloromethane was also prepared inside the glovebox in a sealed vial (rubber septum), removed from the glovebox and cooled to -78 °C. The acid solution was quickly transferred to the solution of Pt-Me and nitrile and kept at -78 °C. The reaction was placed inside the NMR probe at -80 °C and warmed until reactivity was observed by ³¹P-NMR (monitoring the disappearance of Pt-Me and formation of Pt-OTf for HOTf or Pt-NCC₆F₅ for HNTf₂) until completion.

Chapter 3

Reversibility in Pt(II)-Mediated Polycyclizations

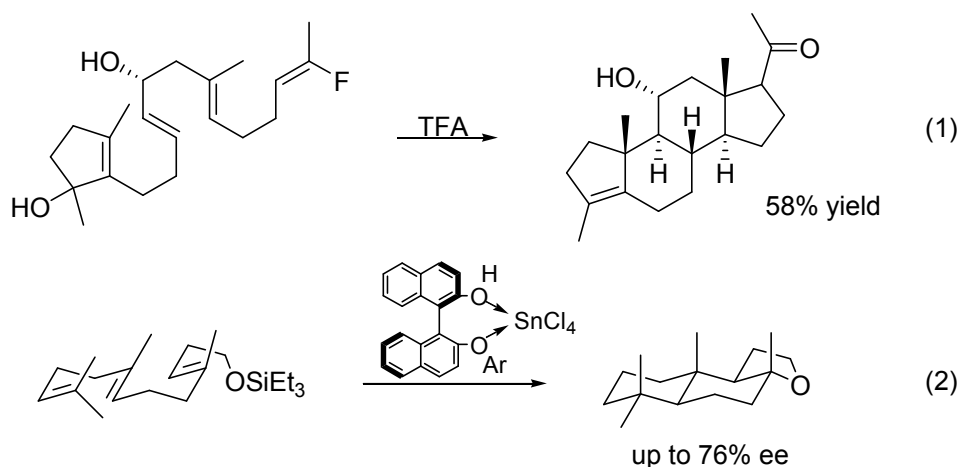
3.1 Introduction

As previously described in Chapter 1, Section 1.1, the ability to control polyene cascade cyclizations with the same efficiency and selectivity as enzymes has been of great interest to synthetic chemists.¹ The greatest challenge to overcome when performing nonenzymatic polycyclizations is controlling diastereo- and enantioselectivity. Two examples of success in this area are depicted in equations 1 and 2. The first reaction shows the cyclization of a monocyclic tetraene to a tetracyclic product with five new asymmetric carbon centers using trifluoroacetic acid in moderate yields.² The second reaction, described recently by Yamamoto, shows the use of a chiral Brønsted-Lewis acid to generate a tricyclic product with good enantioselectivity.³

¹ (a) Sutherland, J. K. In *Comprehensive Organic Synthesis*; Trost, B. M., Ed.; Pergamon Press: 1991; Vol. 1, p 341-377. (b) Wendt, K. U.; Shultz, G. E.; Corey, E. J.; Liu, D. R. *Angew. Chem. Int. Ed.* **2000**, *39*, 2812-2833. (c) Bartlett, P. A. In *Asymmetric Synthesis*; Morrison, J. D., Ed.; Academic Press: New York, 1984; Vol. 3, p 341-409.

² Johnson, W. S; Lyle, T. A.; Daub, G. W. *J. Org. Chem.* **1982**, *47*, 161-163.

³ Ishihara, K.; Ishibashi, H.; Yamamoto, H. *J. Am. Chem. Soc.* **2002**, *124*, 3647-3655.



While the ability to perform stereoselective nonenzymatic cyclizations is quite impressive, these examples raise the question: how is selectivity achieved without a defined cavity to encourage polyene preorganization as is the case with enzymes? The answer to this question is not simple nor is it completely solved, and studies in this area, including the results presented here, are ongoing.⁴ While more details are described in the following sections, a brief explanation of the selectivities observed in previous polycyclizations is given here.

Figure 3.1 shows a generic bicyclization where four stereorelationships are defined. The dictation of diastereoselectivity (ring fusion, centers A and B) for the cyclization of polyenes is in most cases predicted by the Stork-Eschenmoser (S-E) postulate which states that the ring junction formed in a cyclization reaction is determined by the geometry of the starting alkene. *E*-alkenes give *trans*-ring junctions while *Z*-alkenes give predominantly *cis*-ring junctions.⁵ Other relationships including adjacent ring orientations (centers A and C), ring substituents (R and R') and the stereochemistry

⁴ Yoder, R. A.; Johnston, J. N. *Chem. Rev.* **2005**, 105, 4730-4756 and references within.

⁵ (a) Stork, G.; Burgstahler, A. W. *J. Am. Chem. Soc.* **1955**, 77, 5068-5077. (b) Eschenmoser, A.; Ruzika, L.; Jeger, O.; Arigoni, D. *Helv. Chim. Acta.* **1955**, 38, 1890-1904.

defined by termination (center D) are controlled by several factors.^{1c} These factors include but are not limited to: the initiating electrophile, the terminating group, rigidity of carbocations prior to termination, and more importantly interactions observed in cyclization transition states.^{1c}

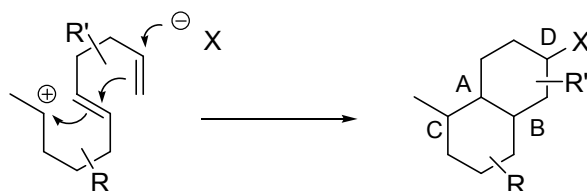


Figure 3.1. Stereorelationships defined by polyolefin cyclization.^{1c}

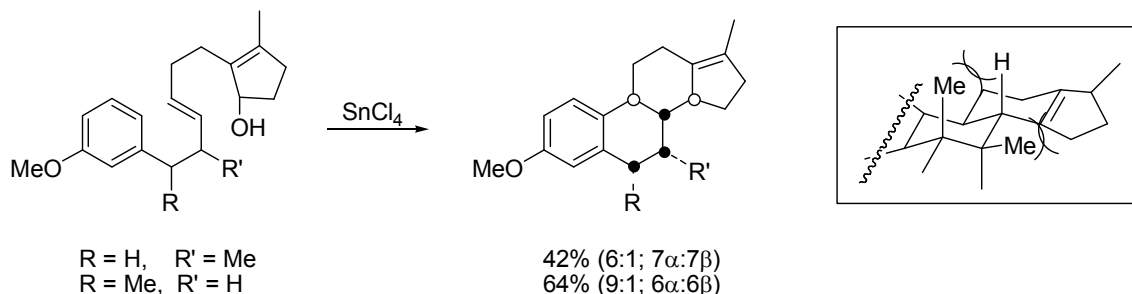
One example of substituent effects on stereochemistry relevant to the studies addressed here is shown in Scheme 3.1. Substituents positioned on the A-ring are known to aid in stereocontrol of the entire polycyclization simply because these effects are coming into play early on as the first ring is being formed.⁶ If substituents on other rings affect the overall stereochemistry of cyclization, it may be inferred that the cyclization is by some degree concerted. The example in Scheme 3.1 of B-ring substituents affecting stereochemistry was reported in which achiral polyenes were cyclized to give tetracyclic products with high diastereoselectivity.⁷ In the case of Me substitution in the 7 position, the high diastereoselectivity (6:1; 7 α :7 β) was attributed to the interaction in the transition state between an equatorial Me and the cyclopentene ring, resulting in a preferred axial orientation of the Me group. Surprisingly, the methyl group in the 6 position on the B-ring surprisingly was still extremely stereoselective (9:1; 6 α :6 β) even though it was one

⁶ (a) Lansbury, P. T.; Briggs, P. C.; Demmin, T. R.; DuBois G. E. *J. Am. Chem. Soc.* **1971**, 93, 1311-1313. (b) Lansbury, P. T.; Demmin, T. R.; DuBois, G. E.; Haddon V. R. *J. Am. Chem. Soc.* **1975**, 97, 394-403. (c) Lansbury, P. T.; DuBois, G. E. *Chem. Commun.* **1971**, 1107-1108. (d) Julia, M.; Fourneron, J. D. *Tetrahedron* **1976**, 32, 1113-1116.

⁷ Marinus B.; Groen, M. B.; Zeelen, F. J. *J. Org. Chem.* **1978**, 43, 1961-1964.

carbon more removed than the double bond, but again, interactions in the transition state of a concerted cyclization would explain the observed diastereoselectivity.

Scheme 3.1

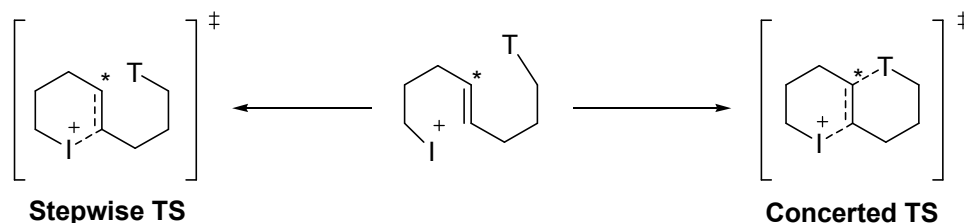


Stereochemistry is also determinant on the nature of the cyclization, be it stepwise or concerted. By nature, concerted reactions are usually stereospecific while stepwise reactions are mostly unselective.⁸ The mode of cyclization (concerted or stepwise) depends on the free energy of formation of the transition state. If the initiating group is a stabilized carbocation, then a considerable degree of bond formation is required to reach the transition state. This results in a concerted cyclization since significant positive charge buildup at C* forces the terminating group to aid in the stabilization of charge buildup in the transition state (Scheme 3.2).^{1c} The drawback for a concerted cyclization is the highly ordered transition state required for cyclization, which is disfavored entropically and normally limits stereospecific concerted cyclizations to mono- and

⁸ For examples of stereospecific concerted reactions see: (a) Koster, F. H.; Wolf, H. *Tetrahedron Lett.* **1981**, 22, 3937-3940. (b) Johnson, W. S.; Harding, K. E. *J. Org. Chem.* **1967**, 32, 478-479. (c) Johnson, W. S.; Lunn, W. H.; Fitz, K. *J. Am. Chem. Soc.* **1964**, 86, 1972-1978. (d) Van Tamelen, E. E.; Schwartz, M. A.; Hessler, E. J.; Storni, A. *Chem. Commun.* **1966**, 409-411. For nonselective stepwise cyclizations, see reference 5. For an example of a selective stepwise cyclization see: Nishizawa, M.; Takenaka, H.; Hayashi, Y. *J. Am. Chem. Soc.* **1985**, 107, 522-523.

bicyclizations.⁹ On the other hand, if there is little charge build up at C*, or if the terminating group is a poor nucleophile, then the cyclization is often stepwise in nature.^{1c}

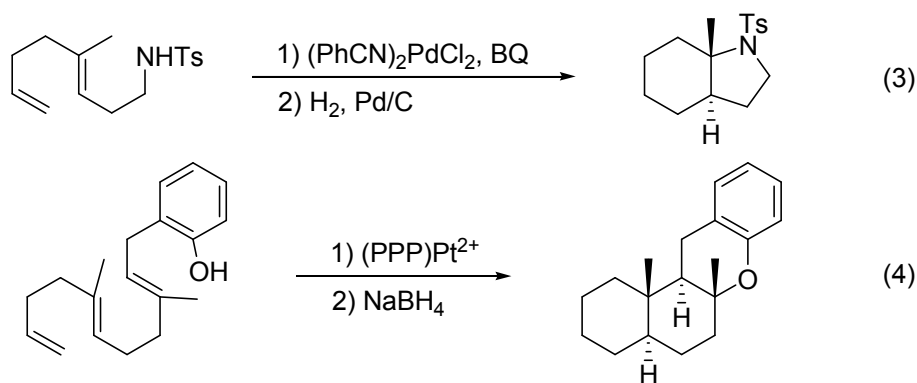
Scheme 3.2^{1c}



Recent studies on electrophilic Pt(II) and Pd(II) complexes showed that these compounds efficiently initiated polyolefin cyclizations, preferentially activating terminal (monosubstituted) olefins in polyolefin starting materials.¹⁰ This preference for olefin coordination is opposite that of the electrophiles used to initiate the reactions described above. In polycyclizations using PdCl₂ or (PPP)Pt²⁺, the products are predominantly composed of a *trans* ring juncture (eqs. 3 and 4).^{10g,h} These reactions were found to be quite diastereoselective, suggesting that they were concerted (though not likely synchronous) cyclizations. However, polycyclizations which were terminated by cyclopropanation, had been shown to be stepwise and putative cationic intermediates had been trapped with benzyl alcohol (Scheme 4.1, Chapter 4).^{10a} Studies on carbocation trapping showed kinetic evidence for reversibility in Pt(II) initiated diene cycloisomerizations although no direct observations of the equilibrating species was made.

⁹ Prestwich, G. D.; Labovitz, J. N. *J. Am. Chem. Soc.* **1974**, *96*, 7103-7105.

¹⁰ (a) Kerber, W. D.; Gagné, M. R. *Org. Lett.* **2005**, *7*, 3379-3381. (b) Kerber, W. D.; Koh, J. H.; Gagné, M. R. *Org. Lett.* **2004**, *6*, 3013-3015. (c) Cucciolito, M. E.; D'Amora, A.; Vitagliano, A. *Organometallics* **2005**, *24*, 3359-3361. (d) Hahn, C. *Chem. Eur. J.* **2004**, *10*, 5888-5899. (e) Hahn, C.; Morvillo, P.; Herdtweck, E.; Vitagliano, A. *Organometallics* **2002**, *21*, 1807-1818. (f) Hahn, C.; Morvillo, P.; Vitagliano, A. *Eur. J. Inorg. Chem.* **2001**, 419-429. (g) Koh, J. H.; Mascarenhas, C.; Gagné, M. R. *Tetrahedron* **2004**, *60*, 7405-7410. (h) Koh, J. H.; Gagné, M. R. *Angew. Chem. Int. Ed.* **2004**, *43*, 3459-3461.



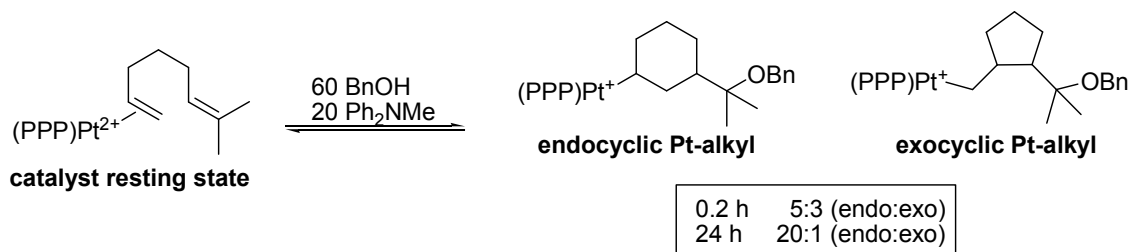
While examining the effects of ligand variations on $(\text{PPP})\text{Pt}(\text{II})$ -mediated cyclizations, an intriguing result was obtained. Using the electron rich EtPPEt ligand (see Chapter 2 for nomenclature), an equilibrium between the Pt-olefin complex and the cyclized Pt-alkyl was directly observed. The first section of this chapter discusses the variables which control electrophilic Pt(II)-initiated reversible cyclizations. The stereochemical consequences of bi- and tricyclization with polyenol substrates including medium range stereocontrol are also discussed.

3.2 Results and Discussion

A. Factors Governing Reversibility. In previous examples of $(\text{PPP})\text{Pt}(\text{II})$ -mediated cyclizations, the alkene activation/cyclization appeared to be rapid, generating very stable Pt-alkyl complexes.^{10g,h} The initiation/cyclization step was also fast in the case of catalytic cyclizations which produced bicyclopropanes from 1,6- and 1,7-dienes.^{10a,b} In an attempt to trap a carbocationic Pt-alkyl in the cyclopropanation systems, excess BnOH and Ph_2NMe were added to convert the catalyst resting state (Pt-olefin) to a mixture of endo- and exocyclic Pt-alkyls (Scheme 3.3).^{10a} Over time, the mixture of Pt-alkyls slowly converged to the endocyclic Pt-alkyl, consistent with a scenario in which

cyclization is both rapid and reversible.^{10a} While kinetic evidence for this reversibility was presented, the equilibrating species were not observed.

Scheme 3.3



While studying the effects of metal electrophilicity on cyclization, a startling observation was made. Following protonolysis of $[(EtPPP)PtMe][BF_4]$ with $[Ph_2NH_2][BF_4]$, cyclization of a 1,5-dienyl sulfonamide (**1**) gave a mixture of three compounds by ³¹P NMR. The *trans* J_{Pt-P} couplings suggested that these species were the $Pt(\eta^2\text{-alkene})$ (**A**; $J_{Pt-P} = 2762$ Hz), the Pt-alkyl (**B**; $J_{Pt-P} = 1281$ Hz), and some Pt-Cl (**C**; $J_{Pt-P} = 3030$ Hz) as shown in equation 5 and Figure 3.2. Compound **A** was unexpected because all previous studies involving dienyl substrates with intramolecular carbocation traps had shown that cyclization rapidly formed a Pt-alkyl. After one hour a ~1:2 ratio of $Pt(\eta^2\text{-alkene})$ ¹¹ (**A**) to Pt-alkyl (**B**) was observed by ³¹P NMR. At later times, the ³¹P NMR spectrum became more complex as chloride abstraction from the solvent generated $(EtPPP)PtCl$, among other decomposition species.¹² Although decomposition occurred, an equilibrium constant was measured at early times and estimated to be ~60.

¹¹ The $Pt(\eta^2\text{-alkene})$ is observed in a 2:1 ratio which correlates to the *E*:*Z* ratio of diene **1**. The complex upfield splitting of the $Pt(\eta^2\text{-alkene})$ is presumably a result of hindered rotation of the bound olefin by the terminal phosphine substituents. The same splitting pattern is observed in $[(EtPPP)Pt(1\text{-hexene})][BF_4]_2$.

¹² (a) Liaw, B.; Lobana, T. S.; Lin, Y.; Wang, J.; Liu, C. W. *Inorg. Chem.* **2005**, *44*, 9921-9929. (b) Angulo, I. M.; Bouwman, E.; Lok, S. M.; Lutz, M.; Mul, W. P.; Spek, A. L. *Eur. J. Inorg. Chem.* **2001**,

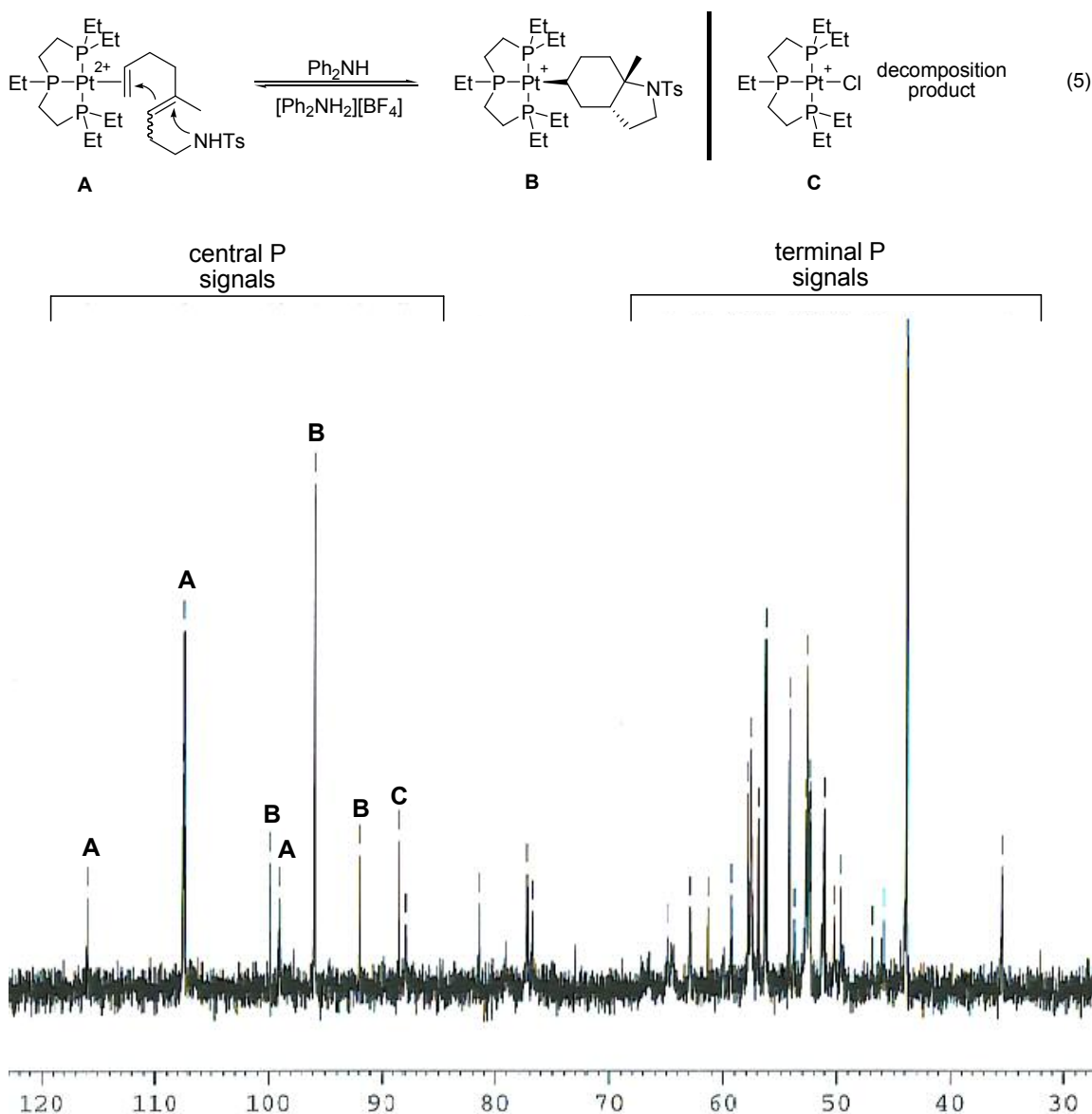


Figure 3.2. ^{31}P NMR of cyclization of **1** with $(\text{EtPPPEt})\text{Pt}^{2+}$ in CH_2Cl_2 .

From this starting point, an investigation into the factors controlling cyclization was undertaken. A solvent screen was performed in an attempt to find a less reactive solvent.

Using $[(\text{EtPPPEt})\text{PtMe}][\text{BF}_4]^{13}$ as the precursor to the cyclization initiator, cyclization of

1465-1473. (c) Oster, S. S.; Lachicotte, R. J.; Jones, W. D. *Inorg. Chim. Acta* **2002**, 330, 118-124. (d) Wang, Q.; Marr, A. C.; Blake, A. J.; Wilson, C.; Schröder, M. *Chem. Commun.* **2003**, 2776-2777.

¹³ Protonolysis of the precursor Pt-Me with $[\text{Ph}_2\text{NH}_2][\text{BF}_4]$ to give $(\text{EtPPPEt})\text{Pt}^{2+}$ is rapid (<10 min), see: Feducia, J. A.; Campbell, A. N.; Anthis, J. W.; Gagné, M. R. *Organometallics* **2006**, 25, 3114-3117.

1 in various solvents showed that more polar solvents favored the dicationic Pt(η^2 -alkene) complex over the monocationic Pt-alkyl (Table 3.1). Fortunately, the solvent halide abstraction previously observed in dichloromethane could be avoided in other solvents. Several additional polar aprotic solvents were tested, however, studies were limited to the four shown in Table 3.1 due to the limited solubility of [Ph₂NH₂][BF₄]. Nitromethane ($K_{eq} = 0.68$; Figure 3.3) was selected for further analysis of this equilibrium since cyclization in this solvent favored the Pt-olefin complex. The equilibrium constant was calculated from the following equation where [Pt-alkyl] and [Pt(η^2 -alkene)] were obtained from ³¹P NMR:¹⁴

$$K_{eq} = \frac{[\text{Pt-alkyl}][\text{Ph}_2\text{NH}_2^+]}{[\text{Pt}(\eta^2\text{-alkene})][\text{Ph}_2\text{NH}]}$$

Table 3.1. Solvent effects on the cyclization of **1** with (EtPPPEt)Pt²⁺.^a

Entry	Solvent	K_{eq} ^b	ΔG (kcal/mol)
1	CH ₂ Cl ₂ ^c	60	-2.0
2	ClCH ₂ CH ₂ Cl ^c	110	-2.8
3	EtNO ₂	3.2	-1.9
4	MeNO ₂	0.68	0.23

^a Reaction conditions: [Pt] = 0.027 M, [Ph₂NH₂][BF₄] = 0.27 M, [**1**] = 0.27 M, 25(1) °C. ^b Relative concentrations determined by ³¹P NMR. Average of three measurements. ^c [Pt] = 0.012 M.

¹⁴ [Pt] was obtained by determining the ratio of Pt-alkyl:Pt(η^2 -alkene) by ³¹P NMR. The concentration of acid and base were calculated from the ratio of Pt-alkyl:Pt(η^2 -alkene). 100% cyclization would result in 10 equiv. of acid present in solution while 0% cyclization would result in 9 equiv. of acid and 1 equiv. of base.

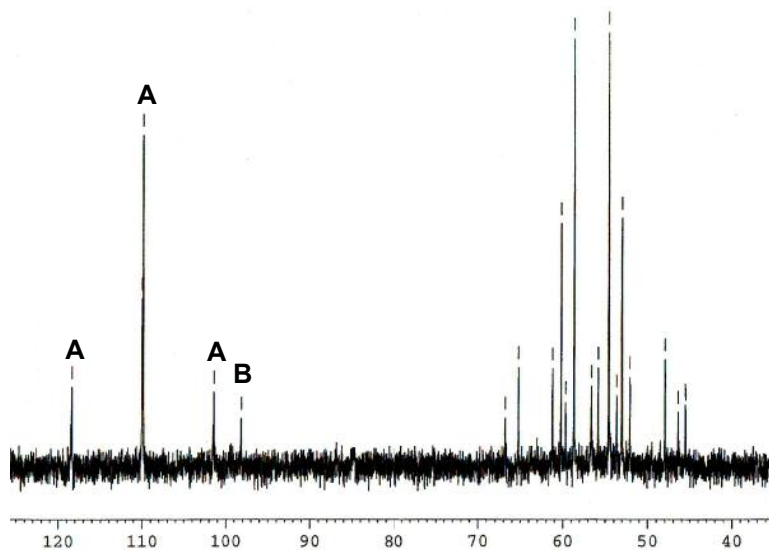


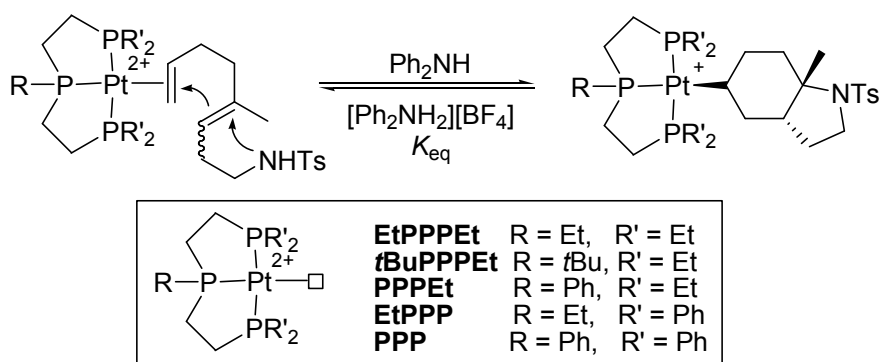
Figure 3.3. ^{31}P NMR of cyclization of **1** with $(\text{EtPPPEt})\text{Pt}^{2+}$ in MeNO_2 .

Since previous reports with more electron poor PPP ligands showed no signs of reversibility for the cyclization reaction (eq. 5), the effect of ligand substituents on the equilibrium constant were systematically studied in nitromethane.¹⁵ By modifying the donor properties of the phosphine substituents, the electrophilicity of the metal center could be systematically tuned, as shown with the protonation studies from Chapter 2. Table 3.2 shows the results from this analysis. As expected, less basic ligands shift the cyclization equilibrium towards the cyclized monocationic Pt-alkyl species. The more electron withdrawing ligands are expected to increase the electrophilicity of the η^2 -coordinated alkene, favoring the cyclized product. One interesting observation from this ligand screen was the minimal effect of the bulky *tert*-butyl group on the cyclization equilibrium. As previously reported (Chapter 2, Table 2.1), $[(t\text{BuPPPEt})\text{PtMe}][\text{BF}_4]$ had a slower rate of protonolysis than the analogous complex with PPPEt as the supporting ligand even though *t*BuPPPEt should be more electron donating. This was rationalized

¹⁵ While using **1** as a trapping ligand during protonolysis studies, there was no observation of a $\text{Pt}(\eta^2\text{-alkene})$ when using PPP or EtPPP as the supporting ligand.

by the encumbrance of the Pt center by the *t*Bu substituent at the central phosphine. However, the trend shown in Table 3.2 indicates that the steric bulk in the central position had little effect on the cyclization equilibrium. While no Pt(η^2 -alkene) species (<5%) was detected with (PPP)Pt²⁺, the detectable limit of reversibility was observed using EtPPP as the tridentate ligand ($K_{eq} = 1100$; Figure 3.4).

Table 3.2. Ligand effects on the cyclization of **1** with (RPPPR')Pt²⁺.^a



Entry	Solvent	K_{eq}^b	ΔG (kcal/mol)
4	EtPPPEt	0.68	0.23
5	<i>t</i>BuPPPEt	7.2	-1.2
6	PPPEt	14	-1.6
7	EtPPP	1100	-4.1
8	PPP	>4200	< -4.9

^a Reaction conditions: [Pt] = 0.027 M, [Ph₂NH₂][BF₄] = 0.27 M, [**1**] = 0.27 M, 25(1) °C.

^b Relative concentrations determined by ³¹P NMR. Average of three measurements.

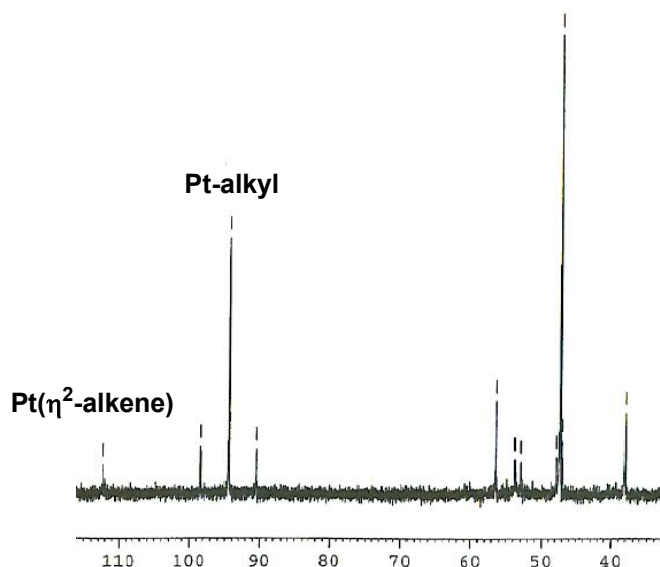


Figure 3.4. ^{31}P NMR of cyclization of **1** with $(\text{EtPPP})\text{Pt}^{2+}$ in MeNO_2 .

Based on the cyclization reaction, it is anticipated that stronger bases should drive the equilibrium more towards the cyclized product and that stronger acids should promote retrocyclization to the $\text{Pt}(\eta^2\text{-alkene})$ complex. Experiments to confirm this were limited to bulky diaryl ammonium acids since the conjugate bases of smaller, more electron rich ammonium acids function as ligands for $\text{Pt}(\text{II})$ and therefore poison cyclization reactions. With $(\text{EtPPPEt})\text{Pt}^{2+}$, the K_{eq} using $[\text{Ph}_2\text{NH}_2][\text{BF}_4]$ was found to be 0.68 (Table 3.1). When this acid was replaced with the less acidic $[\text{Ph}_2\text{NMeH}][\text{BF}_4]$, the equilibrium shifted towards the Pt-alkyl (**B**; eq. 5) demonstrating that the stronger base, Ph_2NMe , promoted cyclization more effectively than Ph_2NH as anticipated ($K_{\text{eq}} = 11$).

Adding base or acid to a preequilibrated system shifted the ratios of **A** and **B** in an expected fashion, demonstrating that a true equilibrium existed. As detailed in Table 3.3, addition of 5 equivalents of Ph_2NH to a system with **A** as the predominant species (entry 4, Table 3.1) decreased the ratio of **A**:**B** from 14:1 to almost 2:1. Using $(\text{EtPPP})\text{Pt}^{2+}$ to mediate the cyclization of **1** gave an equilibrium that favored the Pt-alkyl . Addition of

acid to this mixture resulted in a decrease in the concentration of the Pt-alkyl species relative to the Pt(η^2 -alkene).

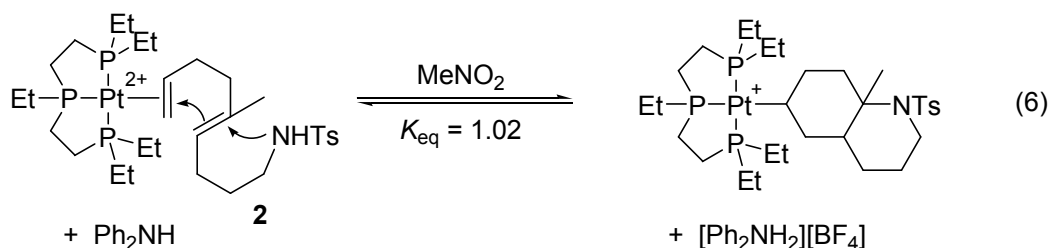
Table 3.3. Acid or base additive effects on the cyclization of **1**.^a

Entry	Additive	A : B
4	None	4 : 1
4*	Ph ₂ NH	1.6 : 1
7	None	1 : 10
7*	Ph ₂ NH ₂ ⁺	1 : 4

^a Reaction conditions: [Pt] = 0.027 M, [Ph₂NH₂][BF₄] = 0.27 M, [1] = 0.27 M, 25(1) °C. ^b Relative concentrations determined by ³¹P NMR. Average of three measurements.

Similar to the other factors examined (solvent polarity, electrophilicity of Pt, and acid/base strength), it was anticipated that ring strain in the cyclized organic moiety would also effect the equilibrium in a predictable manner. To investigate this factor, the dienyl sulfonamide substrate **2**, in which the bicyclic product had a less-strained 6,6 ring structure upon cyclization was subjected to reversible conditions using (EtPPPEt)Pt²⁺. The less strained aza-decalin structure shifted the equilibrium to the cyclized complex ($K_{eq} = 1.02$; eq. 6). The magnitude of the shift was considerably less than expected, perhaps as a result of the fact that the product of the 6,5 bicyclic fragment was *cis*-fused and the 6,6 was *trans*-fused (*vide infra*). The difference in K_{eq} was predicted to be larger since the strain energy associated with *cis*-hydrindan is 6.3 kcal/mol whereas the strain energy calculated for *trans*-decalin is -1.9 kcal/mol, a difference of over 8 kcal/mol.¹⁶

¹⁶ (a) Wiberg, K. B. *Angew. Chem. Int. Ed.* **1986**, 25, 312-322. (b) Allinger, N. L.; Tribble, M. T.; Miller, M. A.; Wertz, D. H. *J. Am. Chem. Soc.* **1971**, 93, 1637-1648.



In summary, these studies explored a number of variables that influenced the driving force for (PPP)Pt²⁺ mediated polycyclization reactions. These variables included solvent polarity, metal electrophilicity, acid strength, and ring strain in the bicyclic products. In the existing equilibrium between a Pt(η^2 -alkene) and a Pt-alkyl, cyclization was favored by less polar solvents, more electrophilic metal centers, weaker acids, and a less strained bicyclic product. The data presented here provided a semi-quantitative description of the magnitude of these effects. Establishing the governing factors that govern the reversible cyclization reaction could guide further studies on the stereochemical consequences of cation-olefin polycyclizations.

B. Stereocontrol in Reversible Polycyclizations. Since diene **1** is a 2:1 mixture of *E* and *Z* isomers, generation of a mixture of two diastereomeric Pt-alkyls, one with a *trans* ring juncture and one with a *cis* ring juncture, should be possible. The results presented in section 3.2 showed only one Pt-alkyl was observed by ³¹P NMR. Two possibilities were considered to explain the formation of only a single alkyl: 1) only one isomer is cyclized to generate the observed alkyl in a concerted mechanism,¹⁷ or 2) that the sulfonamide is a poor nucleophilic trap and therefore a discrete 3° carbocation exists prior to C-N bond formation allowing for thermodynamic control over the cyclization (i.e. nonconcerted B-ring formation).

¹⁷ DFT calculations on a 1,6-dienyl phenol indicated that in the presence of base, cyclization was semi-concerted. Nowroozi-Isfahani, T.; Musaev, D. G.; Morokuma, K.; Gagné, M. R. accepted to *Organometallics*.

The structure of the Pt-alkyl was identified by X-ray crystallography of the PPP analog. Figure 3.5 is an ORTEP representation of the Pt-alkyl cation (**3**)¹⁸ and clearly shows a *cis* ring juncture for the bicyclic fragment; contrary to the *trans* bicyclic products typically obtained from catalytic and stoichiometric cyclizations.^{10g,h} To rule out the possibility of selective concerted cyclization of the *Z* isomer to give **3** (following the Stork-Eschenmoser postulate), the *E* isomer was synthesized and subjected to cyclization conditions. The Pt-alkyl obtained from this reaction was the same by ³¹P NMR, indicating that the isomer of product formed did not depend on the *E/Z* ratio of the starting diene. More importantly, this result indicated that the cyclization of **1** involved a stepwise formation of the A/B-ring structure in the Pt-alkyl.

¹⁸ This structure displays the largest C-P-C angle deviations for PPP at the central phosphorus (117.0°). For a discussion see reference 11.

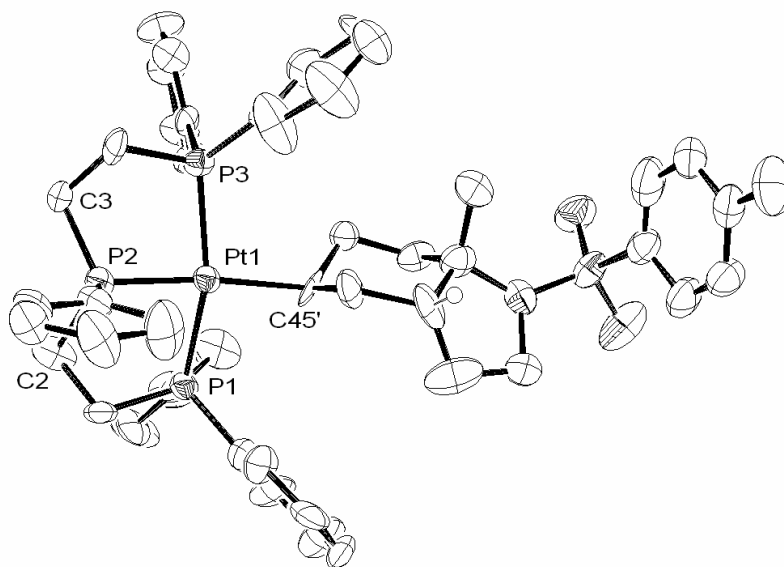
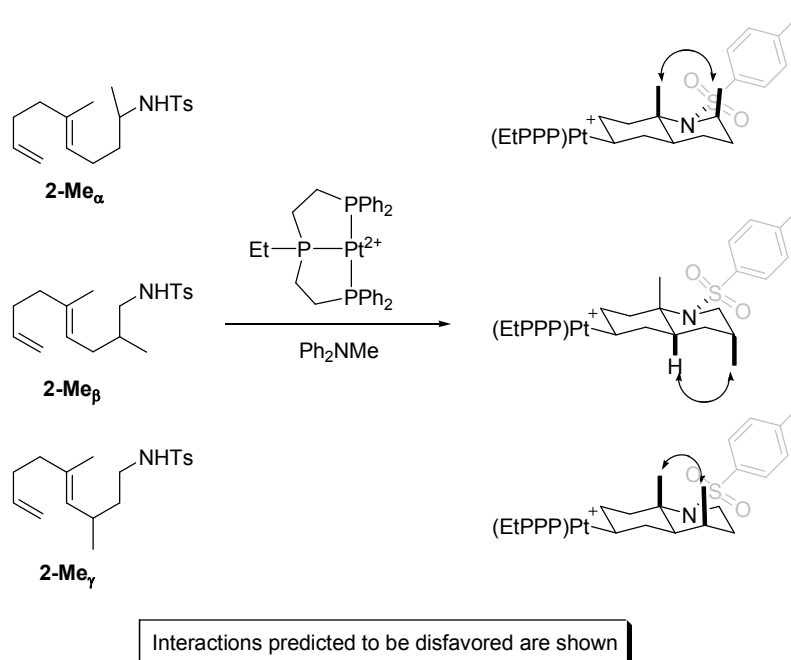


Figure 3.5. ORTEP representation of **3**. Hydrogen atoms and BF_4^- counter ion omitted for clarity. Selected bond lengths (Å): Pt-P₁ = 2.269(4), Pt-P₂ = 2.247(3), Pt-P₃ = 2.308(4), Pt-C₄₅ = 2.150(1). Selected bond angles (deg): P₁-Pt-P₂ = 84.51(16), P₂-Pt-P₃ = 84.63(16), P₁-Pt-C₄₅ = 92.2(4), P₃-Pt-C₄₅ = 100.6(4), C₃-P₂-C₂ = 117.0(6).

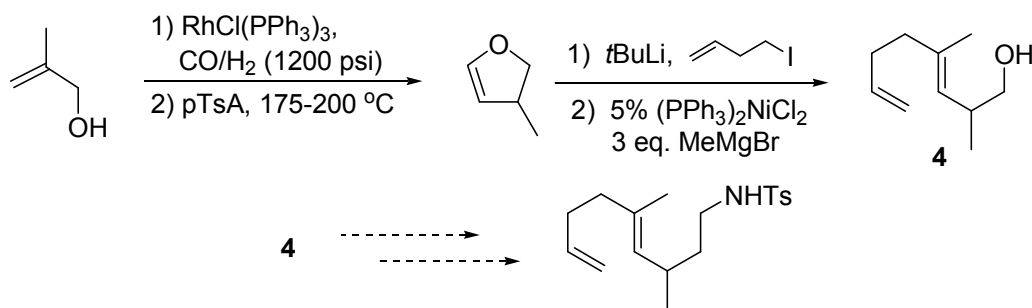
Returning to the idea of using reversibility of the cyclization reaction to correct errors in cascade cyclizations, substrates with substitution on the B-ring were targeted. Initially, the goal was to synthesize B-ring methyl substituted analogs of **2**. These substrates were selected because the proposed kinetic product of cyclization would be a *trans* aza-decalin structured Pt-alkyl, in which significant diaxial interactions (Scheme 3.4) could lead to a mixture of diastereomers. Under thermodynamic control with less electrophilic (RPPPR')Pt²⁺ complexes, this mixture would be expected to converge to the most thermodynamically stable Pt-alkyl.

Scheme 3.4

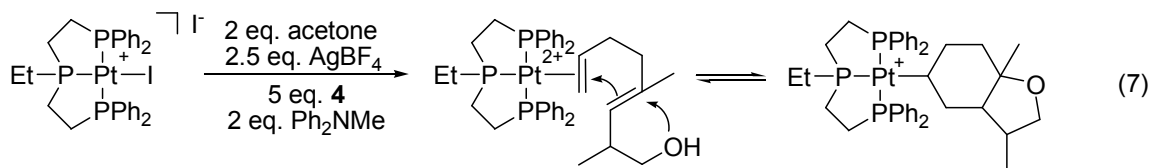


Unfortunately, synthesis of these substrates proved difficult and cyclization attempts with **2-Me_α** (Scheme 3.4) only led to formation of the Pt(η^2 -alkene) species by ^{31}P NMR. Along the synthetic pathway to synthesizing **2-Me_γ**, a methyl substituted dienyl alcohol (**4**) was isolated (Scheme 3.5). A surprising observation was made when **4** was reacted under reversible conditions with $[(\text{EtPPP})\text{PtMe}][\text{BF}_4]$ and 10 equivalents of $[\text{Ph}_2\text{NH}_2][\text{BF}_4]$. Intuition built up from the previous studies examining the factors of reversibility would have predicted a larger K_{eq} because of the good nucleophilic trap present in the substrate (-OH) and the use of a more electron withdrawing ligand (EtPPP, $K_{\text{eq}} = 1100$). Instead, the ^{31}P NMR spectrum indicated a mixture of Pt(η^2 -alkene) species and several peaks in the Pt-alkyl region (90-100 ppm). Over time the spectrum simplified to mostly one Pt-alkyl resonance, a small amount (~5%) of the olefin bound Pt species, and several minor products.

Scheme 3.5



In an attempt to produce a cleaner system, $[(\text{EtPPP})\text{Pt-I}][\text{I}]$ was used as the precursor to $(\text{EtPPP})\text{Pt}^{2+}$ via Ag^+ abstraction as shown in equation 7. Using this procedure, the precursor complex was completely converted to an active dicationic acetone adduct prior to addition of substrate.¹⁹ This contrasted the protonolysis activation route, which was slower and made analysis by ^{31}P NMR more difficult. When this reaction was performed, three species were observed after a few hours in the ^{31}P NMR spectrum, namely the $\text{Pt}(\eta^2\text{-alkene})$ at 100.4 ppm ($J_{\text{Pt-P}} = 2904$ Hz) and two Pt-alkyl species (90.9 ppm, $J_{\text{Pt-P}} = 1241$ Hz; 90.2 ppm, $J_{\text{Pt-P}} = 1239$ Hz) in a 1:1 ratio. Over time, the ^{31}P NMR (Figure 3.6) clearly showed conversion of the three Pt resonances to the Pt-alkyl (**5**) at 90.9 ppm. This experiment was remarkable in that it unambiguously displayed 1,6 stereoinduction in a cascade polycyclization reaction. Moreover, the selectivity was clearly a result of reversibility in the bicyclization (*vide infra*).



¹⁹ Using acetone as a trap for dicationic $(\text{PPP})\text{Pt}^{2+}$ complexes has been shown to be effective in trapping the dication prior to addition of the starting dienes, see reference 8a.

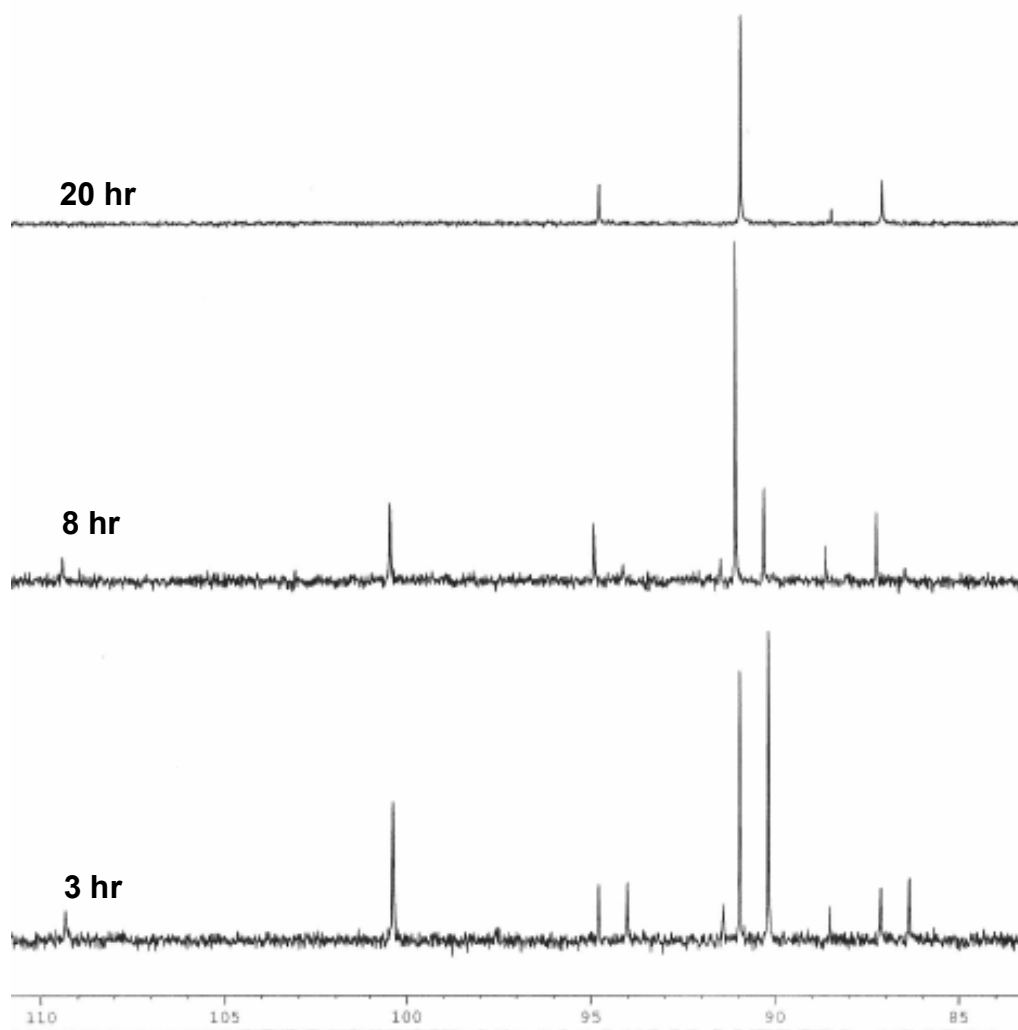


Figure 3.6. ^{31}P NMR stack plot of cyclization of **4** with $(\text{EtPPP})\text{Pt}^{2+}$.

Upon completion of this reaction, the Pt-alkyl species was isolated and characterized. Fortunately, crystals of the thermodynamic Pt-alkyl (**5**) suitable for X-ray crystallography were obtained, and the bicyclic fragment was shown to have a *cis* ring junction similar to **1** (Figure 3.7). As with **3**, complex **5** has Pt in an equatorial position on the cyclohexyl A-ring and has the heteroatom of the bicyclic fragment in a 1,4-*trans* relationship (see Figure 3.5 for comparison). The C-P-C bond angle at the central phosphorus is much

smaller in **5** (110.8°) than in **3** (117.0°) which indicates much less strain at the central phosphorus for this square planar complex.

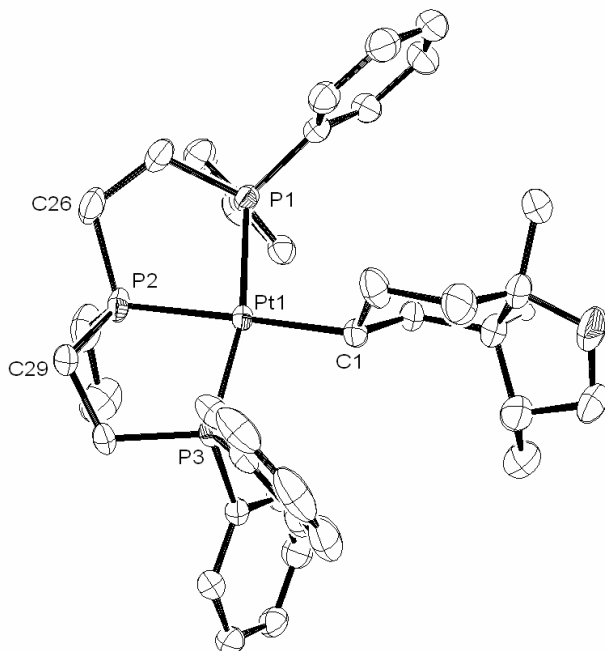


Figure 3.7. ORTEP representation of **5**. Hydrogen atoms and BF_4^- counter ion omitted for clarity. Selected bond lengths (Å): Pt-P₁ = 2.3032(8), Pt-P₂ = 2.3016(8), Pt-P₃ = 2.2722(8), Pt-C₁ = 2.134(3). Selected bond angles (deg): P₁-Pt-P₂ = 82.35(3), P₂-Pt-P₃ = 85.87(3), P₁-Pt-C₁ = 101.07(9), P₃-Pt-C₁ = 90.04(9), C₂₆-P₂-C₂₉ = 110.85(18).

Reaction of **4** with $(\text{PPP})\text{Pt}^{2+}$ was performed to identify the kinetic product of cyclization since the cyclization half-reaction was faster with the more electrophilic $(\text{PPP})\text{Pt}^{2+}$ complex. Substrate **4** underwent rapid cyclization (>20 min) to one cationic $(\text{PPP})\text{Pt}$ -alkyl product (**6**) by ^{31}P NMR (89.6 ppm, $J_{\text{Pt-P}} = 2904$ Hz). No $\text{Pt}(\eta^2\text{-alkene})$ was observed in the ^{31}P NMR. Isolation and crystallographic (X-ray) analysis of the organometallic Pt-alkyl product revealed that the kinetic product had a *trans* ring juncture (Figure 3.8). This *trans* ring juncture was also observed in previous polycyclizations

with Pt(II), suggesting that these previous studies yielded the kinetic product of cyclization.²⁰

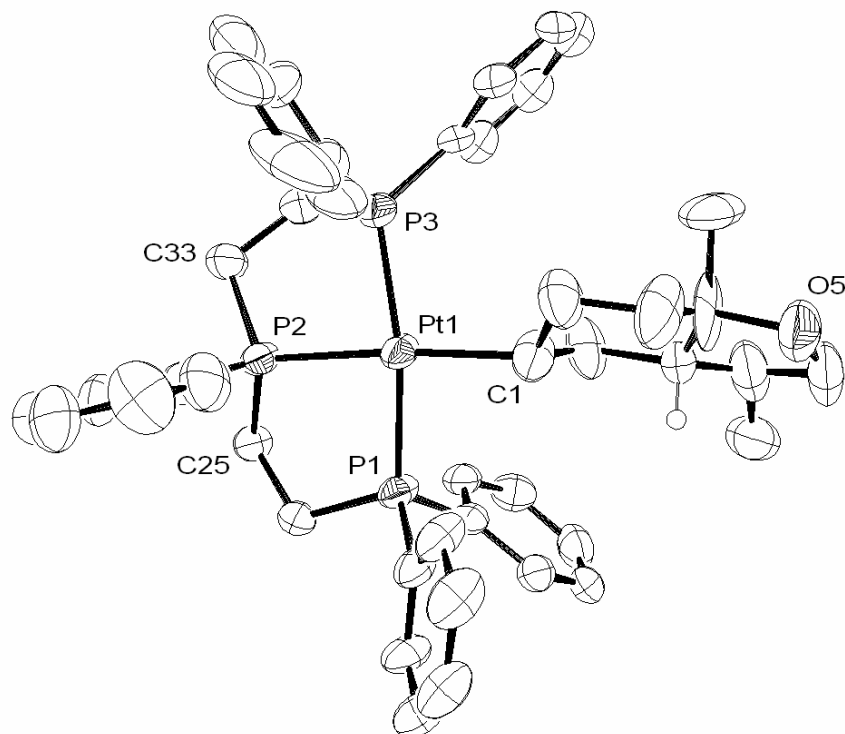


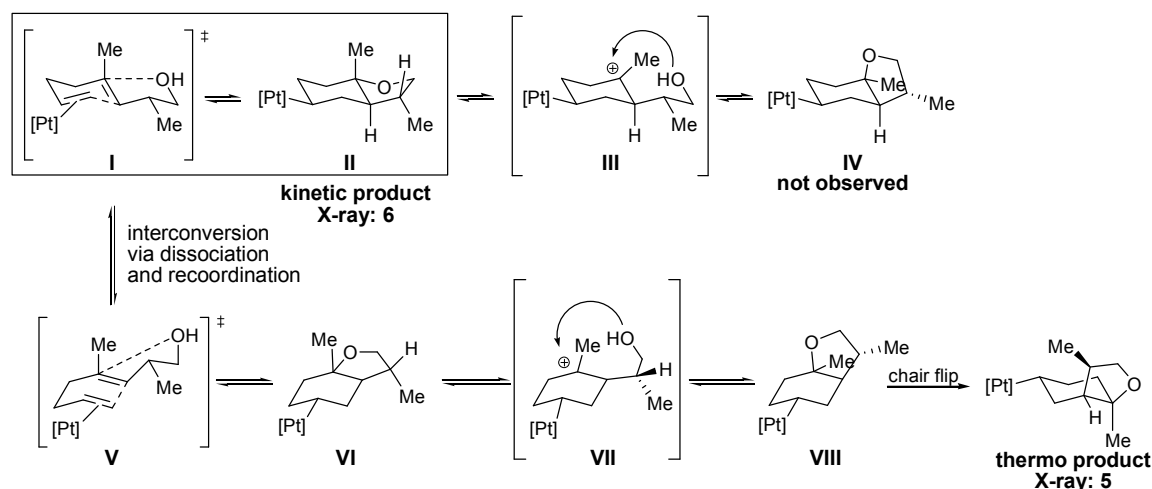
Figure 3.8. ORTEP representation of **6**. Hydrogen atoms and BF_4^- counter ion omitted for clarity. Selected bond lengths (Å): Pt-P₁ = 2.262(3), Pt-P₂ = 2.290(3), Pt-P₃ = 2.290(3), Pt-C₁ = 2.158(11). Selected bond angles (deg): P₁-Pt-P₂ = 84.80(10), P₂-Pt-P₃ = 83.15(10), P₁-Pt-C₁ = 90.6(4), P₃-Pt-C₁ = 101.7(4), C₂₇-P₂-C₃₃ = 112.2(5).

Scheme 3.6 outlines a simple mechanistic pathway for accessing the kinetic *trans* product and a more complex mechanism for converting it to the thermodynamically preferred *cis* form. One key feature of the mechanistic hypothesis is the kinetic preference of the chair-equatorial transition structure (**I**). The kinetic product can thus be rationalized by a cascade bicyclization to give **II**. In this cyclization, the stereochemical outcome is governed by the Stork-Eschenmoser postulate (*E* olefin → *trans* ring junction)

²⁰ Mullen, C. A.; Gagné, M. R. manuscript in preparation. Also see reference 10h.

as depicted in the boxed section of Scheme 3.6. The stereochemistry predicted by **II** is the same as that determined from the X-ray analysis of **6**, indicating that the kinetic product was indeed a result of a chair-equatorial transition state structure. This kinetically favored cyclization mode is the most important geometry for generating the *trans* products seen in other Pt(II) cyclizations.¹⁷

Scheme 3.6



The X-ray structure of **5** revealed that the thermodynamic product did not result from the simplest conversion of **II** to a *cis* isomer. Such a product (**IV**) would result from a simple C-O bond ionization followed by trapping from the opposite face. Instead, the thermodynamic product must have arisen from a more complex sequence of steps that involved *cis-trans* olefin isomerization and boat cyclization geometries.²¹ A possible mechanism for conversion of **II** to **VIII** is detailed in Scheme 3.6. First, complex retrocyclization (C-O and C-C bond scission) of **II** regenerates the starting Pt-olefin

²¹ The Pt-alkyl **5** is in a chair conformation however to obtain the stereochemistry observed requires formation of the *cis* ring junction via a boat conformation of **4**. Isomerization of **IV** to **VIII** which involves complete retrocyclization has also been considered but is not shown.

complex **I**. From this point, cyclization of the substrate via the boat conformation **VI** followed by ionization of the C-O linkage and recoordination from the top face gives the *cis* Pt-alkyl **VIII**. A boat-chair ring flip gives **5**, the thermodynamic product of bicyclization. The conversion of **6** to **5** therefore requires reversible C-O and C-C bond formation but also productive cyclization via a boat conformation.²² These results implied that decreasing the electrophilicity of the metal center by modifying the substituents on the supporting ligand (PPP → EtPPP) opened up higher energy pathways that allowed for access to the more thermodynamically preferred products of multicyclization.

To estimate the relative energies of some of the stereoisomers accessible on the isomerization energy surface, semi-empirical AM1 calculations were made on model compounds. The possible bicyclic isomers were modeled by replacing the metal-ligand complex with an equatorial Me group. The model for *trans* product **II** was lower in energy than the boat conformation **IV** by 1.6 kcal/mol. Interestingly, the models for the chair and boat *cis* Pt-alkyls **IV** and **VIII** had the same relative energy (1.30 kcal/mol). Consistent with **5** being the thermodynamically favored product, its model structure has the lowest AM1 energy of all the isomers studied.

²² Molecular mechanics indicate that the chair conformer of cyclohexane is more stable than the boat conformer by 6.4 kcal/mol, see: (a) Allinger, N. L.; Miller, M. A.; VanCatledge, F. A.; Hirsch, J. A. *J. Am. Chem. Soc.* **1967**, *89*, 4345-4357. (b) Allinger, N. L. *J. Am. Chem. Soc.* **1977**, *99*, 8127-8134.

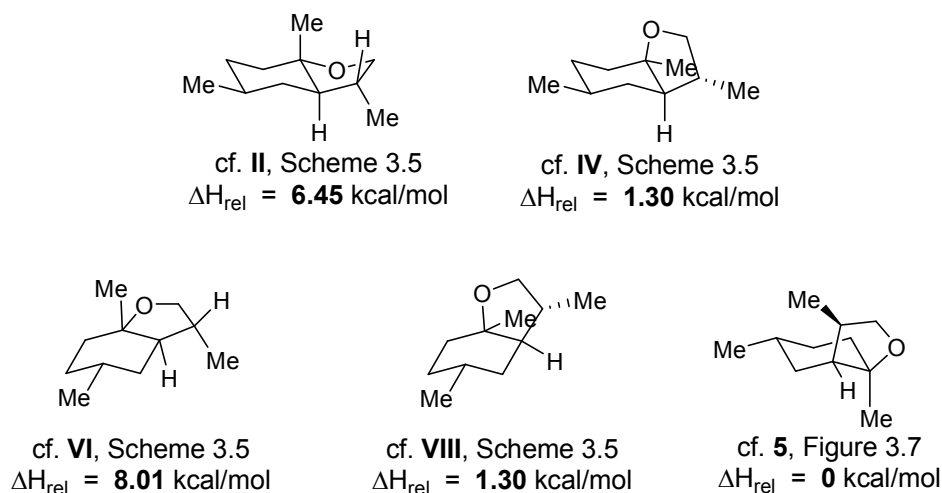
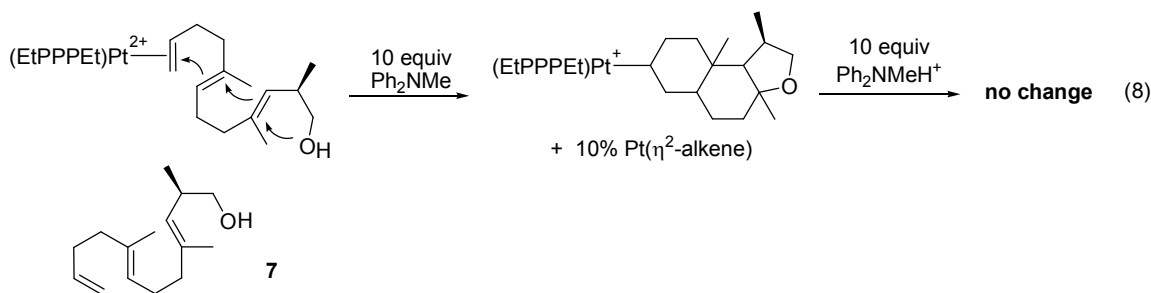


Figure 3.9. Models of Pt-alkyls for AM1 calculations.

To determine the limitations of stereocontrol with dicationic Pt initiators, the trienol substrate **7** was exposed to reversible cyclization conditions with $(\text{EtPPPEt})\text{Pt}^{2+}$. Unexpectedly, the only product observed from this reaction was a $\text{Pt}(\eta^2\text{-alkene})$ species at 110.1 ppm ($J_{\text{Pt-P}} = 2747$ Hz). Only upon addition of ten equivalents of base (Ph_2NMe) was a significant amount²³ of cyclized product observed (δ 98.2 br, $J_{\text{Pt-P}} = 1250$ Hz). For the trienol systems, the broad peak for the central phosphine of the Pt-alkyl was a result of two coincidental P signals corresponding to two Pt-alkyls. The resolution was slightly more pronounced for the terminal phosphines although the ratio of Pt-alkyls could not be accurately determined by ^{31}P NMR. To determine if this system was reversible, increasing amounts of $[\text{Ph}_2\text{NMeH}][\text{BF}_4]$ (up to 10 equivalents) were added to the reaction mixture and the ratio of Pt-alkyl to $\text{Pt}(\eta^2\text{-alkene})$ was monitored by ^{31}P NMR (eq. 8). No change in the ratio was observed upon addition of acid to the system indicating that the

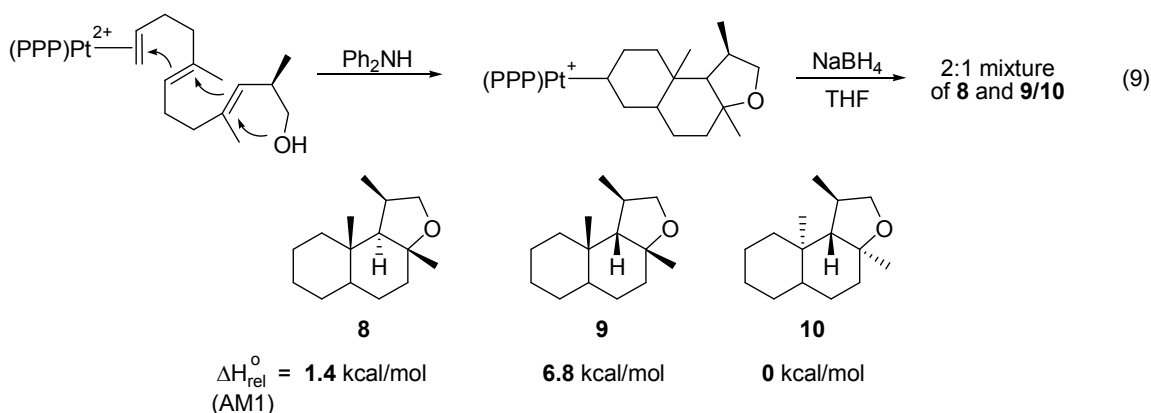
²³ >10% of the $\text{Pt}(\eta^2\text{-alkene})$ was observed after 24 h at 23 °C. The terminal P shift (~45.2 ppm) shows up as two overlapping yet unresolved singlets.

tricyclization of **7** was not reversible even with the least electrophilic tridentate ligand tested.



Using more electron withdrawing ligands, namely EtPPP and PPP, to generate a more electrophilic Pt(II) initiator drove the reaction to the cyclized product. In the case of PPP, no Pt(η^2 -alkene) was observed, only two Pt-alkyl species (89.8 br; $J_{\text{Pt-P}} = 1281$ Hz), whose ratio did not change over time. Isolation of the mixture and cleavage of the organic fragment yielded a 2:1 ratio of diastereomers which were inseparable by chromatography but appeared to be the *trans/cis* isomers **8** and **9** at the B/C-ring junction as shown in equation 9.²⁴ Compound **10** must also be considered as a possibility for one of the diastereomers formed as it would result from initiating a chair-chair cyclization from the opposite diastereoface as **7**.

²⁴ Assignments were made by comparison to ^1H NMR for dinorambrox derivatives (*trans*-dinorambrox Me groups: 0.76, 1.09 ppm; **8**: 0.74, 1.08 ppm). Ohloff, G.; Giersch, W.; Pickenhagen, W.; Furrer, A.; Frei, B. *Helv. Chim. Acta* **1985**, 68, 2022-2029.



The results with the trienyl substrate **7** showed that cyclization was nonselective in contrast to the bicyclic analog **4**. With trienyl alcohol **7**, the poor diastereoselectivity upon cyclization (2:1) implied that little organization of the C-ring existed prior to initiation of the cascade cyclization. The *trans* product (the presumed kinetic product) was the major diastereomer and no $\text{Pt}(\eta^2\text{-alkene})$ species were observed, suggesting that the tricyclization products have a much larger energy barrier for the retrocyclization than in the case of the dienyl alcohol **4**. This higher barrier arises from the larger ΔG for the cyclization of a triene over a diene.²⁵ Overcoming the barrier for cyclization (i.e. sufficient charge buildup at C-5), by the use of more electron withdrawing triphos ligands or external base, most likely resulted in concerted formation of the A- and B-rings with little organization of the C-ring prior to furan formation. From these results, the assumption was made that in the case of the trienyl substrate, the cyclization was not reversible and that there was a barrier for cyclization that less electrophilic Pt(II) complexes could not overcome.

²⁵ A large favorable enthalpy change is associated with the transformation of a C-C π bond into a C-C σ bond ($\Delta H_f^{\circ} = -20.3 \text{ kcal/mol}$), see Stull, D. R.; Westrum, E. F., Jr.; Sinke, G. C. In *The Chemical Thermodynamics of Organic Compounds*; Wiley: New York, 1969.

The difference in reactivity between the bi- and tricyclic systems results from the different terminating groups for the B-ring formation. In the cases of the dienol substrate **4**, the trapping nucleophile for C-5 is OH, which is more efficient than the third alkene in **7** at stabilizing the developing A-ring cyclization while simultaneously moving the reaction forward. Since there is expected to be significant neighboring group participation by –OH in the stabilization of any charge buildup at C-5 in the transition structure of **4**, it is proposed that the barrier for retrocyclization is lower, thereby permitting thermodynamic control of the Pt-alkyl product formed. By analogy, the poorer alkene trap in **7** requires a more electrophilic initiating alkene to undergo concerted cyclization of the A- and B-rings. The trienol cyclization is therefore under kinetic control, which generates Pt-alkyls with poor diastereoselectivity.

3.3 Conclusions

The first half of this study investigated the reactivity of (RPPPR')Pt²⁺ complexes varying in electrophilicity, with polyolefin substrates bearing sulfonamide nucleophiles. This study produced the first direct observation of a reversible cyclization (³¹P NMR) wherein both the dicationic η^2 -alkene Pt(II) adduct and the cyclized monocationic Pt-alkyl could be observed. More polar solvents, less electrophilic Pt(II) centers, weaker bases, and substrate ring strain all drove the cyclization equilibrium more towards the Pt(η^2 -alkene). An X-ray structure of **3** showed that the favored ring junction for a [6,5]-bicyclic sulfonamide was *cis* in contrast to previous studies which resulted in *trans*-fused polycyclic products.

Once an understanding on how to control the equilibrium was developed, attempts were made to use the reversible nature of cyclization to influence the stereochemistry of a cyclization reaction. When a methyl group β to the trapping nucleophile was in place, the dieny substrate **4** was shown to undergo reversible cyclization and also to induce stereocontrol by a mechanism which included some degree of retrocyclization. Attempts to extend the observed stereinduction to trienyl substrate **7** resulted in a nonselective cyclization (2:1 dr) with the more electrophilic (PPP)Pt²⁺ complex. This result suggested that triene cyclization was probably not reversible and that less electrophilic (RPPPR')Pt²⁺ initiators could not generate enough partial positive charge (δ^+) at the key C-5 position to ionize the third alkene for cyclization. These studies suggested that when the cyclizations were reversible, a mechanism for stereochemical error correction is available.

3.4 Experimental

Synthesis of Dienes

General Methods. All reactions were performed under an inert atmosphere of N₂ using standard Schlenk techniques or using an MBraun Lab-Master 100 glove box. Solvents for equilibrium studies (CH₂Cl₂, ClCH₂CH₂Cl, MeNO₂ and EtNO₂) were dried over CaH₂, distilled and degassed by several successive freeze-pump-thaw cycles and stored in a glove box. All starting [(RPPPR)PtMe][BF₄] compounds,¹¹ [Ph₂NH₂][BF₄],²⁶ [Ph₂NMeH][BF₄],²³ and **1**^{10g} were prepared by published procedures. Diphenylamine and 2,3-dihydropyran were purchased from Aldrich and used as received. NMR spectra were

²⁶ Forschner, T. C.; Cutler, A. R. *Organometallics* **1985**, 4, 1247.

recorded on a Bruker Avance 400 MHz or Bruker Avance 500 MHz spectrometer; chemical shifts are given in ppm and are referenced to residual solvent resonances (^1H and ^{13}C). ^{31}P NMR chemical shifts are referenced to an external PPh_3 standard in C_6D_6 sealed in a capillary tube.

2: Prepared by a similar procedure to **1**^{10g} using 2,3-dihydropyran in place of dihydrofuran. The crude material was separated by silica gel chromatography using 4:1 hexanes/EtOAc to yield 647.6 mg (54%) of a pale yellow oil; ^1H NMR: (400 MHz, CDCl_3) δ 7.72 (d, 2 H, $J = 7.6$ Hz), 7.28 (d, 2 H, $J = 7.6$ Hz), 5.73 (m, 1 H), 4.94 (m, 3 H), 4.37 (br, 1 H), 2.91 (q, 2 H, $J = 6.8$ Hz), 2.41 (s, 3 H), 2.08 (m, 2 H), 1.96 (m, 4 H), 1.58 (s, 3 H), 1.48 (m, 2 H); ^{13}C NMR (100 MHz, CDCl_3) δ 143.2, 138.5, 136.9, 135.7, 129.6, 127.0, 123.1, 114.3, 42.8, 38.9, 32.2, 29.4, 24.8, 21.5, 15.9. HRMS (ESI) $[\text{M}+\text{K}]^+/z$ calc. 346.124, found 346.120.

4: Prepared by a published procedure^{10g} using 3-methyl-2,3-dihydrofuran.²⁷ The crude material was purified by silica gel chromatography using 9:1 hexanes/EtOAc to yield 797.1 mg (65%) of a clear oil; ^1H NMR: (400 MHz, CDCl_3) δ 5.73 (m, 1 H), 4.96 (m, 2 H), 4.85 (d, 1 H, $J = 9.6$ Hz), 3.45 (m, 1 H), 3.25 (t, 1 H, $J = 9.2$ Hz), 2.60 (m, 1 H), 2.12 (m, 4 H), 1.63 (s, 3 H), 1.41 (m, 1 H), 0.92 (d, 3 H, $J = 10.8$ Hz); ^{13}C NMR (100 MHz, CDCl_3) δ 158.0, 138.2, 115.2, 101.4, 77.4, 37.7, 31.2, 27.8, 21.2. HRMS (ESI) $[\text{M}+\text{Na}]^+/z$ calc. 177.126, found 177.127.

7: Prepared by a published procedure^{10g} except using 3-methyl-2,3-dihydrofuran.²⁴ The crude material was purified by silica gel chromatography using 9:1 hexanes/EtOAc to yield 370.4 mg (53%) of a clear oil; ^1H NMR: (400 MHz, CDCl_3) δ 5.77 (m, 1 H),

²⁷ Chan, J.; Jamison, T. F. *J. Am. Chem. Soc.* **2004**, *126*, 10682-10691.

5.07 (m, 1 H), 4.98 (d, 1 H, $J = 17.2$ Hz), 4.90 (d, 1 H, $J = 10.4$ Hz), 4.84 (d, 1 H, $J = 9.2$ Hz), 3.44 (m, 1 H), 3.26 (t, 1 H, $J = 9.2$ Hz), 2.59 (m, 1 H), 2.07 (m, 8 H), 1.64 (s, 3 H), 1.58 (s, 3 H), 1.38 (m, 1 H), 0.89 (d, 3 H, $J = 6.8$ Hz); ^{13}C NMR (100 MHz, CDCl_3) δ 139.1, 138.3, 135.3, 127.6, 124.6, 114.7, 68.3, 40.2, 39.4, 35.8, 32.8, 26.8, 17.4, 16.9, 16.4. HRMS (ESI) $[\text{M}+\text{Na}]/z$ calc. 245.1881, found 245.1877.

3: In a glovebox, (PPP)PtI₂ (0.10 mmol) and AgBF₄ (0.23 mmol) were weighed out into a glass vial. Dichloromethane was added to this and the solution was stirred for 10 minutes upon which **1** (0.11 mmol) was added to the solution dropwise. After an additional 10 minutes of stirring AgI began to precipitate and diphenylmethylamine (0.11 mmol) was added to the suspension. This mixture was shielded from light and stirred for 2 hours. The suspension was filtered through celite to remove AgI, washed three times with a saturated NaHCO₃ solution, dried over MgSO₄ and concentrated *in vacuo*. The product was precipitated three times from dichloromethane and Et₂O and dried to give 75.4 mg (68%) of a white solid; ^1H NMR (400 MHz, CDCl_3): δ 7.78 (m, 2 H); 7.51 (m, 25 H); 7.20 (d, 2 H, $J = 8.0$ Hz); 3.35 (m, 3 H); 2.87 (m, 3 H); 2.43 (m, 7 H); 1.79 (m, 1 H); 1.43 (m, 1 H); 1.29 (m, 4 H); 0.97 (m, 4 H); 0.80 (s, 3 H). $^{31}\text{P}\{^1\text{H}\}$ NMR (162 MHz, CDCl_3): δ 90.0 (s, 1 P, $^3J_{\text{Pt-P}} = 1319$ Hz); 44.6 (s, 2 P, $^3J_{\text{Pt-P}} = 2991$ Hz).

5: In a glovebox, (EtPPP)PtI₂ (0.11 mmol) and AgBF₄ (0.29 mmol) were weighed out into a glass vial. Dichloromethane (8 mL) was added to this and the solution was stirred for 10 minutes upon which **4** (0.13 mmol) was added to the solution dropwise. After an additional 10 minutes of stirring AgI began to precipitate and diphenylmethylamine (0.13 mmol) was added to the suspension. This mixture was stirred for 48 hours. The suspension was filtered through celite to remove AgI, washed three times with a saturated

NaHCO₃ solution, dried over MgSO₄ and concentrated *in vacuo*. The product was precipitated three times from dichloromethane and Et₂O and dried to give 53.6 mg (51%) of a white solid. Crystals suitable for X-ray crystallography were grown by vapor diffusion with dichloromethane and diethyl ether; ¹H NMR (500 MHz, CDCl₃): δ 7.68 (m, 4 H); 7.59 (m, 6 H); 7.43 (m, 10 H); 3.70 (t, 1 H, *J* = 8.0 Hz); 3.45 (m, 2 H); 3.09 (t, 1 H, *J* = 8.0 Hz); 2.65 (m, 2 H); 2.34 (m, 5 H); 1.77 (m, 1 H); 1.67 (m, 2 H); 1.33 (m, 2 H); 1.03 (m, 1 H); 0.85 (m, 4 H); 0.78 (m, 2 H); 0.71 (m, 1 H); 0.57 (d, 3 H, *J* = 6.5 Hz); 0.48 (s, 3 H). ³¹P{¹H} NMR (162 MHz, CDCl₃): δ 90.9 (s, 1 P, ³*J*_{Pt-P} = 1241 Hz); 43.8 (s, 2 P, ³*J*_{Pt-P} = 3012 Hz).

6: In a glovebox, (PPP)PtI₂ (0.53 mmol) and AgBF₄ (0.133 mmol) were weighed out into a glass vial. Dichloromethane (15 mL) and acetone (1.06 mmol) was added to this and the solution was stirred for 1 hour upon which a 3 mL solution of **4** (0.58 mmol) and Ph₂NMe (1.06 mmol) in dichloromethane was added to the solution dropwise. This mixture was stirred for 1 hour. The suspension was filtered through celite to remove AgI, washed three times with a saturated NaHCO₃ solution, washed once with brine and dried over MgSO₄. The filtrate from drying was concentrated *in vacuo*. The product was precipitated three times from dichloromethane and Et₂O and dried to give 380.3 mg (74%) of a white solid. Crystals suitable for X-ray crystallography were grown by vapor diffusion with dichloromethane and pentane; ³¹P{¹H} NMR (162 MHz, CDCl₃): δ 89.6 ppm, *J*_{Pt-P} = 2904 Hz; 44.6 (s, ³*J*_{Pt-P} = 2897 Hz, 2P).

Typical Procedure for Equilibrium Measurements. A solution of 0.008 mmol of [(RPPPR)PtMe][BF₄], 0.08 mmol [Ph₂NH₂][BF₄], and 0.08 mmol of substrate (**1**, **2**, **4**, or

7) in 300 μL of CH_3NO_2 ²⁸ (or other solvent for Table 2.1) was sealed in a J-Young NMR tube at 25(1) $^\circ\text{C}$. The reaction was monitored by ^{31}P NMR until no change in peak intensity was observed. Equilibrium constants were calculated from the average molar ratios of the $\text{Pt}(\eta^2\text{-alkene})$ and $\text{Pt}(\text{alkyl})$ complexes.

²⁸ Commercial MeNO_2 contains traces of propionitrile that poison the Pt^{2+} catalyst, for purification see: Parrett, F. W.; Sun, M. S. *J. Chem. Educ.* **1977**, *54*, 448.

Chapter 4

Designing Modular Catalysts to Improve Diene Cycloisomerization

4.1 Introduction

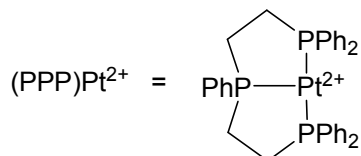
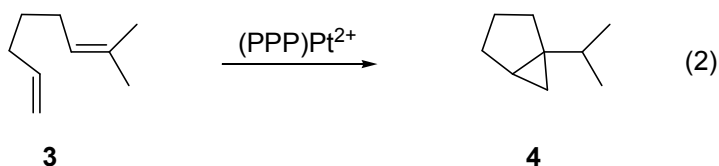
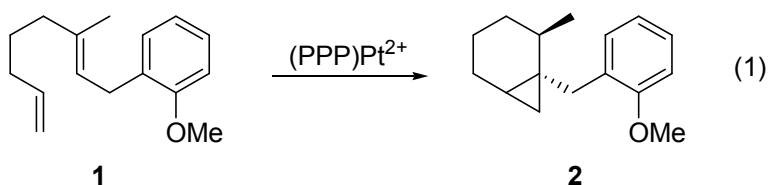
Metal catalyzed cycloisomerization reactions are highly atom economical methods to increase molecular complexity in one step from simple achiral starting materials. Enynes are well established substrates for this type of reactivity with Pt, Pd, Ru, and Au being exemplary catalysts for these transformations.^{1,2} While enynes can lead to products where all unsaturation from the starting material has been consumed, diene substrates typically give products with incomplete consumption of unsaturation under cycloisomerization conditions. Along this line, enynes have been known to isomerize to cyclopropanes while this type of transformation for dienes is uncommon and was only recently discovered with group 10 metals.³

¹ (a) Aubert, C.; Buisine, O.; Malacria, M. *Chem. Rev.* **2002**, *102*, 813-834. (b) Trost, B. M. *Acc. Chem. Res.* **1990**, *23*, 34-42. (c) Trost, B. M.; Krische, M. J. *Synlett* **1998**, 1-16. (d) Widenhoefer, R. A. *Acc. Chem. Res.* **2002**, *35*, 905-913. (e) Echavarren, A. M.; Nevado, C. *Chem. Soc. Rev.* **2004**, *33*, 431-436. (f) Diver, S. T.; Giessert, A. J. *Chem. Rev.* **2004**, *104*, 1317-1382. (g) Ma, S.; Yu, S.; Gu, Z. *Angew. Chem. Int. Ed.* **2006**, *45*, 200-203.

² Mechanistic reviews: (a) Lloyd-Jones, G. C. *Org. Biomol. Chem.* **2003**, *1*, 215-236. (b) Méndez, M.; Mamane, V.; Fürstner, A. *Chemtracts* **2003**, *16*, 397-425.

³ (a) Kerber, W. D.; Gagné, M. R. *Org. Lett.* **2005**, *7*, 3379-3381. (b) Kerber, W. D.; Koh, J. H.; Gagné, M. R. *Org. Lett.* **2004**, *6*, 3013-3015. (c) Cucciolito, M. E.; D' Amora, A.; Vitagliano, A. *Organometallics* **2005**, *24*, 3359-3361.

Group 10 metals are known to activate olefins for nucleophilic addition and preferentially bind less substituted olefins.⁴ This binding preference is opposite that of typical electrophilic reagents used to activate olefins such as Hg^{2+} , Ag^+ , H^+ , or Br^+ .⁵ Recently, Pt^{2+} catalysts with tridentate pincer ligands were shown to inhibit β -H elimination (common turnover pathway) and generate cyclopropanes as the major product of cycloisomerization.³ In particular, $(\text{PPP})\text{Pt}^{2+}$ efficiently catalyzed the cycloisomerization of 1,6- and 1,7-dienes to [3.1.0] and [4.1.0] bicyclic products (eqs. 1 and 2).



⁴ Hegedus, L. S. In *Transition Metals in the Synthesis of Complex Organic Molecules*; University Science Books: Mill Valley, CA, 1994; pp 199-236.

⁵ (a) Hegedus, L. S. In *Comprehensive Organic Synthesis*; Trost, B. M., Ed.; Pergamon Press: Elmsford, NY, 1991; Vol. 4, pp 551-569. (b) Bartlett, P. A. In *Asymmetric Synthesis*; Morrison, J. D., Ed.; Academic Press: New York, 1984; Vol. 3, pp 411-454. (c) Ishibani, H.; Ishihara, K.; Yamamoto, H. *J. Am. Chem. Soc.* **2004**, *126*, 11122-11123. (d) Uyanik, M.; Ishihara, K.; Yamamoto, K. *Bioorg. Med. Chem.* **2005**, *13*, 5055-5065.

The [3.1.0] bicyclic skeleton obtained from these Pt^{2+} catalyzed cycloisomerizations is a key feature common to naturally occurring bicyclic terpenes (Figure 4.1).⁶ Compounds of this type are typically found in essential oils as well as in flavor and fragrance applications (owing to their volatility).⁷ The biosynthesis of terpenes with this structure is believed to follow from the generation of carbocationic intermediates from unsaturated polyprenoids which are subsequently quenched by C-C bond formation to give polycyclic products.⁸ Interestingly, the mechanism for the biosynthesis of terpenoids is similar to that observed for the Pt^{2+} catalyzed cycloisomerization of 1,6-dienes to [3.1.0] bicyclopropanes.

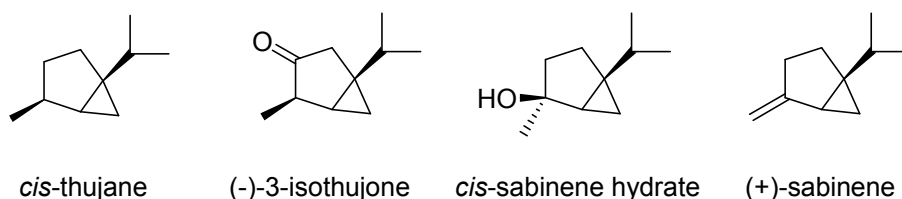


Figure 4.1. Examples of [3.1.0] bicyclic natural products.

Previous work had shown that tridentate (PPP)Pt(II) catalysts generated terpene-like products from acyclic 1,6- and 1,7-dienes.³ Deconstructing these first-generation catalysts into mixed diphosphine/monophosphine combinations (P_2P) led to more active catalysts for the cycloisomerization of 1,6- and 1,7-dienes into bicyclo-[3.1.0] and -[4.1.0] products. When the diphosphine had a small bite angle, reaction rates were 20-fold faster than with PPP, although reaction rates and diastereoselectivities were also sensitive to the monophosphine. Rates, selectivities, and substrate compatibility were all

⁶ Croteau, R. *Chem. Rev.* **1987**, 87, 929-954.

⁷ Croteau, R. In *Recent Developments in Flavor and Fragrance Chemistry: Proceedings of the 3rd International Harmann & Reimer Symposium*; VCH: Weinheim, 1993; p 263.

⁸ *Biosynthesis of Isoprenoid Compounds*; Porter, J. W.; Spurgeon, S. L., Eds.; John Wiley & Sons: New York, 1981; Vol. 1.

significantly improved over first-generation PPP catalysts. This chapter describes the development of modular catalysts and the improvements discovered upon applying them towards cycloisomerization. Efforts towards asymmetric catalysis using modular catalysts are also discussed.

4.2 Results and Discussion

A. First Generation PPP Catalysts. Previous studies have detailed the transformation of 1,6- and 1,7-dienyl starting materials to bicyclopropane products using (PPP)Pt²⁺ as the active catalyst species.^{3a,b} In these systems, a precursor [(PPP)PtMe][BF₄] catalyst was activated by *in situ* protonolysis in the presence of a weak trapping ligand (acetone) followed by addition of a dienyl substrate to generate terpene like products where both degrees of unsaturation in the starting material were consumed. Table 4.1 highlights the results from this initial work. While the reactivity observed in these systems was novel, successful cyclizations produced only moderate yields and required heat and an external amine base (to reduce background acid catalysis of the starting dienes).

Table 4.1. Cycloisomerization of dienes with [(PPP)PtMe][BF₄].^a

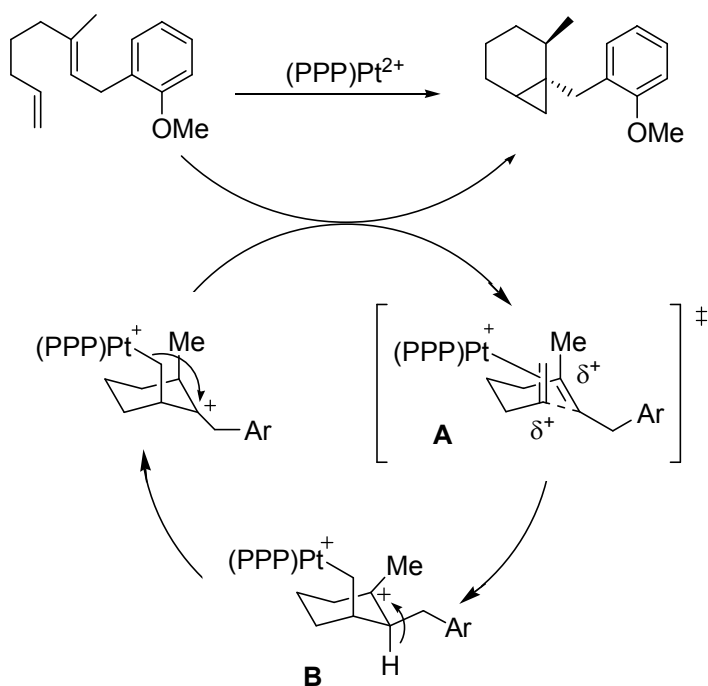
entry	diene	product	time, yield ^b
1			16 h, 83 19 : 1 dr ^c
2			25 h, 61
3			15 h, 65 47 : 1 dr ^c
4			36 h, 53
5			12 h, 53

^aReaction conditions: 5% (PPP)Pt²⁺ (from *in situ* protonolysis), 10% Ph₂NMe, CD₃NO₂, 40 °C. ^bIsolated. ^cBy GC.

In order to understand the mechanism of cyclopropane formation, deuterium labeling studies were performed on **1**.^{3b} The mechanism, as depicted by Scheme 4.1, begins with activation of the terminal olefin in a pseudoaxial orientation (**A**). Upon activation, the internal double bond closes the 6-membered ring to produce the cyclic Pt-alkyl cation **B**. A subsequent 1,2-hydride shift generates a carbocation γ to the metal center which is captured by the Pt-C bond, similar to Sn, Fe, and Ti systems, to give a cyclopropane product and Pt²⁺.⁹

⁹ (a) Davis, D. D.; Johnson, H. T. *J. Am. Chem. Soc.* **1974**, *96*, 7576-7577. (b) Fleming, I.; Urch, C. J. *Tetrahedron Lett.* **1983**, *24*, 4591-4594. (c) McWilliam, D. C.; Balasubramanian, T. R.; Kuivila, H. G. *J. Am. Chem. Soc.* **1978**, *100*, 6407-6413. (d) Lambert, J. B.; Salvador, L. A.; So, J. H. *Organometallics* **1993**, *12*, 697-703. (e) Casey, C. P.; Smith-Vosejpka, L. J. *Organometallics* **1992**, *11*, 738-744. (f) Brookhart, M.; Liu, Y. *J. Am. Chem. Soc.* **1991**, 939-944. (g) Casey, C. P.; Strotman, N. A. *J. Am. Chem. Soc.* **2004**, *126*, 1699-1704, and references therein.

Scheme 4.1



The development of cyclopropanation catalysts hinged on the ligands supporting the metal center blocking the coordination site *cis* to the incoming dienyl substrate. By doing so, β-hydride elimination from the Pt-alkyl formed during cyclization could be completely inhibited as a reaction pathway.¹⁰ PPP was shown to be an acceptable ligand for cyclopropanation but modifying the ligand structure was not trivial¹¹ and produced less active catalysts. Cyclopropanation using the less electrophilic [(PPPEt)PtMe][BF₄] or [(EtPPP)PtMe][BF₄] catalysts was much slower and gave lower yields of

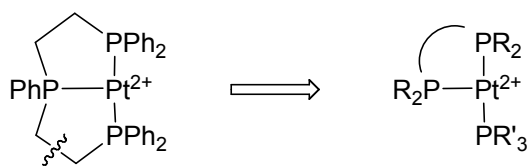
¹⁰ For other systems which take advantage of this principal see: (a) Hahn, C.; Cucciolito, M. E.; Vitagliano, A. *J. Am. Chem. Soc.* **2002**, *124*, 9038-9039. (b) Hahn, C. *Chem. Eur. J.* **2004**, *10*, 5888-5899. (c) Hahn, C.; Morvillo, P.; Herdtweck, E.; Vitagliano, A. *Organometallics* **2002**, *21*, 1807-1818. (d) Hahn, C.; Morvillo, P.; Vitagliano, A. *Eur. J. Inorg. Chem.* **2001**, 419-429. (e) Michael, F. E.; Cochran, B. M. *J. Am. Chem. Soc.* **2006**, *128*, 4246-4247.

¹¹ Ligand modification of PPP architecture required multi-step phosphine synthesis using careful Schlenk techniques to avoid oxidation of the ligand. For typical procedure, see: DuBois, D. L.; Miedaner, A.; Haltiwanger, R. C. *J. Am. Chem. Soc.* **1991**, *113*, 8753-8764.

cyclopropane products.¹² Since these ligands were achiral, cyclopropanation was never performed asymmetrically which served as a concern for optimization and overall utility of this reaction.

B. Modular Catalyst Development. Due to the inherent limitations of PPP ligands, a new strategy for optimizing catalysts for cyclopropanation was implemented. This strategy involved deconstructing the linked tridentate ligand architecture of PPP to a modular combination of bi- and monodentate phosphine ligands (Scheme 4.2). A modular design would allow for independent assessment of catalyst properties including: bite angle and steric effects, electronics, and diastereo- or enantioselectivities among others. Since a wide range of bidentate and monodentate phosphines are commercially available, a rapid screening of these ligand properties could be performed thereby resulting in an efficient method for catalyst optimization. More importantly, asymmetric catalysis could also be optimized for this cycloisomerization since a large number of commercially available chiral phosphine ligands exist.

Scheme 4.2



Activation in the first generation PPP catalysts was performed by *in situ* protonolysis of a precursor [(PPP)PtMe][BF₄] complex with HNTf₂ in the presence of acetone, a weak trapping ligand. This method of activation provided a clean, reproducible means to an active catalyst for cyclopropanation. Previous studies on the protonolysis of cationic tridentate Pt(II) compounds showed that torsional strain in the square planar

¹² [(EtPPP)PtMe][BF₄] with **5** gave **6** in 22% GC yield after 24 h at 60 °C . [(EtPPPEt)PtMe][BF₄] with **5** gave **6** in 4% GC yield after 7 h at 70 °C . Unpublished results by Dr. William Kerber.

[(PPP)PtMe][BF₄] complex resulted in successful cleavage of the Pt-C bond by protonolysis while modular [(P₂)(PR₃)PtMe][BF₄] complexes were stable to strong acids even at elevated temperatures.¹³ Since modular catalysts were inactive towards activation by protonolysis, active catalysts were generated by *in situ* halide abstraction of [(P₂)(PR₃)PtI][I] by Ag⁺ salts. Iodide precursors were found to be significantly easier to activate than chloride precursors. Similar to the first generation catalysts, nitromethane proved to be the optimal solvent for cyclization as less polar solvents like CH₂Cl₂ or EtNO₂ were slower and generated more unsaturated byproducts. In PPP systems, external amine base (Ph₂NMe) was required to limit the formation of Brønsted products however; this additive only slowed the rates of cyclopropanation in reactions with modular catalysts. This rate retardation is presumably due to amine base inhibiting activation of the Pt-I precursor by Ag⁺. Therefore, typical conditions for modular catalyst screening were as follows: 5 mol% [(P₂)(PR₃)PtI][I], 11 mol% AgBF₄, and **1** in CD₃NO₂¹⁴ at room temperature. Substrate **1** was chosen not only because changes in rates, yields, and diastereoselectivity could be examined, but also because the characterization of many of the side products from the cyclization of **1** had previously been performed thereby simplifying the analysis of product mixtures.

Changes in bite angle size had been shown to be an important factor governing catalytic activity in various systems, therefore the first variable to be examined by this

¹³ Feducia, J. A.; Campbell, A. N.; Anthis, J. W.; Gagné, M. R. *Organometallics* **2006**, 25, 3114-3117.

¹⁴ CD₃NO₂ was utilized since traces of nitrile present in reagent grade CH₃NO₂ poison the catalyst. For preparative work, nitromethane that had been twice precipitated from a 50:50 solution with Et₂O at -78°C was sufficiently pure for use. See: Parrett, F. W.; Sun, M. S. *J. Chem. Educ.* **1977**, 54, 448-449.

modular approach was the effect of bidentate phosphine bite angle on cyclopropanation.¹⁵ These experiments were performed by adding one equivalent of PMePh₂ to (P₂)PtI₂ in CD₃NO₂ and then activating with AgBF₄ in the presence of **1**. PMePh₂ was chosen as the monodentate phosphine for bite angle studies since the sterics and electronics of this monodentate ligand closely resembled one arm of a deconstructed PPP ligand. As shown in Table 4.2, the rates and diastereoselectivity of product formation were very sensitive to changes in the carbon spacer of the bidentate ligand. These results showed that as the carbon number in the linker was increased, the rates, yields, and dr decreased. Incorporating benzene as the spacer also provided poor results. Since sterics seemed to correlate with reactivity, the tetramethylated analogs of dppe and dppm (dmpe and dmpm respectively) were tested. Unfortunately, the (dmpe/dmpm)Pt(II) dichlorides and diiodides were either insoluble in CD₃NO₂ or formed unreactive dimers.¹⁶ From this analysis, the smallest bite angle ligand, dppm (72°), gave the most reactive catalyst for the conversion of **1** to **2** with the highest diastereoselectivity (1.5 h, 26:1 dr, 79% GC yield). These results were greatly improved over the first generation PPP systems, with much faster rates (1.5 h at 23 °C versus 16 h at 40 °C), higher diastereomeric ratio (26:1 versus 19:1) and comparable yields.

¹⁵ (a) Freixa, Z.; van Leeuwen, P. W. N. M. *J. Chem. Soc., Dalton Trans.* **2003**, 1890-1901. (b) van Leeuwen, P. W. N. M.; Kamer, P. C. J.; Reek, J. N. H.; Dierkes, P. *Chem. Rev.* **2000**, *100*, 2741-2770. (c) Raebiger, J. W.; Miedaner, A.; Curtis, C. J.; Miller, S. M.; Anderson, O. P.; DuBois, D. L. *J. Am. Chem. Soc.* **2004**, *126*, 5502-5514.

¹⁶ (a) Ling, S. S. M.; Puddephatt, R. J. *Inorg. Chim. Acta* **1983**, *77*, L95-L96. (b) Azam, K. A.; Ferguson, G.; Ling, S. S. M.; Puddephatt, R. J.; Srokowski, D. *Inorg. Chem.* **1985**, *24*, 2799-2802. (c) Xia, B.; Zhang, H.; Che, C.; Leung, K.; Phillips, D. L.; Zhu, N.; Zhou, Z. *J. Am. Chem. Soc.* **2003**, *125*, 10362-10374. (d) Xia, B.; Che, C.; Phillips, D. L.; Leung, K.; Cheung, K. *Inorg. Chem.* **2002**, *41*, 3866-3875.

Table 4.2. The effect of bidentate ligand on the cycloisomerization of **1**.^a

P ₂ (°) ^b	t (h)	dr	yield ^c
dppm (72°)	1.5	26:1	79%
dppbz (83°)	5	12:1	25%
dppe (85°)	6	19:1	56%
dppp (91°)	15	5:1	45%
dppb (98°)	7	7:1	16%

^a Reaction conditions: 5% (P₂)PtI₂ (0.06 M in CD₃NO₂), 5% PMePh₂, 11% AgBF₄, 23 °C. ^b See reference 12b. ^c By GC.

One important observation from the bidentate bite angle studies was that no dehydrogenated products were detected by GC/MS. These types of compounds would arise from β -hydride elimination from a putative Pt-alkyl after phosphine dissociation from a *cis* coordination site. Since these compounds were not observed, and because no free phosphine was observed in the ³¹P NMR during the reaction, it was presumed that the catalyst structure remained intact throughout the reaction as initially envisioned. In addition to this, the improvement in reaction times and lower reaction temperature resulted in higher yields since the dienyl starting material was not exposed to the reaction conditions long enough for significant amounts of side products to form.

The next step to developing an optimal cyclopropanation catalyst was an examination of the monodentate phosphine. These reactions were performed with dppm since this ligand excelled in previous cyclopropanation reactions. As shown in Table 4.3, the data from this study was scattered although some relationships were established. Large monodentate ligands (P(NMe₂)₃ and PCy₃) gave little to no yield of cyclopropane although an increase in steric bulk did increase the diastereoselectivity of the bicyclopropane product. While rates and yields varied, the diastereomeric ratio directly

correlated with the cone angle for the following ligands¹⁷: P(OMe)₃ (107°, 5:1); PMe₃ (118°, 12:1); PEt₃ (132°, 20:1); PPh₃ (145°, 38:1). These results showed that PMePh₂ gave the best combination of rate and diastereoselectivity (1.5 h, 26:1), PMe₃ was optimal for yield (94%) and PPh₃ gave the best diastereoselectivity (38:1).

Table 4.3. The effect of monodentate ligand on the cycloisomerization of **1** to **2**.^a

PR ₃	t (h)	dr ^b	yield ^b
P(OMe) ₃	1	5:1	74%
PMe₃	3	12:1	94%
PMe ₂ Ph	1	17:1	83%
PEt ₃	3	20:1	87%
P(2-furyl) ₃	3.5	23:1	43%
PMePh ₂	1.5	26:1	79%
PPh ₃	0.8	38:1	64%
P(4-OMePh) ₃	0.5	15:1	81%
P(C ₆ F ₅) ₃	3	24:1	53%
P(NMe ₂) ₃	48	78:1	10%
PCy ₃	- ^c	-	-

^a Reaction conditions: 5% (P₂)PtI₂ (0.06 M in CD₃NO₂), 5% PMePh₂, 11% AgBF₄, 23 °C. ^b By GC. ^c Reaction resulted in conversion of diene to unknown products.

Although phosphine ligands proved to be optimal ligands for cyclopropanation, other ligand types were tested (Figure 4.2). Pyridine and oxazolidone catalysts showed consumption of starting material but only generated small amounts of cyclopropane product. The anion of 4-*tert*-butylphenol was chosen as a ligand to generate a neutral catalyst precursor, however, this catalyst did not convert 1,6-dienes to the desired bicyclo-[3.1.0] products. The active species in solution using these monodentate ligands was not determined by ³¹P NMR. Due to the ambiguous role of these types of ligands in catalysis, there was no direct method to select new monodentate ligands for further screening. Fortunately phosphine ligands, as shown, were quite adept for this reaction.

¹⁷ Tolman, C. A. *Chem. Rev.* **1977**, 77, 313-348.

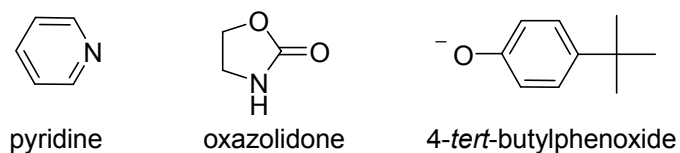


Figure 4.2. Non-phosphine monodentate ligands tested for modular catalysts.

Since dppm and PMe_3 gave the highest yield for the transformation of **1** to **2** with a fast rate and good diastereoselectivity, this modular catalyst combination was used to test the substrate scope for cyclopropanation (Table 4.4). In all cases, the reactions were 10-20 times faster than the first generation $(\text{PPP})\text{Pt}^{2+}$ catalysts and they could be carried out at ambient temperatures except in a couple of cases.

Table 4.4 shows rate and product yield improvements over the first generation PPP catalysts for the hydrocarbon substrates (entries 2-4). Like the triphos catalysts, the modular dppm catalyst also formed [4.1.0] bicyclic products from 1,7-dienes (entry 4) at a slower rate than the 1,6-diene to [3.1.0]-product conversion. Not only were rates and product yields enhanced with modular catalysts, functional group compatibility was also expanded using $(\text{dppm})(\text{PMe}_3)\text{Pt}^{2+}$. Along with malonates, acetal and sulfone functionalities were compatible with this catalyst system, which showed that these catalysts not only had a high propensity for cyclopropane formation but were also very carbophilic (entry 5-7). Even more surprising was the ketone substrate in entry 8 which cycloisomerized to the bicyclo-[3.1.0] ketone **16**, resembling the bare skeleton of thujone and thujanol derivatives (Figure 4.1). This substrate was much slower presumably due to competitive coordination of the ketone and terminal olefin to Pt^{2+} but upon heating to 40 °C still transformed into ketone **16**.¹⁸

¹⁸ Because of extensive splitting and the number of species in solution, *in situ* monitoring by ^{31}P NMR was uninformative although no olefin bound species were observed.

Table 4.4. Cycloisomerization of dienes with (dppm)(PMe₃)Pt²⁺.^a

entry	diene	product	time, yield ^b
1			3 h, 86 12 : 1 dr ^c
2			3 h, 70 (80)
3			1.5 h, 72 (81) 57 : 1 dr ^c
4			19 h, 62 (74)
5			3 h, 71 4.5 : 1 ^c 5-exo : 6-endo
6			1 h, 78 5.8 : 1 ^d 5-exo : 6-endo
7			3 h, 73
8			45 h ^e , 64 (82)
9			94 h ^e , 18
10			10 min, --
11		--	NR

21a,b
a: Ar = Ph
b: Ar = 3,4,5-(OMe)₃C₆H₂

^a Reaction conditions: 5% (dppm)PtI₂ (0.06 M in CD₃NO₂), 5% PMe₃, 11% AgBF₄, 23 °C. ^b Isolated yield; GC yield prior to isolation in parentheses. ^c By GC. ^d By ¹H NMR. ^e 10% catalyst loading, 40 °C.

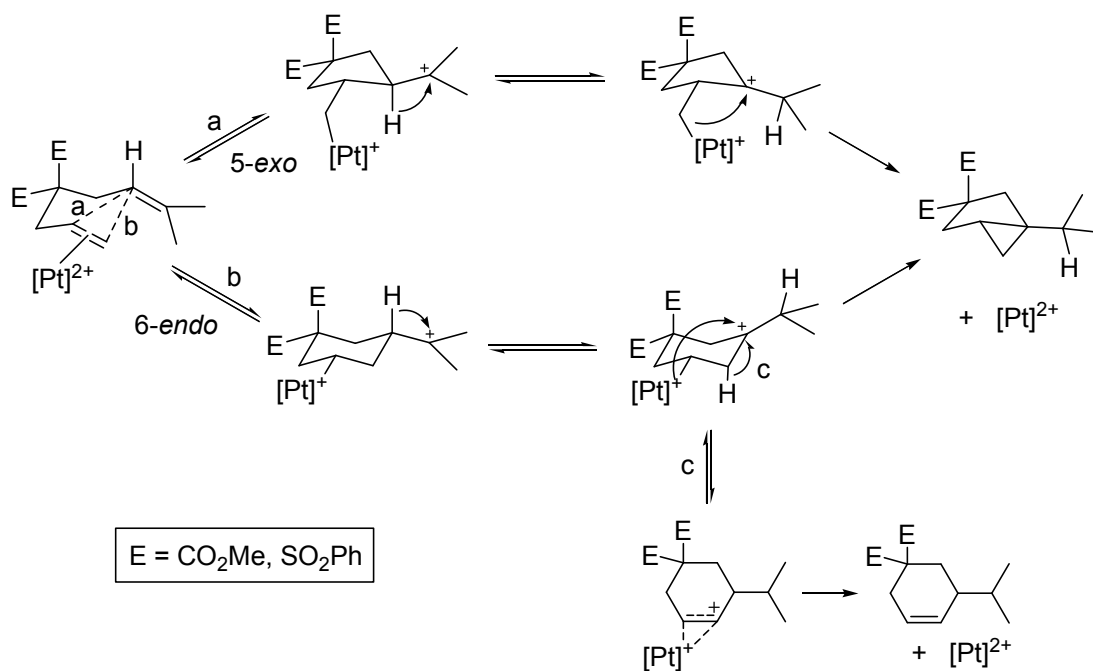
Entry 9 describes another limitation of this catalyst with the cycloisomerization of the allyl crotylmalonate **17**. Following a similar mechanism of cyclopropane formation as previously described (Scheme 4.1) would require the generation of a secondary carbocation subsequent to C-C bond formation. While the secondary carbocation is much less stable than the tertiary carbocations typically formed, with heat and long reaction times, cyclopropane formation was observed albeit in low yields (18% isolated yield of **18**). The sulfonamide **19** was extremely reactive under these conditions with complete consumption of starting material within 10 minutes at room temperature. Unfortunately, no cyclopropane **20** was observed, only higher molecular weight products were identified by GC/MS. This result was similar to the reaction of **19** with (PPP)Pt²⁺ in which polymerization inside the reaction vessel was observed. Substrates **21a** and **21b** were unreactive to the active Pt catalyst. This result was surprising since the benzyl cation generated upon cyclization of **21a/b** should be more stable than the secondary cation generated in the case of **17** (entry 9) which provided small amounts of cyclopropane product.

In the cases where side product formation was competitive (entries 5 and 6), modular systems provided a better ratio of cyclopropane to cyclohexene products. The malonate substrate **9** (Table 4.1, entry 5; Table 4.4, entry 5) gave a 3:1 ratio of cyclopropane to cyclohexene with (PPP)Pt²⁺ and a 4.5:1 ratio with the (dppm)(PMe₃)Pt²⁺ catalyst. Similarly, the sulfone substrate **11** (Table 4.4, entry 6) was more selective for cyclopropane product formation with the modular system (6:1) than the (PPP)Pt²⁺ catalyst (1:5).¹⁹ Cyclohexene substrates were not surprising products considering the

¹⁹ Results for sulfone substrate **11** with (PPP)Pt²⁺ were unpublished but performed under the same conditions described in Table 4.1.

possible mechanisms for product formation from 1,6-dienyl substrates (Scheme 4.3). Previous mechanistic experiments with triphos catalysts showed that initial ring closure can occur by either a 5-*exo* or 6-*endo* pathway. Following a 6-*endo* pathway, a second 1,2-hydride shift prior to cyclopropane ring formation (c) would generate a carbocation β to Pt. This carbocation could be considered as a slipped form of an η^2 -alkene which would be displaced by another molecule of starting material to give the observed cyclohexene product.

Scheme 4.3



While it was not obvious why (dppm)(PMe₃)Pt²⁺ had a higher propensity than (PPP)Pt²⁺ to catalyze the cyclopropanation of 1,6- and 1,7-dienyl substrates, the X-ray structure (Figure 4.3) of the precursor catalyst, [(dppm)(PMe₃)PtI][I], portrayed the small bite angle of dppm clearly. The dppm bite angle in this complex (72°) was similar to previously reported structures^{12b} and resulted in an obvious distortion of the square plane around Pt such that the bond angles around the site of alkene coordination were increased

(P_3 -Pt- $P_1 = 188.7^\circ$). The enlargement of the site of activation and the minimal steric encumbrance of PMe_3 provides ample room for dienyl substrates to coordinate and undergo cycloisomerization. The $(dppm)(PMe_3)Pt^{2+}$ framework resulted in a potent catalyst for the selective cycloisomerization of 1,6- and 1,7-dienes to bicyclopropane products. This catalyst is still the most efficient, functional group tolerant catalyst for these transformations.

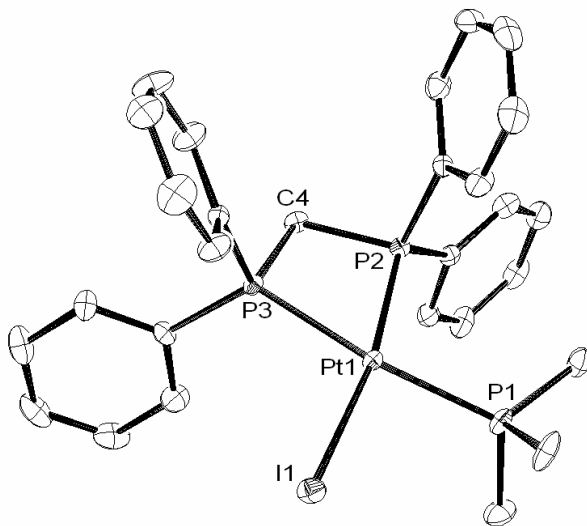
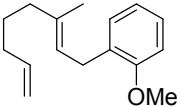
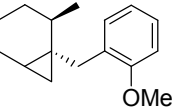
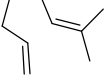
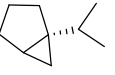
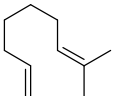
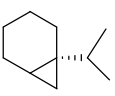
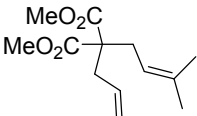
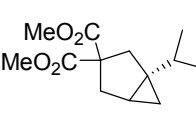
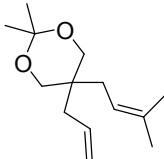
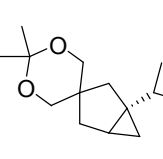
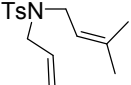
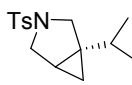


Figure 4.3. ORTEP representation of $[(dppm)(PMe_3)PtI][I]$. Hydrogen atoms and I^- counter ion omitted for clarity. Selected bond lengths (Å): Pt- $P_1 = 2.3172(13)$, Pt- $P_2 = 2.2410(13)$, Pt- $P_3 = 2.3242(12)$, Pt-I = 2.6329(4). Selected bond angles (deg): P_1 -Pt- $P_2 = 99.16(5)$, P_2 -Pt- $P_3 = 72.13(5)$, P_1 -Pt-I = 90.98(4), P_3 -Pt-I = 97.73(3).

C. Asymmetric Catalysis. While development of an achiral catalyst proved to be quite successful, efforts to develop an asymmetric version of cyclopropane formation were desired. To this end, a screen of commercially available chiral bidentate ligands revealed that (a) only small monodentate ligands were suitable with the larger chiral ligands and (b) the chiral BINAP architecture (with PMe_3 as the monodentate ligand)

gave the best results for the transformation of **1** to **2**. Table 4.5 shows the results from the screen of dienylyl substrates with the optimal chiral catalyst [(*R*-xylyl-BINAP)(PMe₃)Pt][BF₄]₂.²⁰ While these catalysts had slower reaction rates and poor yields compared to the achiral dppm analog, enantioselectivities were generally high with the substrates tested.

Table 4.5. Cycloisomerization reactions with ((*R*)-xylyl-BINAP)(PMe₃)Pt²⁺.^a

entry	diene	product	yield ^b , %ee
1			70%, 95/67 4:1 dr ^c
2			55%, 92
3			43%, 69 ^d
4			47%, 87
5			70%, 93
6			50%, 88 ^e

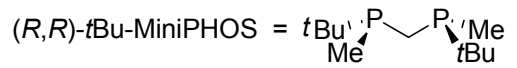
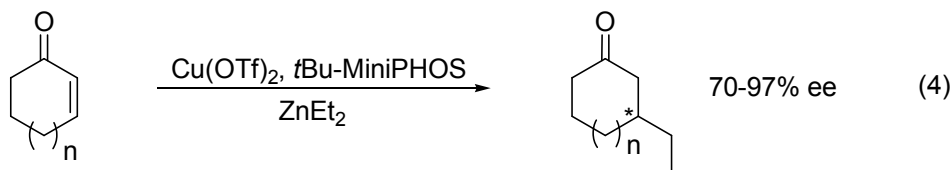
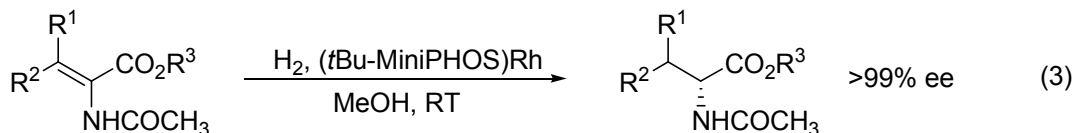
^a Reaction conditions: 5% (*R*-xylyl-BINAP)PtI₂ (0.05 M in CD₃NO₂), 5% PMe₃, 12% AgBF₄, 23 °C.

^b Isolated yield. ^c By GC. ^d 10% catalyst loading. ^e 40 °C.

Since yields and rates were poor with commercially available bidentate phosphine ligands, a chiral variant of dppm was synthesized. Typically, chiral bidentate ligands had chirality incorporated either on the carbon linker or the phosphorus centers although a convenient approach to synthesizing C₂-symmetric P-chiral diphosphines had been

²⁰ Commercially available chiral bidentate ligands were screened by Alison Campbell.

developed.²¹ *t*Bu-MiniPHOS²² was found to be a good chiral ligand for reactions including asymmetric hydrogenations with Rh and Cu catalyzed Michael reactions (eqs. 3 and 4 respectively). *t*Bu-MiniPHOS, like dppm, contained a methylene bridge, therefore synthesis of this ligand was pursued as a potential candidate for a modular asymmetric cyclopropanation catalyst.



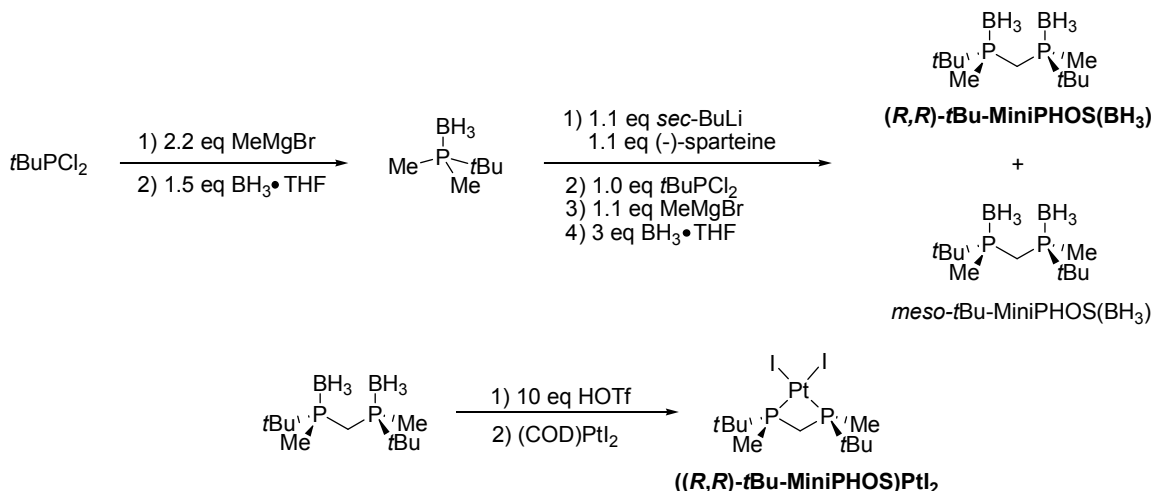
The synthesis of (*t*Bu-MiniPHOS)PtI₂ is outlined by Scheme 4.4 and began with the addition of methyl Grignard to *tert*-butyldichlorophosphine followed by borane protection of the alkyldimethylphosphine intermediate. After an aqueous workup, no further purification was required and these intermediates were produced with good yields (80-85%). The next step was an enantioselective deprotonation of *t*BuMe₂P(BH₃) with *sec*-BuLi and (-)-sparteine, followed by coupling of this anion to *t*BuPCl₂. In the same pot, this mixture was treated with MeMgBr and BH₃•THF to produce a mixture of enantiopure and *meso* phosphine-boranes. Optically active ligand could be obtained from this mixture by simple recrystallization from MeOH albeit with very low yields (~20%).

²¹ Muci, A. R.; Campos, K. R.; Evans, D. A. *J. Am. Chem. Soc.* **1995**, *117*, 4075-4076.

²² (a) Yamanoi, Y.; Imamoto, T. *J. Org. Chem.* **1999**, *64*, 2988-2989. (b) Yasutake, M.; Gridnev, I. D.; Higashi, N.; Imamoto, T. *Org. Lett.* **2001**, *3*, 1701-1704.

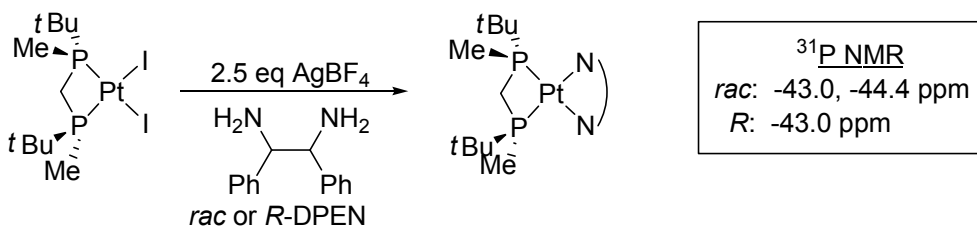
Borane deprotection with a large excess of triflic acid at low temperature followed by a basic workup under nitrogen generated the free ligand which was directly transferred to a solution of (COD)PtI₂ to give the MiniPHOS-Pt complex.

Scheme 4.4



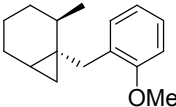

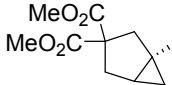
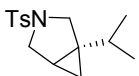
Enantiopurity of the resulting (*t*Bu-MiniPHOS)PtI₂ was tested by coordinating a chiral bidentate ligand to Pt and observing the diastereomeric ratio by ³¹P NMR. The bidentate ligand chosen for this analysis was DPEN. Using *rac*-DPEN both diastereomers were identified (Scheme 4.5) and only one diastereomer was observed when (*R*)-DPEN was coordinated to Pt. This suggested that only one enantiomer of the borane protected MiniPHOS was obtained during ligand synthesis.

Scheme 4.5



With enantiopure catalyst in hand, a screen of substrates and monodentate phosphines was performed to compare to the chiral BINAP catalysts (Table 4.6). Although the bite angle should be similar between the achiral dppm ligand and *t*Bu-MiniPHOS, the electron donating nature of the phosphine atoms was greatly increased by changing the P substituents from aryl to alkyl groups. The much slower rates for [3.1.0]-bicyclopropane formation were most likely a direct result of this large decrease in electrophilicity at the Pt center (entries 2-4). Unlike the dppm systems (Table 4.3), the *t*Bu-MiniPHOS catalyst showed little correlation between cone angle of the monodentate ligand and diastereoselectivity for bicyclopropane product **2**. One encouraging result from the substrate screen however, was the successful cycloisomerization of **19** to the aza-bicycle **20**. Previously, the only $(P_2)(PR_3)Pt^{2+}$ complexes which catalyzed this transformation were those incorporating BINAP or SEGPHOS bidentate ligands. In comparison to the chiral systems examined in Table 4.5, the enantioselectivities observed with *t*Bu-MiniPHOS were well below the 85-95% ee typically obtained using (*R*)-xylyl-BINAP, although both systems behaved best with PMe_3 as the monodentate ligand.

Table 4.6. Cycloisomerization reactions with ((*R,R*)-*t*Bu-MiniPHOS)PtI₂.^a

entry	diene	product	PR ₃	time	yield ^b , %ee ^c
1	1		P(OMe) ₃	4 h	87% (5:1 dr), 25/8
			PMe ₃	4 h	80% (4:1 dr), 23/58
			PMePh ₂	3 h	92% (2:1 dr), 0/10
			PPh ₃	3 h	64% (3:1 dr), 0/26
2	3		P(OMe) ₃	12 h	90%, 18
			PMe ₃	29 h	20%, 54
3	9		PMe ₃	29 h	67%, 48
			PMePh ₂	20 h	62%, 17
4	19		PMe ₃	29 h	63%, 48
			PMePh ₂	20 h	20%, 28

^a Reaction conditions: 5% ((*R,R*)-*t*Bu-MiniPHOS)PtI₂ (0.06 M in CD₃NO₂), 5% PR₃, 11% AgBF₄, 23 °C. ^b GC yield. ^c Enantioselectivities were obtained by chiral GC (β-cyclosil column).

While *t*Bu-MiniPHOS did not improve upon the rates or selectivities seen with (*R*)-xylyl-BINAP catalysts, this ligand showed that *P*-chirality may be used with moderate success for asymmetric cyclopropanations. Perhaps a MiniPHOS ligand with aryl instead of *tert*-butyl substituents would increase rates and selectivities by increasing the electrophilicity of the metal center and changing the chiral cavity around the site of activation. The smaller phenyl groups could also allow for the utility of monodentate phosphines with a larger range of cone angles.

4.3 Conclusions

In summary, the development of a second generation of catalysts for the cycloisomerization of 1,6- and 1,7-dienes to [3.1.0]- and [4.1.0]-bicyclopropanes was reported. These results described how deconstructing the tridentate architecture of the PPP ligand into a modular combination of bidentate and monodentate ligands provided an efficient approach to catalyst discovery and optimization. Reaction rates, functional

group compatibility, and yields were all improved over the first generation triphos-based catalysts. The selection of the small bite angle diphosphine dppm in combination with PMe_3 generated the optimum catalyst for this reaction. This catalyst was also the most efficient to date for the cycloisomerization of 1,6- and 1,7-dienes into bicyclopropanes. The modular approach to catalyst design also enabled chiral catalysts to be quickly optimized. While xylyl-BINAP proved to be the best diphosphine for asymmetric cyclizations, a methylene bridged *P*-chiral diphosphine, *t*Bu-MiniPHOS showed promise as an alternative to larger chiral bidentate ligands. The results from *t*Bu-MiniPHOS suggested that further screening with electron withdrawing substituents on the diphosphine should be pursued. Overall, these catalysts efficiently operated at the 5 mol% level, at ambient temperatures, and showed tolerance to functional groups that included sulfonamides, acetals, esters, sulfones, and ketones.

4.4 Experimental

Synthesis of Dienes

General Methods. All reactions were performed under an inert atmosphere of N_2 using standard Schlenk techniques or using an MBraun Lab-Master 100 glove box. Diethyl ether and dichloromethane were sparged with dry argon and passed through a column of activated alumina. DMF was dried overnight and subsequently distilled from CaH_2 . Cycloisomerization substrates **3** and **5** are commercially available from Aldrich. All other chemicals were used as received from Aldrich. Substrates **1**^{3b}, **7**^{3a}, **9**^{3a}, **17**²³, and

²³ Chuang, C. *Tet. Lett.* **1992**, 33, 6311-6314.

21²³ were prepared and purity was compared to literature procedures. Substrate **11**²⁴ was prepared by a literature procedure for an analogous compound. Substrate **15**²⁵ was prepared by a literature method for an analogous compound and its purity was compared to known spectral data.²⁶ NMR spectra were recorded on a Bruker Avance 400 MHz spectrometer; chemical shifts are given in ppm and are referenced to residual solvent resonances (¹H and ¹³C). Elemental microanalyses were performed by Robertson-Microlit Laboratories, Madison, NJ.

11: The crude material was separated on silica gel using 4:1 hexanes/EtOAc to yield 1.2764 g (71%) of a white solid; ¹H NMR: (400 MHz, CDCl₃) δ 8.04 (d, 4 H, *J* = 7.2 Hz), 7.68 (t, 2 H, *J* = 7.6 Hz), 7.55 (t, 4 H, *J* = 8.0 Hz), 5.98 (m, 1 H), 5.29 (m, 1 H), 5.20 (d, 1 H, *J* = 10.4 Hz), 5.15 (d, 1 H, *J* = 17.2 Hz), 3.00 (d, 2 H, *J* = 6.4 Hz), 2.91 (d, 2 H, *J* = 6.0 Hz), 1.69 (s, 3 H), 1.52 (d, 3 H, *J* = 7.6 Hz); ¹³C NMR (100 MHz, CDCl₃) δ 136.8, 136.4, 134.4, 131.5, 130.1, 128.4, 120.3, 115.1, 90.7, 33.0, 27.8, 26.0, 18.2. Anal. Calcd for C₂₁H₂₄O₄S₂: C, 62.35; H, 5.98. Found: C, 62.40; H, 5.77.

13: To a suspension of 288.8 mg LiAlH₄ (7.61 mmol) in 35 mL of Et₂O was added 1.6821 g of substrate **9** (7.0 mmol) at 23 °C. The solution was refluxed for 16 h then cooled to room temperature, quenched with H₂O and 1 M NaOH and extracted three times with Et₂O. The organic extracts were washed once with H₂O and once with brine. The extracts were dried over MgSO₄, filtered, and concentrated *in vacuo*. The crude diol product was carried on without further purification. To a solution of 133.2 mg *p*-TsOH•H₂O (0.7 mmol) in 150 mL of dichloromethane was added 1.2899 g of the crude

²⁴ Oppolzer, W.; Ruiz-Montes, J. *Helv. Chim. Acta* **1993**, *76*, 1266-1274.

²⁵ Lee, A. S.; Lin, L. *Tet. Lett.* **2000**, *41*, 8803-8806.

²⁶ Merrifield, J. H.; Godschalx, J. P.; Stille, J. K. *Organometallics* **1984**, *3*, 1108-1112.

diol (7.0 mmol) followed by 1.3 mL 2,2-dimethoxypropane (10.5 mmol). The solution was stirred for 4 h and quenched with a saturated solution of NaHCO₃. The organic layer was extracted and washed once each with H₂O and brine. The extracts were dried over MgSO₄, filtered and concentrated *in vacuo*. The crude material was flashed on silica gel with 20:1 hexanes/EtOAc to yield 1.1307 g (72%) of a clear oil; ¹H NMR: (400 MHz, CDCl₃) δ 5.77 (m, 1 H), 5.10 (m, 3 H), 3.57 (m, 4 H), 2.09 (t, 4 H, *J* = 7.2 Hz), 1.73 (s, 3 H), 1.64 (s, 3 H), 1.41 (s, 6 H); ¹³C NMR (100 MHz, CDCl₃) δ 134.6, 133.4, 118.6, 118.1, 97.9, 67.3, 36.8, 36.2, 30.5, 26.1, 24.3, 23.4, 17.9. Anal. Calc. for C₁₄H₂₄O₂: C, 74.95; H, 10.78. Found: C, 75.22; H, 10.58.

19: To a suspension of NaH (3.10 mmol) in 4 mL DMF at 0 °C was added via cannula 4-methyl-*N*-allylbenzenesulfonamide²⁷ (3.10 mmol) in 3 mL DMF. The mixture was raised to 23 °C and stirred for 1 h. 1-bromo-3-methylbut-2-ene (3.10 mmol) was then added via syringe, and the mixture was stirred for 3 h at 80 °C. The reaction was quenched with water, extracted three times with Et₂O, and the combined organic extracts washed twice with water and brine. The solution was dried over MgSO₄, filtered, and concentrated *in vacuo*. The crude product was purified by silica gel chromatography on silica gel in 10:1 hexanes/EtOAc to yield 670 mg (77%) of colorless oil; ¹H NMR: (300 MHz, CDCl₃) δ 7.69 (d, 2 H, *J* = 8.1 Hz), 7.28 (d, 2 H, *J* = 8.1 Hz), 5.64 (m, 1 H), 5.13 (m, 2 H), 4.97 (m, 1 H), 3.77 (m, 4 H), 2.42 (s, 3 H), 1.65 (s, 3 H), 1.58 (s, 3 H); ¹³C NMR: (100 MHz, CDCl₃) δ 143.0, 137.6, 136.7, 133.2, 129.5, 127.1, 118.8, 188.3, 49.3, 44.4, 25.7, 21.4, 17.8. Anal. Calc. for C₁₅H₂₁NO₂S: C, 64.48; H, 7.58; N, 5.01. Found: C, 64.74; H, 7.84; N, 4.93.

²⁷ Terada, Y.; Arisawa, M.; Nishida, A. *Angew. Chem. Int. Ed.* **2004**, *43*, 4063-4067.

Catalytic Cycloisomerizations

General Methods. All reactions were performed under an inert atmosphere of N₂ using an MBraun Lab-Master 100 glove box. Dichloromethane was dried by passage through a column of activated alumina. CD₃NO₂ was distilled from CaH₂. MeNO₂²⁸ was purchased from Aldrich and used as received. All bidentate and monodentate ligands used for catalyst screening were purchased from Strem Chemicals, stored in a glovebox and used as received. (P₂)PtI₂ catalyst precursors were prepared by a known literature procedure.²⁹ All solvents were degassed by several successive freeze-pump-thaw cycles and stored in a glovebox. GC was performed on an HP 6890 with a DB-1 (for **4**, **6**, **8**, **16**) or HP-5 (for **2**, **10**, **14**, **18**, **20**) column. Chiral GC was performed on a HP 6890 with an Agilent β-cyclosil column. AgNO₃ impregnated silica gel was prepared according to a literature procedure.³⁰

Typical Procedure: To a 0.06 M suspension of 13 μmol (dppm)PtI₂ (or other (P₂)PtI₂ complex for Table 4.2) in CD₃NO₂ was added 1 equiv. of PMe₃ (or other PR₃ for Table 4.3) in a glass scintillation vial. The suspension was stirred until (dppm)PtI₂ was completely dissolved and 20 equiv. of diene was added, followed by 5.6 mg AgBF₄ (29 μmol). The solution was stirred until complete by GC. The reaction was quenched by addition of MeNO₂ (containing traces of propionitrile). For **4**, **6**, **8**, and **16**, the MeNO₂/hydrocarbon biphasic was extracted with three small portions of pentane and

²⁸ Commercial MeNO₂ contains traces of propionitrile that poison the Pt²⁺ catalyst. Commercial CD₃NO₂ (Cambridge) is free of nitriles and its use was cost effective because of the small solvent volume used for a typical cycloisomerization reaction (~200 μL).

²⁹ Colacot, T. J.; Qian, H.; Cea-Olivares, R.; Hernandez-Ortega, S. *J. Organomet. Chem.* **2001**, 637-639, 691-697.

³⁰ Ag⁺ silica was developed for separation of alkene byproducts from saturated cyclopropane products, see: Tong-Shuang, L.; Ji-Tai, L.; Hui-Zhang, L. *J. Chrom. A.* **1995**, 715, 372-375.

directly loaded onto a Ag^+ silica column. For **2**, **10**, **12**, **14**, **18**, and **20** the organic product was extracted with Et_2O and washed with H_2O several times to remove MeNO_2 . The extracts were dried over MgSO_4 , filtered, concentrated *in vacuo* and loaded onto a Ag^+ silica column.

2: Prepared from **1** as above with the crude material purified by chromatography on Ag^+ impregnated silica with 400:1 hexanes/ EtOAc to yield 51.5 mg (86%) of a clear oil. The enantiomeric purity was confirmed by GC (Agilent β -cyclosil, 80 °C for 5 min, 2 °C/min to 170 °C, hold 10 min): t_R 42.5 min (minor); 42.8 min (major). ^1H NMR: (400 MHz, CDCl_3) δ 7.24 (d, 1 H, $J = 7.2$ Hz), 7.16 (m, 1 H), 6.89 (m, 1 H), 6.83 (d, 1 H, $J = 7.8$ Hz), 3.79 (s, 3 H), 3.18 (d, 1 H, $J = 14.4$ Hz), 2.08 (d, 1 H, $J = 14.4$ Hz), 1.97 (m, 1 H), 1.67 (m, 1 H), 1.33 (m, 2 H), 1.27 (m, 1 H), 0.99 (m, 2 H), 0.94 (d, 3 H, $J = 6.6$ Hz), 0.64 (m, 1 H), 0.27 (dd, 1 H, $J = 4.2, 9.0$ Hz), 0.17 (t, 1 H, $J = 4.8$ Hz).

4: Prepared from **3** as above with the crude material purified by chromatography on Ag^+ impregnated silica with n-pentane. The solvent was removed by fractional distillation to yield 87.0 mg (70%) of a 33% w/w solution in n-pentane. The enantiomeric purity was confirmed by GC (Agilent β -cyclosil, isothermal 40 °C): t_R 17.3 min (minor); 18.7 min (major). ^1H NMR: (400 MHz, CDCl_3) δ 1.64 (m, 2 H), 1.55 (m, 3 H), 1.38 (m, 1 H), 1.15 (m, 1 H), 0.95 (m, 1 H), 0.91 (d, 3 H, $J = 6.8$ Hz), 0.85 (d, 3 H, $J = 6.8$ Hz), 0.24 (t, 1 H, $J = 4.0$ Hz), 0.17 (dd, 1 H, $J = 4.8, 8.0$ Hz).

6: Prepared from **5** as above with the crude material purified by chromatography on Ag^+ impregnated silica with n-pentane. The solvent was removed by fractional distillation to yield 99.5 mg (72%) of a 13% w/w solution in n-pentane; ^1H NMR: (400 MHz, CDCl_3) δ 1.99 (sep, 1 H, $J = 6.9$ Hz), 1.66 (m, 1 H), 1.45 (m, 1 H), 1.33 (m, 2 H),

1.16 (m, 1 H), 0.94 (m, 1 H), 0.91 (d, 3 H, $J = 7.2$ Hz), 0.89 (d, 3 H, $J = 6.8$ Hz), 0.75 (dd, 1 H, $J = 3.6, 7.8$ Hz), 0.26 (t, 1 H, $J = 4.2$ Hz), 0.21 (dd, 1 H, $J = 4.5, 7.8$ Hz).

8: Prepared from **7** as above with the crude material purified by chromatography on Ag^+ impregnated silica with n-pentane. The solvent was removed by fractional distillation to yield 93.2 mg (62%) of a 37% w/w solution in n-pentane. The enantiomeric purity was confirmed by GC (Agilent β -cyclosil, isothermal 40 °C): t_R 35.5 min (minor); 39.4 min (major). ^1H NMR: (400 MHz, CDCl_3) δ 1.81 (m, 1 H), 1.63 (m, 2 H), 1.42 (m, 1 H), 1.18 (m, 4 H), 0.89 (d, 3 H, $J = 6.0$ Hz), 0.88 (d, 3 H, $J = 6.0$ Hz), 0.80 (m, 1 H), 0.62 (m, 1 H), 0.29 (dd, 1 H, $J = 4.2, 9.0$ Hz), 0.12 (t, 1 H, $J = 4.8$ Hz).

10: Prepared from **9** as above with the crude material purified by chromatography on Ag^+ impregnated silica with 33:1 hexanes/EtOAc to yield 44.4 mg (71%) of a clear oil. The enantiomeric purity was confirmed by GC (Agilent β -cyclosil, 100 °C for 80 min, 2 °C/min to 140 °C, hold 20 min): t_R 66.7 min (major); 70.0 min (minor). ^1H NMR: (400 MHz, CDCl_3) δ 3.71 (s, 3 H), 3.69 (s, 3 H), 2.47 (m, 3 H), 2.33 (dd, 1 H, $J = 1.6, 13.6$ Hz), 1.42 (h, 1 H, $J = 6.8$ Hz), 1.12 (p, 1 H, $J = 4.4$ Hz), 0.95 (d, 3 H, $J = 6.8$ Hz), 0.85 (d, 3 H, $J = 6.8$ Hz), 0.36 (t, 1 H, $J = 6.8$ Hz), 0.08 (dd, 1 H, $J = 4.0, 5.6$ Hz).

12: Prepared from **11** as above with the crude material purified by chromatography on Ag^+ impregnated silica with 24:1 hexanes/EtOAc to yield 82.1 mg (78%) of a white solid; ^1H NMR: (400 MHz, CDCl_3) δ 8.04 (dd, 4 H, $J = 7.6, 17.2$ Hz), 7.69 (t, 2 H, $J = 7.6$ Hz) 7.58 (dt, 4 H, $J = 2.8, 8.0$ Hz), 2.98 (dd, 1 H, $J = 6.0, 16.0$ Hz), 2.61 (m, 3 H), 1.41 (h, 1 H, $J = 6.8$ Hz), 1.29 (m, 1 H), 0.89 (d, 3 H, $J = 6.8$ Hz) 0.57 (m, 5 H); ^{13}C NMR (100 MHz, CDCl_3) δ 137.1, 136.3, 134.51, 134.50, 131.6, 131.3, 128.72, 128.66, 128.5. HRMS (ESI) $[\text{M}+\text{H}]/z$ calc. 405.119, found 405.113.

14: Prepared from **13** as above with the crude material purified by chromatography on Ag⁺ impregnated silica with 200:1 hexanes/EtOAc to yield 72.8 mg (73%) of a colorless oil. The enantiomeric purity was confirmed by GC (Agilent β -cyclosil, 100 °C for 80 min, 2 °C/min to 140 °C, hold 20 min): t_R 58.4 min (major); 60.6 min (minor). ¹H NMR: (400 MHz, CDCl₃) δ 3.49 (m, 4 H), 1.74 (dd, 1 H, J = 5.6, 5.6 Hz), 1.63 (m, 2 H), 1.51 (d, 1 H, J = 14.0 Hz), 1.35 (s, 6 H), 1.26 (m, 1 H), 1.05 (m, 1 H), 0.89 (d, 3 H, J = 6.8 Hz), 0.81 (d, 3 H, J = 7.2 Hz), 0.51 (dd, 1 H, J = 4.8, 5.2 Hz), 0.041 (t, 1 H, J = 4.2 Hz); ¹³C NMR (100 MHz, CDCl₃) δ 97.4, 70.8, 70.6, 43.8, 37.5, 37.1, 36.3, 33.3, 24.3, 23.5, 23.2, 20.2, 20.0, 19.9. HRMS (ESI) [M+H]⁺/z calc. 225.185, found 225.193.

16: Prepared from **15** as above with the crude material purified by chromatography on Ag⁺ impregnated silica with 100:1 n-pentane/Et₂O. The solvent was removed by fractional distillation to yield 46.0 mg (64%) of a 32% w/w solution in n-pentane. An analytically pure sample could be obtained by drying at 0 °C/100 mm Hg with a substantial reduction in yield; ¹H NMR: (400 MHz, CDCl₃) δ 2.60 (dd, 1 H, J = 5.6, 18.8 Hz), 2.45 (d, 1 H, J = 18.8 Hz), 2.14 (m, 2 H), 1.40 (h, 1 H, J = 6.8 Hz), 1.33 (m, 1 H), 0.97 (d, 3 H, J = 6.8 Hz), 0.90 (d, 3 H, J = 6.8 Hz), 0.74 (m, 1 H), 0.049 (t, 1 H, J = 4.8 Hz); ¹³C NMR (100 MHz, CDCl₃) δ 218.4, 42.5, 41.8, 33.0, 30.2, 19.9, 19.8, 18.4, 18.0. HRMS (ESI) [M+Na]⁺/z calc. 161.094, found 161.093.

18: Prepared from **17** (12:1 *trans:cis* ratio) as above with the crude material purified by chromatography on Ag⁺ impregnated silica with 200:1 hexanes/EtOAc to yield 26.4 mg (18%) of a colorless oil; ¹H NMR: (400 MHz, CDCl₃) δ 3.70 (s, 3 H), 3.67 (s, 3 H), 2.51 (m, 3 H), 2.26 (d, 1 H, J = 18.0 Hz), 1.60 (m, 1 H), 1.31 (m, 1 H), 1.08 (m, 1 H), 0.89 (t, 3 H, J = 9.8 Hz), 0.31 (t, 1 H, J = 9.2 Hz), 0.092 (m, 1 H); ¹³C NMR (100 MHz,

CDCl₃) δ 173.4, 172.7, 59.8, 52.9, 52.7, 39.7, 36.6, 30.3, 28.3, 22.7, 14.6, 11.6. HRMS (ESI) [M+H]⁺/z calc. 227.128, found 227.127.

20: Prepared from **19** with the crude material purified by chromatography on silica gel with 6:1 hexanes/EtOAc to yield 65.4 mg (44%) of colorless oil. The enantiomeric purity was confirmed by GC (Agilent β -cyclosil, 170 °C for 5 min, 0.5 °C/min to 210 °C, hold 5 min): t_R 47.7 min (major); 48.3 min (minor). ¹H NMR: (300 MHz, CDCl₃) δ 7.67 (d, 2 H, J = 8.1 Hz), 7.31 (d, 2 H, J = 7.8 Hz), 3.47 (d, 1 H, J = 9.0 Hz), 3.43 (d, 1 H, J = 9.0 Hz), 3.07 (dd, 1 H, J = 9.0, 3.9 Hz), 2.96 (d, 2 H, J = 9.0 Hz), 2.43 (s, 3 H), 1.50 (h, 1 H, J = 6.9 Hz), 1.18 (p, 1 H, J = 3.9 Hz), 0.86 (d, 3 H, J = 6.9 Hz), 0.78 (d, 3 H, J = 6.9 Hz), 0.50 (dd, 1 H, J = 7.8, 5.1 Hz), 0.42 (t, 1 H, J = 4.5 Hz). ¹³C NMR (100 MHz, CDCl₃) δ 143.3, 133.9, 129.6, 127.4, 51.2, 50.4, 33.2, 30.1, 21.5, 20.2, 20.1, 19.5, 12.0. HRMS (ESI) [M + Na]⁺/z calc. 302.12, found 302.20.

[(dppm)(PMe₃)PtI][I]: To a solution of 70.5 mg (dppm)PtI₂ (84.6 μ mol) in 15 mL dichloromethane was added 8.6 μ L PMe₃ (84.6 μ mol). This solution was stirred for 30 minutes, the solvent was removed under reduced pressure and the resulting solid was washed several times with pentane to yield 69.1 mg (90%) of a pale yellow solid. Crystals of **19** suitable for X-ray crystallography were grown from a solution of dichloromethane and n-pentane at -26 °C; ¹H NMR: (400 MHz, CDCl₃) δ 7.82 (m, 8 H), 7.57 (m, 6 H), 7.45 (m, 6 H), 5.26 (t, 2 H, J = 11.0 Hz, ² J_{Pt-H} = 62.4 Hz), 1.57 (m, 9 H); ³¹P{¹H} NMR (161.8 MHz, CDCl₃) δ -17.91 (dt, 1 P, J = 32.3, 416.6 Hz, ¹ J_{Pt-P1} = 2333.4 Hz), -53.2 (m, 1 P, ¹ J_{Pt-P2} = 2935.3 Hz), -54.2 (dd, 1 P, J = 63.4, 416.8 Hz, ¹ J_{Pt-P3} = 1794.2 Hz).

***((R,R)*-*t*Bu-MiniPHOS)PtI₂**: To a solution of 436.5 mg (*R,R*)-*t*Bu-MiniPHOS(BH₃) (1.76 mmol) in 30 mL dichloromethane at 0 °C was added 1.5 mL HOTf (17.6 mmol) dropwise. Warm to room temperature after bubbling ceases and stir for 20 hours. At this point, dilute the reaction mixture with 10 mL of dichloromethane. The reaction was quenched with 25 mL of saturated NaHCO₃ solution and extracted two times with dichloromethane. The combined organic mixture was washed once with water and once with brine. The dichloromethane layer was dried over Na₂SO₄ and cannula filtered directly onto a solution of 580.0 mg of (COD)PtI₂ (1.04 mmol) in 10 mL of dichloromethane. The product precipitates out of solution and is collected by filtration. The remaining solid is washed with ether to remove any excess ligand and precipitated from dichloromethane and diethyl ether to yield 662.6 mg (56%) of a pale yellow solid; ¹H NMR: (400 MHz, CD₂Cl₂) δ 3.30 (t, 2 H, *J* = 10.4 Hz), 1.82 (d, 6 H, ²*J*_{P-H} = 11.0 Hz, ³*J*_{Pt-H} = 42.4 Hz), 1.34 (d, 18 H, ²*J*_{P-H} = 17.6 Hz); ³¹P{¹H} NMR (161.8 MHz, CD₂Cl₂) δ -54.4 (s, ¹*J*_{Pt-P} = 2834 Hz).

Appendix A

X-Ray Structure of [(CyPPP)PtMe][Cl] (Chapter 2)

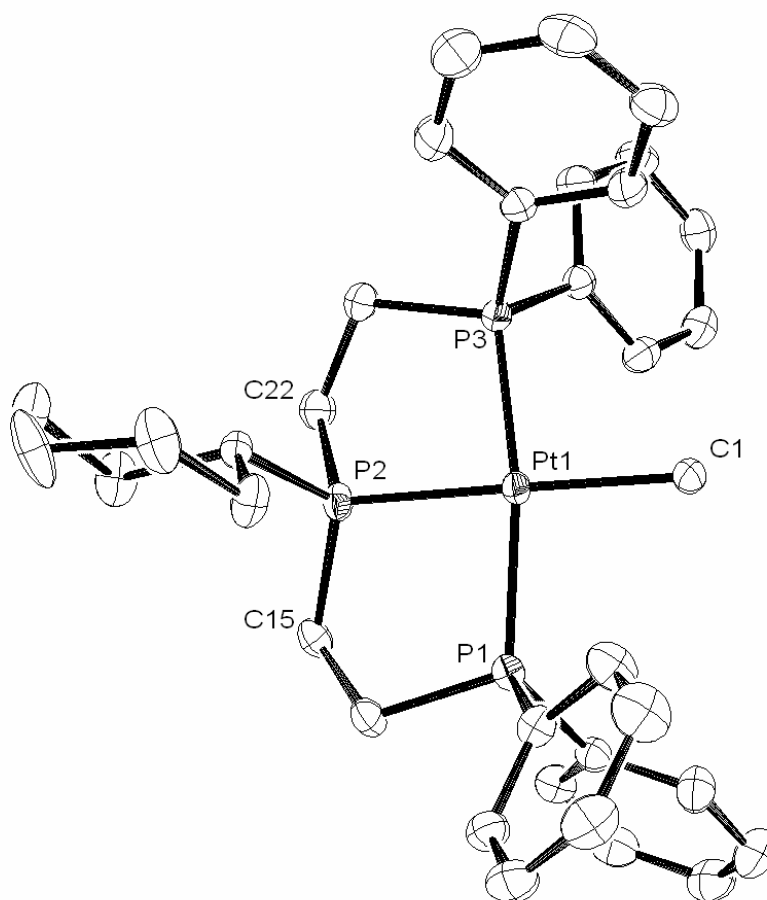


Figure A.1. ORTEP representation of [(CyPPP)PtMe][Cl].

Table A.1. Bond distances (Å) for [(CyPPP)PtMe][Cl].

Bond	Length (Å)	Bond	Length (Å)
Pt(1)-C(1)	2.144(2)	C(18)-H(18B)	0.9700
Pt(1)-P(2)	2.2674(6)	C(19)-C(20)	1.3239
Pt(1)-P(1)	2.2907(6)	C(19)-H(19A)	0.9700
Pt(1)-P(3)	2.2949(6)	C(19)-H(19B)	0.9700
P(1)-C(8)	1.819(3)	C(20)-C(21)	1.5632
P(1)-C(2)	1.823(3)	C(20)-H(20A)	0.9700
P(1)-C(14)	1.852(2)	C(20)-H(20B)	0.9700
P(3)-C(24)	1.813(3)	C(21)-H(21A)	0.9700
P(3)-C(30)	1.817(3)	C(21)-H(21B)	0.9700
P(3)-C(23)	1.851(2)	C(16A)-C(17A)	1.2578
P(2)-C(15)	1.8228(15)	C(16A)-C(21A)	1.5733
P(2)-C(22)	1.8252(15)	C(17A)-C(18A)	1.6787
P(2)-C(16)	1.8353(14)	C(17A)-H(17B)	1.3401
P(2)-C(16A)	1.8690(14)	C(17A)-H(17C)	0.9700
Cl(2)-C(36)	1.769(3)	C(17A)-H(17D)	0.9700
Cl(3)-C(36)	1.774(3)	C(18A)-C(19A)	1.5367
Cl(4)-C(36)	1.760(3)	C(18A)-H(18C)	0.9700
C(1)-H(1A)	0.9600	C(18A)-H(18D)	0.9700
C(1)-H(1B)	0.9600	C(19A)-C(20A)	1.3084
C(1)-H(1C)	0.9600	C(19A)-H(19C)	0.9700
C(2)-C(3)	1.394(3)	C(19A)-H(19D)	0.9700
C(2)-C(7)	1.395(4)	C(20A)-C(21A)	1.5737
C(3)-C(4)	1.391(4)	C(20A)-H(20C)	0.9700
C(3)-H(3)	0.9300	C(20A)-H(20D)	0.9700
C(4)-C(5)	1.383(5)	C(21A)-H(21C)	0.9700
C(4)-H(4)	0.9300	C(21A)-H(21D)	0.9700
C(5)-C(6)	1.377(4)	C(22)-C(23)	1.541(3)
C(5)-H(5)	0.9300	C(22)-H(22A)	0.9700
C(6)-C(7)	1.390(4)	C(22)-H(22B)	0.9700
C(6)-H(6)	0.9300	C(23)-H(23A)	0.9700
C(7)-H(7)	0.9300	C(23)-H(23B)	0.9700
C(8)-C(9)	1.387(4)	C(24)-C(25)	1.398(4)
C(8)-C(13)	1.395(4)	C(24)-C(29)	1.401(3)
C(9)-C(10)	1.396(4)	C(25)-C(26)	1.387(4)
C(9)-H(9)	0.9300	C(25)-H(25)	0.9300
C(10)-C(11)	1.379(5)	C(26)-C(27)	1.377(5)
C(10)-H(10)	0.9300	C(26)-H(26)	0.9300
C(11)-C(12)	1.387(4)	C(27)-C(28)	1.386(4)
C(11)-H(11)	0.9300	C(27)-H(27)	0.9300
C(12)-C(13)	1.384(4)	C(28)-C(29)	1.382(4)
C(12)-H(12)	0.9300	C(28)-H(28)	0.9300
C(13)-H(13)	0.9300	C(29)-H(29)	0.9300
C(14)-C(15)	1.549(3)	C(30)-C(35)	1.394(3)
C(14)-H(14A)	0.9700	C(30)-C(31)	1.397(4)
C(14)-H(14B)	0.9700	C(31)-C(32)	1.393(4)
C(15)-H(15A)	0.9700	C(31)-H(31)	0.9300
C(15)-H(15B)	0.9700	C(32)-C(33)	1.392(4)
C(16)-C(17)	1.3194	C(32)-H(32)	0.9300
C(16)-C(21)	1.5669	C(33)-C(34)	1.378(4)
C(17)-C(18)	1.6519	C(33)-H(33)	0.9300
C(17)-H(17A)	0.9700	C(34)-C(35)	1.392(4)
C(17)-H(17B)	0.9700	C(34)-H(34)	0.9300

C(18)-C(19)	1.5325	C(35)-H(35)	0.9300
C(18)-H(18A)	0.9700	C(36)-H(36)	0.9800

Table A.2. Bond angles (°) for [(CyPPP)PtMe][Cl].

Bonds	Angle (°)	Bonds	Angle (°)
C(1)-Pt(1)-P(2)	177.30(7)	C(19)-C(20)-H(20B)	107.6
C(1)-Pt(1)-P(1)	94.69(6)	C(21)-C(20)-H(20B)	107.6
P(2)-Pt(1)-P(1)	85.25(2)	H(20A)-C(20)-H(20B)	107.0
C(1)-Pt(1)-P(3)	94.97(6)	C(20)-C(21)-C(16)	117.5
P(2)-Pt(1)-P(3)	84.80(2)	C(20)-C(21)-H(21A)	107.9
P(1)-Pt(1)-P(3)	168.45(2)	C(16)-C(21)-H(21A)	107.9
C(8)-P(1)-C(2)	103.51(11)	C(20)-C(21)-H(21B)	107.9
C(8)-P(1)-C(14)	105.08(12)	C(16)-C(21)-H(21B)	107.9
C(2)-P(1)-C(14)	104.53(12)	H(21A)-C(21)-H(21B)	107.2
C(8)-P(1)-Pt(1)	117.16(9)	C(17A)-C(16A)-C(21A)	125.8
C(2)-P(1)-Pt(1)	117.26(8)	C(17A)-C(16A)-P(2)	124.5
C(14)-P(1)-Pt(1)	108.00(8)	C(21A)-C(16A)-P(2)	109.6
C(24)-P(3)-C(30)	104.28(11)	C(16A)-C(17A)-C(18A)	113.3
C(24)-P(3)-C(23)	107.04(12)	C(16A)-C(17A)-H(17B)	99.1
C(30)-P(3)-C(23)	105.15(13)	C(18A)-C(17A)-H(17B)	83.5
C(24)-P(3)-Pt(1)	115.46(9)	C(16A)-C(17A)-H(17C)	108.9
C(30)-P(3)-Pt(1)	116.08(8)	C(18A)-C(17A)-H(17C)	108.9
C(23)-P(3)-Pt(1)	108.05(9)	H(17B)-C(17A)-H(17C)	34.8
C(15)-P(2)-C(22)	111.57(7)	C(16A)-C(17A)-H(17D)	108.9
C(15)-P(2)-C(16)	114.39(7)	C(18A)-C(17A)-H(17D)	108.9
C(22)-P(2)-C(16)	99.84(7)	H(17B)-C(17A)-H(17D)	140.5
C(15)-P(2)-C(16A)	98.40(7)	H(17C)-C(17A)-H(17D)	107.7
C(22)-P(2)-C(16A)	114.47(7)	C(19A)-C(18A)-C(17A)	112.0
C(16)-P(2)-C(16A)	17.8	C(19A)-C(18A)-H(18C)	109.2
C(15)-P(2)-Pt(1)	107.20(4)	C(17A)-C(18A)-H(18C)	109.2
C(22)-P(2)-Pt(1)	105.50(4)	C(19A)-C(18A)-H(18D)	109.2
C(16)-P(2)-Pt(1)	117.80(5)	C(17A)-C(18A)-H(18D)	109.2
C(16A)-P(2)-Pt(1)	119.38(5)	H(18C)-C(18A)-H(18D)	107.9
Pt(1)-C(1)-H(1A)	109.5	C(20A)-C(19A)-C(18A)	119.2
Pt(1)-C(1)-H(1B)	109.5	C(20A)-C(19A)-H(19C)	107.5
H(1A)-C(1)-H(1B)	109.5	C(18A)-C(19A)-H(19C)	107.5
Pt(1)-C(1)-H(1C)	109.5	C(20A)-C(19A)-H(19D)	107.5
H(1A)-C(1)-H(1C)	109.5	C(18A)-C(19A)-H(19D)	107.5
H(1B)-C(1)-H(1C)	109.5	H(19C)-C(19A)-H(19D)	107.0
C(3)-C(2)-C(7)	119.3(2)	C(19A)-C(20A)-C(21A)	122.1
C(3)-C(2)-P(1)	120.7(2)	C(19A)-C(20A)-H(20C)	106.8
C(7)-C(2)-P(1)	119.98(19)	C(21A)-C(20A)-H(20C)	106.8
C(4)-C(3)-C(2)	119.9(3)	C(19A)-C(20A)-H(20D)	106.8
C(4)-C(3)-H(3)	120.1	C(21A)-C(20A)-H(20D)	106.8
C(2)-C(3)-H(3)	120.1	H(20C)-C(20A)-H(20D)	106.6
C(5)-C(4)-C(3)	120.4(3)	C(16A)-C(21A)-C(20A)	111.4
C(5)-C(4)-H(4)	119.8	C(16A)-C(21A)-H(21C)	109.4
C(3)-C(4)-H(4)	119.8	C(20A)-C(21A)-H(21C)	109.4
C(6)-C(5)-C(4)	120.0(3)	C(16A)-C(21A)-H(21D)	109.4
C(6)-C(5)-H(5)	120.0	C(20A)-C(21A)-H(21D)	109.4
C(4)-C(5)-H(5)	120.0	H(21C)-C(21A)-H(21D)	108.0
C(5)-C(6)-C(7)	120.3(3)	C(23)-C(22)-P(2)	107.26(13)
C(5)-C(6)-H(6)	119.9	C(23)-C(22)-H(22A)	110.3

C(7)-C(6)-H(6)	119.9	P(2)-C(22)-H(22A)	110.3
C(6)-C(7)-C(2)	120.1(3)	C(23)-C(22)-H(22B)	110.2
C(6)-C(7)-H(7)	119.9	P(2)-C(22)-H(22B)	110.2
C(2)-C(7)-H(7)	119.9	H(22A)-C(22)-H(22B)	108.5
C(9)-C(8)-C(13)	119.3(2)	C(22)-C(23)-P(3)	110.26(15)
C(9)-C(8)-P(1)	120.3(2)	C(22)-C(23)-H(23A)	109.6
C(13)-C(8)-P(1)	120.4(2)	P(3)-C(23)-H(23A)	109.6
C(8)-C(9)-C(10)	120.2(3)	C(22)-C(23)-H(23B)	109.6
C(8)-C(9)-H(9)	119.9	P(3)-C(23)-H(23B)	109.6
C(10)-C(9)-H(9)	119.9	H(23A)-C(23)-H(23B)	108.1
C(11)-C(10)-C(9)	119.9(3)	C(25)-C(24)-C(29)	118.1(3)
C(11)-C(10)-H(10)	120.1	C(25)-C(24)-P(3)	124.5(2)
C(9)-C(10)-H(10)	120.1	C(29)-C(24)-P(3)	117.27(19)
C(10)-C(11)-C(12)	120.2(3)	C(26)-C(25)-C(24)	120.3(3)
C(10)-C(11)-H(11)	119.9	C(26)-C(25)-H(25)	119.8
C(12)-C(11)-H(11)	119.9	C(24)-C(25)-H(25)	119.8
C(13)-C(12)-C(11)	119.9(3)	C(27)-C(26)-C(25)	120.9(3)
C(13)-C(12)-H(12)	120.0	C(27)-C(26)-H(26)	119.6
C(11)-C(12)-H(12)	120.0	C(25)-C(26)-H(26)	119.6
C(12)-C(13)-C(8)	120.4(3)	C(26)-C(27)-C(28)	119.5(3)
C(12)-C(13)-H(13)	119.8	C(26)-C(27)-H(27)	120.3
C(8)-C(13)-H(13)	119.8	C(28)-C(27)-H(27)	120.3
C(15)-C(14)-P(1)	111.65(14)	C(29)-C(28)-C(27)	120.2(3)
C(15)-C(14)-H(14A)	109.3	C(29)-C(28)-H(28)	119.9
P(1)-C(14)-H(14A)	109.3	C(27)-C(28)-H(28)	119.9
C(15)-C(14)-H(14B)	109.3	C(28)-C(29)-C(24)	121.0(3)
P(1)-C(14)-H(14B)	109.3	C(28)-C(29)-H(29)	119.5
H(14A)-C(14)-H(14B)	108.0	C(24)-C(29)-H(29)	119.5
C(14)-C(15)-P(2)	107.49(12)	C(35)-C(30)-C(31)	119.5(2)
C(14)-C(15)-H(15A)	110.2	C(35)-C(30)-P(3)	121.13(19)
P(2)-C(15)-H(15A)	110.2	C(31)-C(30)-P(3)	119.4(2)
C(14)-C(15)-H(15B)	110.2	C(32)-C(31)-C(30)	119.8(3)
P(2)-C(15)-H(15B)	110.2	C(32)-C(31)-H(31)	120.1
H(15A)-C(15)-H(15B)	108.5	C(30)-C(31)-H(31)	120.1
C(17)-C(16)-C(21)	117.5	C(33)-C(32)-C(31)	120.2(3)
C(17)-C(16)-P(2)	129.8	C(33)-C(32)-H(32)	119.9
C(21)-C(16)-P(2)	112.3	C(31)-C(32)-H(32)	119.9
C(16)-C(17)-C(18)	117.2	C(34)-C(33)-C(32)	120.0(3)
C(16)-C(17)-H(17A)	108.0	C(34)-C(33)-H(33)	120.0
C(18)-C(17)-H(17A)	108.0	C(32)-C(33)-H(33)	120.0
C(16)-C(17)-H(17B)	108.0	C(33)-C(34)-C(35)	120.2(3)
C(18)-C(17)-H(17B)	108.0	C(33)-C(34)-H(34)	119.9
H(17A)-C(17)-H(17B)	107.2	C(35)-C(34)-H(34)	119.9
C(19)-C(18)-C(17)	110.8	C(34)-C(35)-C(30)	120.2(2)
C(19)-C(18)-H(18A)	109.5	C(34)-C(35)-H(35)	119.9
C(17)-C(18)-H(18A)	109.5	C(30)-C(35)-H(35)	119.9
C(19)-C(18)-H(18B)	109.5	Cl(4)-C(36)-Cl(2)	109.88(15)
C(17)-C(18)-H(18B)	109.5	Cl(4)-C(36)-Cl(3)	110.38(15)
H(18A)-C(18)-H(18B)	108.1	Cl(2)-C(36)-Cl(3)	109.80(16)
C(20)-C(19)-C(18)	118.9	Cl(4)-C(36)-H(36)	108.9
C(20)-C(19)-H(19A)	107.6	Cl(2)-C(36)-H(36)	108.9
C(18)-C(19)-H(19A)	107.6	Cl(3)-C(36)-H(36)	108.9
C(20)-C(19)-H(19B)	107.6	C(19)-C(20)-C(21)	118.8
C(18)-C(19)-H(19B)	107.6	C(19)-C(20)-H(20A)	107.6
H(19A)-C(19)-H(19B)	107.0	C(21)-C(20)-H(20A)	107.6

Appendix B

X-Ray Structure of **3** (Chapter 3)

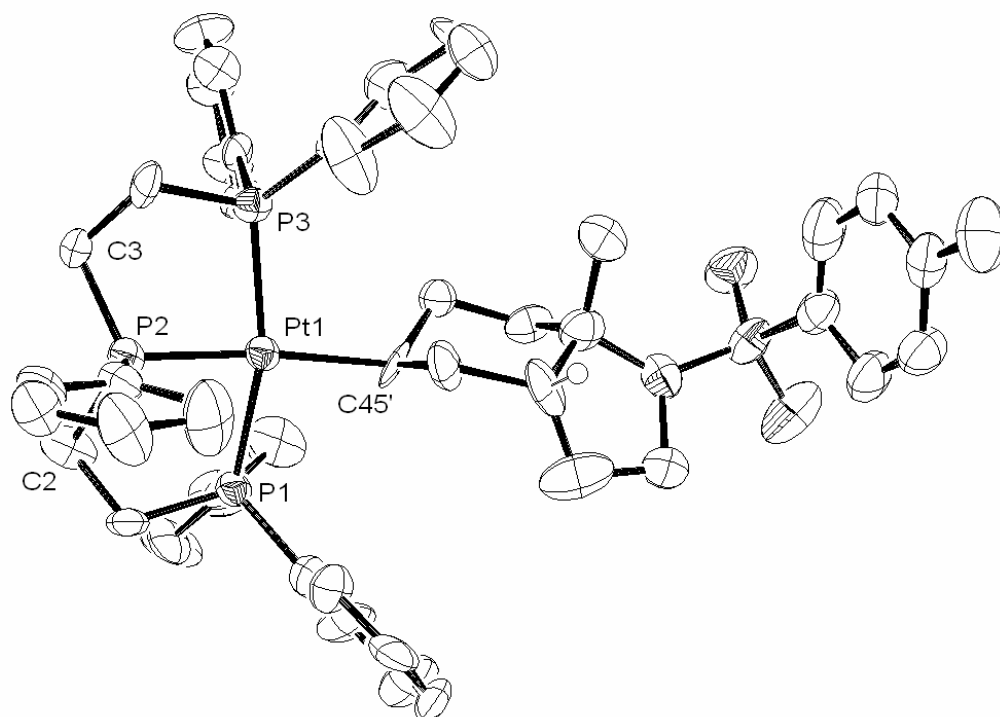


Figure B.1. ORTEP representation of **3**.

Table B.1. Bond distances (Å) for **3**.

Bond	Length (Å)	Bond	Length (Å)
Pt(1)-C(45)	2.150(11)	C(24)-C(25)	1.33(2)
Pt(1)-P(2)	2.247(3)	C(24)-C(29)	1.400(19)
Pt(1)-P(1)	2.269(4)	C(25)-C(26)	1.35(2)
Pt(1)-P(3)	2.308(4)	C(26)-C(27)	1.37(2)
P(1)-C(11)	1.814(15)	C(27)-C(28)	1.40(2)
P(1)-C(1)	1.845(16)	C(28)-C(29)	1.36(2)
P(1)-C(5)	1.854(17)	C(30)-C(31)	1.40(2)
P(2)-C(17)	1.789(13)	C(30)-C(35)	1.41(2)
P(2)-C(3)	1.826(14)	C(31)-C(32)	1.43(2)
P(2)-C(2)	1.842(15)	C(32)-C(33)	1.34(3)
P(3)-C(30)	1.795(15)	C(33)-C(34)	1.33(3)
P(3)-C(29)	1.824(13)	C(34)-C(35)	1.38(2)
P(3)-C(4)	1.847(14)	C(37)-C(45)	1.544(10)
S(1)-O(46)	1.406(12)	C(37)-C(38)	1.547(10)
S(1)-O(47)	1.469(13)	C(38)-C(39)	1.54(2)
S(1)-N(40)	1.605(13)	C(45)-C(44)	1.636(18)
S(1)-C(48)	1.736(17)	C(39)-C(43)	1.50(2)
C(1)-C(2)	1.47(2)	C(39)-N(40)	1.50(2)
C(3)-C(4)	1.49(2)	C(39)-C(55)	1.55(2)
C(5)-C(10)	1.33(2)	N(40)-C(41)	1.54(2)
C(5)-C(6)	1.40(2)	C(41)-C(42)	1.46(3)
C(6)-C(7)	1.38(2)	C(42)-C(43)	1.50(3)
C(7)-C(8)	1.40(3)	C(43)-C(44)	1.59(2)
C(8)-C(9)	1.34(3)	C(48)-C(49)	1.31(3)
C(9)-C(10)	1.38(2)	C(48)-C(53)	1.42(2)
C(11)-C(12)	1.41(2)	C(49)-C(50)	1.38(3)
C(11)-C(16)	1.42(2)	C(50)-C(51)	1.37(2)
C(12)-C(13)	1.37(3)	C(51)-C(52)	1.40(2)
C(13)-C(14)	1.39(3)	C(51)-C(54)	1.50(2)
C(14)-C(15)	1.41(3)	C(52)-C(53)	1.38(2)
C(15)-C(16)	1.37(2)	B(61)-F(62)	1.27(2)
C(17)-C(18)	1.361(19)	B(61)-F(64)	1.335(19)
C(17)-C(22)	1.458(19)	B(61)-F(65)	1.35(2)
C(18)-C(19)	1.397(19)	B(61)-F(63)	1.41(4)
C(19)-C(20)	1.42(2)	C(71)-Cl(2)	1.742(10)
C(20)-C(21)	1.36(2)	C(71)-Cl(1)	1.753(10)
C(21)-C(22)	1.38(2)		

Table B.2. Bond angles (°) for **3**.

Bonds	Angle (°)	Bonds	Angle (°)
C(45)-Pt(1)-P(2)	170.5(4)	C(20)-C(21)-C(22)	121.0(15)
C(45)-Pt(1)-P(1)	92.2(4)	C(21)-C(22)-C(17)	120.1(14)
P(2)-Pt(1)-P(1)	84.51(16)	C(25)-C(24)-C(29)	121.0(14)
C(45)-Pt(1)-P(3)	100.6(4)	C(24)-C(25)-C(26)	120.7(15)
P(2)-Pt(1)-P(3)	84.63(16)	C(25)-C(26)-C(27)	120.9(15)
P(1)-Pt(1)-P(3)	162.28(10)	C(26)-C(27)-C(28)	117.9(16)
C(11)-P(1)-C(1)	108.2(8)	C(29)-C(28)-C(27)	121.3(15)
C(11)-P(1)-C(5)	104.7(7)	C(28)-C(29)-C(24)	118.1(13)
C(1)-P(1)-C(5)	105.9(6)	C(28)-C(29)-P(3)	121.8(11)
C(11)-P(1)-Pt(1)	111.2(5)	C(24)-C(29)-P(3)	119.9(11)
C(1)-P(1)-Pt(1)	107.7(5)	C(31)-C(30)-C(35)	115.1(16)
C(5)-P(1)-Pt(1)	118.6(5)	C(31)-C(30)-P(3)	123.5(14)
C(17)-P(2)-C(3)	103.3(7)	C(35)-C(30)-P(3)	121.4(12)
C(17)-P(2)-C(2)	105.9(7)	C(30)-C(31)-C(32)	120.7(18)
C(3)-P(2)-C(2)	117.0(6)	C(33)-C(32)-C(31)	120.2(18)
C(17)-P(2)-Pt(1)	112.9(4)	C(34)-C(33)-C(32)	120.8(16)
C(3)-P(2)-Pt(1)	109.9(5)	C(33)-C(34)-C(35)	120.9(17)
C(2)-P(2)-Pt(1)	107.9(6)	C(34)-C(35)-C(30)	122.0(17)
C(30)-P(3)-C(29)	107.8(7)	C(45)-C(37)-C(38)	107.3(13)
C(30)-P(3)-C(4)	106.4(7)	C(39)-C(38)-C(37)	119(3)
C(29)-P(3)-C(4)	102.6(7)	C(37)-C(45)-C(44)	118(3)
C(30)-P(3)-Pt(1)	120.7(5)	C(37)-C(45)-Pt(1)	142(2)
C(29)-P(3)-Pt(1)	112.0(5)	C(44)-C(45)-Pt(1)	99.7(8)
C(4)-P(3)-Pt(1)	105.7(5)	C(43)-C(39)-N(40)	102.2(13)
O(46)-S(1)-O(47)	119.3(8)	C(43)-C(39)-C(38)	115.1(13)
O(46)-S(1)-N(40)	107.8(8)	N(40)-C(39)-C(38)	105.3(12)
O(47)-S(1)-N(40)	106.8(9)	C(43)-C(39)-C(55)	110.5(14)
O(46)-S(1)-C(48)	108.7(9)	N(40)-C(39)-C(55)	111.7(13)
O(47)-S(1)-C(48)	105.1(8)	C(38)-C(39)-C(55)	111.5(13)
N(40)-S(1)-C(48)	108.9(8)	C(39)-N(40)-C(41)	111.6(13)
C(2)-C(1)-P(1)	109.7(11)	C(39)-N(40)-S(1)	130.8(13)
C(1)-C(2)-P(2)	106.8(11)	C(41)-N(40)-S(1)	114.8(11)
C(4)-C(3)-P(2)	105.1(10)	C(42)-C(41)-N(40)	99.9(15)
C(3)-C(4)-P(3)	113.2(11)	C(41)-C(42)-C(43)	108.1(18)
C(10)-C(5)-C(6)	122.1(17)	C(39)-C(43)-C(42)	103.7(15)
C(10)-C(5)-P(1)	122.6(14)	C(39)-C(43)-C(44)	110.4(13)
C(6)-C(5)-P(1)	115.2(13)	C(42)-C(43)-C(44)	122.9(16)
C(7)-C(6)-C(5)	118(2)	C(43)-C(44)-C(45)	110.7(11)
C(6)-C(7)-C(8)	120(2)	C(49)-C(48)-C(53)	119.3(16)
C(9)-C(8)-C(7)	118.4(18)	C(49)-C(48)-S(1)	121.1(14)
C(8)-C(9)-C(10)	123(2)	C(53)-C(48)-S(1)	119.5(14)
C(5)-C(10)-C(9)	118.1(19)	C(48)-C(49)-C(50)	123.8(18)
C(12)-C(11)-C(16)	116.9(15)	C(51)-C(50)-C(49)	119.2(19)
C(12)-C(11)-P(1)	122.9(14)	C(50)-C(51)-C(52)	117.5(17)
C(16)-C(11)-P(1)	120.2(13)	C(50)-C(51)-C(54)	123(2)
C(13)-C(12)-C(11)	120.5(18)	C(52)-C(51)-C(54)	119.5(17)
C(12)-C(13)-C(14)	121.3(16)	C(53)-C(52)-C(51)	122.5(17)
C(13)-C(14)-C(15)	119.7(17)	C(52)-C(53)-C(48)	117.5(17)
C(16)-C(15)-C(14)	118(2)	F(62)-B(61)-F(64)	115.9(18)
C(15)-C(16)-C(11)	123.0(17)	F(62)-B(61)-F(65)	120.1(18)
C(18)-C(17)-C(22)	115.8(12)	F(64)-B(61)-F(65)	114.9(16)
C(18)-C(17)-P(2)	124.9(11)	F(62)-B(61)-F(63)	97(3)

C(22)-C(17)-P(2)	119.1(10)	F(64)-B(61)-F(63)	100(2)
C(17)-C(18)-C(19)	123.9(13)	F(65)-B(61)-F(63)	103.6(18)
C(18)-C(19)-C(20)	118.1(15)	Cl(2)-C(71)-Cl(1)	109.4(12)
C(21)-C(20)-C(19)	119.5(15)		

Appendix C

X-Ray Structure of 5 (Chapter 3)

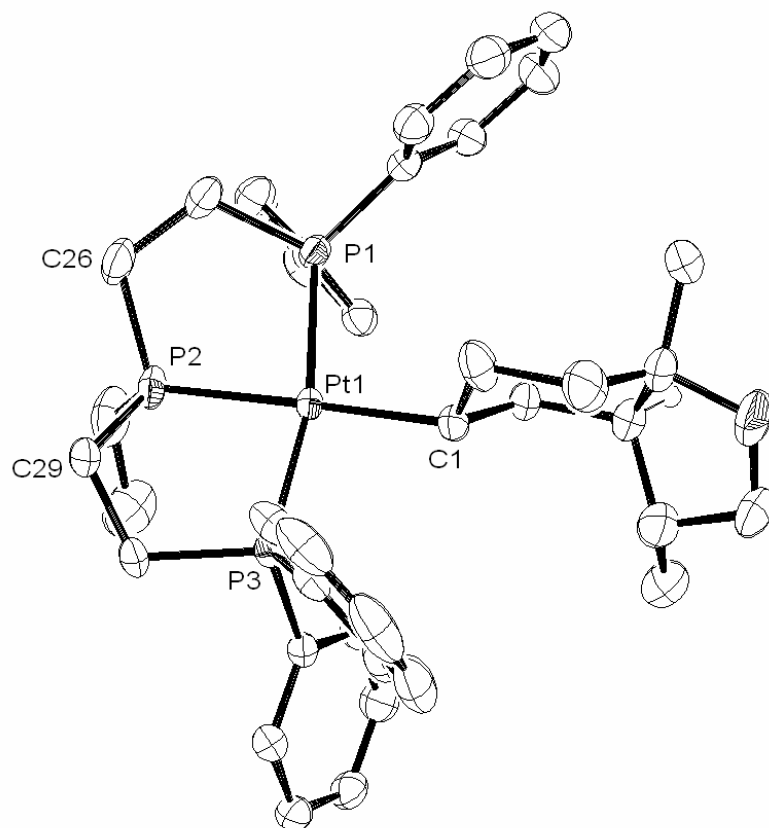


Figure C.1. ORTEP representation of 5.

Table C.1. Bond distances (Å) for **5**.

Bond	Length (Å)	Bond	Length (Å)
Pt(1)-C(1)	2.134(3)	C(14)-C(15)	1.388(6)
Pt(1)-P(3)	2.2722(8)	C(15)-C(16)	1.399(6)
Pt(1)-P(2)	2.3016(8)	C(16)-C(17)	1.397(5)
Pt(1)-P(1)	2.3032(8)	C(19)-C(24)	1.397(5)
P(1)-C(12)	1.819(3)	C(19)-C(20)	1.397(5)
P(1)-C(19)	1.822(3)	C(20)-C(21)	1.400(5)
P(1)-C(25)	1.846(4)	C(21)-C(22)	1.382(6)
P(2)-C(29)	1.842(4)	C(22)-C(23)	1.394(7)
P(2)-C(27)	1.843(5)	C(23)-C(24)	1.390(6)
P(2)-C(26)	1.850(4)	C(25)-C(26)	1.541(6)
P(3)-C(31)	1.818(3)	C(27)-C(28)	1.475(8)
P(3)-C(37)	1.822(4)	C(29)-C(30)	1.542(5)
P(3)-C(30)	1.861(3)	C(31)-C(36)	1.400(5)
C(1)-C(2)	1.512(5)	C(31)-C(32)	1.403(4)
C(1)-C(9)	1.541(6)	C(32)-C(33)	1.392(5)
C(2)-C(3)	1.556(5)	C(33)-C(34)	1.397(5)
C(3)-C(4)	1.525(7)	C(34)-C(35)	1.392(6)
C(3)-C(7)	1.562(6)	C(35)-C(36)	1.394(5)
C(4)-O(18)	1.457(5)	C(37)-C(38)	1.401(5)
C(4)-C(10)	1.528(6)	C(37)-C(42)	1.403(5)
C(4)-C(8)	1.534(7)	C(38)-C(39)	1.402(6)
C(6)-O(18)	1.412(6)	C(39)-C(40)	1.391(8)
C(6)-C(7)	1.540(6)	C(40)-C(41)	1.381(8)
C(7)-C(11)	1.526(7)	C(41)-C(42)	1.397(6)
C(8)-C(9)	1.534(6)	B(1)-F(2)	1.315(6)
C(12)-C(17)	1.405(5)	B(1)-F(1)	1.333(6)
C(12)-C(13)	1.410(5)	B(1)-F(4)	1.375(7)
C(13)-C(14)	1.397(6)	B(1)-F(3)	1.418(6)

Table C.2. Bond angles (°) for **5**.

Bonds	Angle (°)	Bonds	Angle (°)
C(1)-Pt(1)-P(3)	90.04(9)	O(18)-C(6)-C(7)	107.8(3)
C(1)-Pt(1)-P(2)	173.01(10)	C(11)-C(7)-C(6)	116.1(4)
P(3)-Pt(1)-P(2)	85.87(3)	C(11)-C(7)-C(3)	113.5(4)
C(1)-Pt(1)-P(1)	101.07(9)	C(6)-C(7)-C(3)	101.4(4)
P(3)-Pt(1)-P(1)	166.86(3)	C(4)-C(8)-C(9)	112.8(4)
P(2)-Pt(1)-P(1)	82.35(3)	C(8)-C(9)-C(1)	112.8(4)
C(12)-P(1)-C(19)	105.17(15)	C(17)-C(12)-C(13)	118.8(3)
C(12)-P(1)-C(25)	104.01(17)	C(17)-C(12)-P(1)	121.4(3)
C(19)-P(1)-C(25)	107.12(17)	C(13)-C(12)-P(1)	119.8(3)
C(12)-P(1)-Pt(1)	125.26(11)	C(14)-C(13)-C(12)	120.5(4)
C(19)-P(1)-Pt(1)	110.17(11)	C(15)-C(14)-C(13)	120.0(4)
C(25)-P(1)-Pt(1)	103.82(12)	C(14)-C(15)-C(16)	120.3(4)
C(29)-P(2)-C(27)	109.9(2)	C(17)-C(16)-C(15)	119.9(4)
C(29)-P(2)-C(26)	110.85(18)	C(16)-C(17)-C(12)	120.5(4)
C(27)-P(2)-C(26)	99.6(2)	C(6)-O(18)-C(4)	109.8(3)
C(29)-P(2)-Pt(1)	104.73(13)	C(24)-C(19)-C(20)	118.7(3)
C(27)-P(2)-Pt(1)	121.81(16)	C(26)-C(25)-P(1)	112.1(3)

C(26)-P(2)-Pt(1)	109.86(13)	C(25)-C(26)-P(2)	111.4(2)
C(31)-P(3)-C(37)	105.96(16)	C(28)-C(27)-P(2)	115.7(4)
C(31)-P(3)-C(30)	104.83(15)	C(30)-C(29)-P(2)	109.2(2)
C(37)-P(3)-C(30)	105.07(17)	C(29)-C(30)-P(3)	113.2(2)
C(31)-P(3)-Pt(1)	116.13(11)	C(36)-C(31)-C(32)	119.3(3)
C(37)-P(3)-Pt(1)	115.68(10)	C(36)-C(31)-P(3)	119.1(2)
C(30)-P(3)-Pt(1)	108.12(12)	C(32)-C(31)-P(3)	121.6(2)
C(2)-C(1)-C(9)	110.1(3)	C(33)-C(32)-C(31)	120.5(3)
C(2)-C(1)-Pt(1)	114.2(2)	C(32)-C(33)-C(34)	119.9(3)
C(9)-C(1)-Pt(1)	112.4(2)	C(35)-C(34)-C(33)	119.9(3)
C(1)-C(2)-C(3)	111.4(3)	C(34)-C(35)-C(36)	120.4(3)
C(4)-C(3)-C(2)	114.7(3)	C(35)-C(36)-C(31)	120.1(3)
C(4)-C(3)-C(7)	100.8(4)	C(38)-C(37)-C(42)	120.1(4)
C(2)-C(3)-C(7)	117.5(3)	C(38)-C(37)-P(3)	122.3(3)
O(18)-C(4)-C(3)	104.5(4)	C(42)-C(37)-P(3)	117.7(3)
O(18)-C(4)-C(10)	106.8(3)	C(37)-C(38)-C(39)	119.3(4)
C(3)-C(4)-C(10)	112.8(4)	C(40)-C(39)-C(38)	120.1(5)
O(18)-C(4)-C(8)	108.3(4)	C(41)-C(40)-C(39)	120.7(4)
C(3)-C(4)-C(8)	111.3(3)	C(40)-C(41)-C(42)	120.0(4)
C(10)-C(4)-C(8)	112.7(4)	C(41)-C(42)-C(37)	119.8(4)
C(24)-C(19)-P(1)	122.8(3)	F(2)-B(1)-F(1)	109.5(5)
C(20)-C(19)-P(1)	118.5(3)	F(2)-B(1)-F(4)	107.0(5)
C(19)-C(20)-C(21)	120.7(4)	F(1)-B(1)-F(4)	108.3(6)
C(22)-C(21)-C(20)	119.9(4)	F(2)-B(1)-F(3)	120.0(6)
C(21)-C(22)-C(23)	119.8(4)	F(1)-B(1)-F(3)	106.8(4)
C(24)-C(23)-C(22)	120.4(4)	F(4)-B(1)-F(3)	104.8(4)
C(23)-C(24)-C(19)	120.4(4)		

Table C.3. Torsion angles ($^{\circ}$) for **5**.

Bonds	Angle ($^{\circ}$)	Bonds	Angle ($^{\circ}$)
C(1)-Pt(1)-P(1)-C(12)	-17.64(18)	C(15)-C(16)-C(17)-C(12)	-1.0(6)
P(3)-Pt(1)-P(1)-C(12)	129.65(18)	C(13)-C(12)-C(17)-C(16)	1.1(5)
P(2)-Pt(1)-P(1)-C(12)	156.18(15)	P(1)-C(12)-C(17)-C(16)	-176.7(3)
C(1)-Pt(1)-P(1)-C(19)	109.30(16)	C(7)-C(6)-O(18)-C(4)	0.7(6)
P(3)-Pt(1)-P(1)-C(19)	-103.41(17)	C(3)-C(4)-O(18)-C(6)	-25.2(5)
P(2)-Pt(1)-P(1)-C(19)	-76.87(12)	C(10)-C(4)-O(18)-C(6)	-145.0(5)
C(1)-Pt(1)-P(1)-C(25)	-136.28(17)	C(8)-C(4)-O(18)-C(6)	93.5(5)
P(3)-Pt(1)-P(1)-C(25)	11.0(2)	C(12)-P(1)-C(19)-C(24)	-87.2(3)
P(2)-Pt(1)-P(1)-C(25)	37.54(14)	C(25)-P(1)-C(19)-C(24)	23.0(4)
C(1)-Pt(1)-P(2)-C(29)	-24.4(8)	Pt(1)-P(1)-C(19)-C(24)	135.3(3)
P(3)-Pt(1)-P(2)-C(29)	30.00(13)	C(12)-P(1)-C(19)-C(20)	94.0(3)
P(1)-Pt(1)-P(2)-C(29)	-144.15(13)	C(25)-P(1)-C(19)-C(20)	-155.7(3)
C(1)-Pt(1)-P(2)-C(27)	-149.7(8)	Pt(1)-P(1)-C(19)-C(20)	-43.4(3)
P(3)-Pt(1)-P(2)-C(27)	-95.3(2)	C(24)-C(19)-C(20)-C(21)	1.6(5)
P(1)-Pt(1)-P(2)-C(27)	90.5(2)	P(1)-C(19)-C(20)-C(21)	-179.6(3)
C(1)-Pt(1)-P(2)-C(26)	94.7(8)	C(19)-C(20)-C(21)-C(22)	-1.5(6)
P(3)-Pt(1)-P(2)-C(26)	149.10(16)	C(20)-C(21)-C(22)-C(23)	0.6(6)
P(1)-Pt(1)-P(2)-C(26)	-25.06(16)	C(21)-C(22)-C(23)-C(24)	0.2(7)
C(1)-Pt(1)-P(3)-C(31)	-79.44(15)	C(22)-C(23)-C(24)-C(19)	-0.1(7)
P(2)-Pt(1)-P(3)-C(31)	106.24(12)	C(20)-C(19)-C(24)-C(23)	-0.8(6)
P(1)-Pt(1)-P(3)-C(31)	132.59(16)	P(1)-C(19)-C(24)-C(23)	-179.6(3)
C(1)-Pt(1)-P(3)-C(37)	45.70(17)	C(12)-P(1)-C(25)-C(26)	179.8(3)

P(2)-Pt(1)-P(3)-C(37)	-128.62(13)	C(19)-P(1)-C(25)-C(26)	68.8(3)
P(1)-Pt(1)-P(3)-C(37)	-102.27(18)	Pt(1)-P(1)-C(25)-C(26)	-47.8(3)
C(1)-Pt(1)-P(3)-C(30)	163.15(17)	P(1)-C(25)-C(26)-P(2)	28.5(4)
P(2)-Pt(1)-P(3)-C(30)	-11.17(14)	C(29)-P(2)-C(26)-C(25)	118.6(3)
P(1)-Pt(1)-P(3)-C(30)	15.2(2)	C(27)-P(2)-C(26)-C(25)	-125.7(3)
P(3)-Pt(1)-C(1)-C(2)	132.1(2)	Pt(1)-P(2)-C(26)-C(25)	3.3(3)
P(2)-Pt(1)-C(1)-C(2)	-173.7(6)	C(29)-P(2)-C(27)-C(28)	-66.4(5)
P(1)-Pt(1)-C(1)-C(2)	-54.9(3)	C(26)-P(2)-C(27)-C(28)	177.2(5)
P(3)-Pt(1)-C(1)-C(9)	-101.5(2)	Pt(1)-P(2)-C(27)-C(28)	56.5(5)
P(2)-Pt(1)-C(1)-C(9)	-47.3(9)	C(27)-P(2)-C(29)-C(30)	85.6(3)
P(1)-Pt(1)-C(1)-C(9)	71.5(2)	C(26)-P(2)-C(29)-C(30)	-165.3(3)
C(9)-C(1)-C(2)-C(3)	54.4(4)	Pt(1)-P(2)-C(29)-C(30)	-46.9(3)
Pt(1)-C(1)-C(2)-C(3)	-178.0(2)	P(2)-C(29)-C(30)-P(3)	40.0(4)
C(1)-C(2)-C(3)-C(4)	-52.7(5)	C(31)-P(3)-C(30)-C(29)	-139.2(3)
C(1)-C(2)-C(3)-C(7)	65.4(5)	C(37)-P(3)-C(30)-C(29)	109.4(3)
C(2)-C(3)-C(4)-O(18)	165.4(4)	Pt(1)-P(3)-C(30)-C(29)	-14.7(3)
C(7)-C(3)-C(4)-O(18)	38.2(4)	C(37)-P(3)-C(31)-C(36)	-123.1(3)
C(2)-C(3)-C(4)-C(10)	-79.0(5)	C(30)-P(3)-C(31)-C(36)	126.0(3)
C(7)-C(3)-C(4)-C(10)	153.7(3)	Pt(1)-P(3)-C(31)-C(36)	6.8(3)
C(2)-C(3)-C(4)-C(8)	48.8(5)	C(37)-P(3)-C(31)-C(32)	59.6(3)
C(7)-C(3)-C(4)-C(8)	-78.4(4)	C(30)-P(3)-C(31)-C(32)	-51.2(3)
O(18)-C(6)-C(7)-C(11)	146.5(5)	Pt(1)-P(3)-C(31)-C(32)	-170.4(2)
O(18)-C(6)-C(7)-C(3)	23.1(5)	C(36)-C(31)-C(32)-C(33)	0.5(5)
C(4)-C(3)-C(7)-C(11)	-161.7(4)	P(3)-C(31)-C(32)-C(33)	177.7(3)
C(2)-C(3)-C(7)-C(11)	72.9(5)	C(31)-C(32)-C(33)-C(34)	-0.4(5)
C(4)-C(3)-C(7)-C(6)	-36.5(4)	C(32)-C(33)-C(34)-C(35)	0.0(6)
C(2)-C(3)-C(7)-C(6)	-161.9(4)	C(33)-C(34)-C(35)-C(36)	0.4(6)
O(18)-C(4)-C(8)-C(9)	-163.2(4)	C(34)-C(35)-C(36)-C(31)	-0.3(6)
C(3)-C(4)-C(8)-C(9)	-48.9(5)	C(32)-C(31)-C(36)-C(35)	-0.1(5)
C(10)-C(4)-C(8)-C(9)	79.0(5)	P(3)-C(31)-C(36)-C(35)	-177.4(3)
C(4)-C(8)-C(9)-C(1)	53.9(5)	C(31)-P(3)-C(37)-C(38)	15.0(3)
C(2)-C(1)-C(9)-C(8)	-56.3(4)	C(30)-P(3)-C(37)-C(38)	125.7(3)
Pt(1)-C(1)-C(9)-C(8)	175.1(3)	Pt(1)-P(3)-C(37)-C(38)	-115.2(3)
C(19)-P(1)-C(12)-C(17)	-18.1(3)	C(31)-P(3)-C(37)-C(42)	-165.7(2)
C(25)-P(1)-C(12)-C(17)	-130.5(3)	C(30)-P(3)-C(37)-C(42)	-55.0(3)
Pt(1)-P(1)-C(12)-C(17)	110.9(3)	Pt(1)-P(3)-C(37)-C(42)	64.1(3)
C(19)-P(1)-C(12)-C(13)	164.1(3)	C(42)-C(37)-C(38)-C(39)	1.3(5)
C(25)-P(1)-C(12)-C(13)	51.7(3)	P(3)-C(37)-C(38)-C(39)	-179.4(3)
Pt(1)-P(1)-C(12)-C(13)	-66.9(3)	C(37)-C(38)-C(39)-C(40)	-0.1(6)
C(17)-C(12)-C(13)-C(14)	-0.8(5)	C(38)-C(39)-C(40)-C(41)	-0.7(6)
P(1)-C(12)-C(13)-C(14)	177.0(3)	C(39)-C(40)-C(41)-C(42)	0.3(6)
C(12)-C(13)-C(14)-C(15)	0.4(6)	C(40)-C(41)-C(42)-C(37)	0.9(6)
C(13)-C(14)-C(15)-C(16)	-0.3(6)	C(38)-C(37)-C(42)-C(41)	-1.7(5)
C(14)-C(15)-C(16)-C(17)	0.6(6)	P(3)-C(37)-C(42)-C(41)	179.0(3)

Appendix D

X-Ray Structure of 6 (Chapter 3)

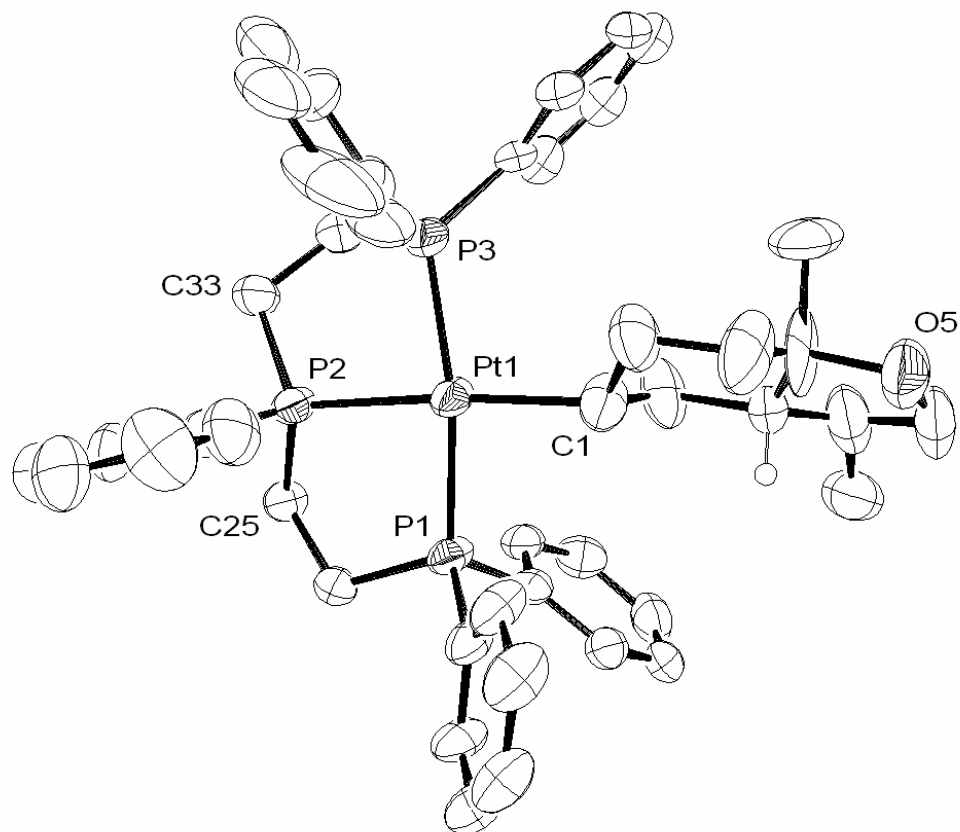


Figure D.1. ORTEP representation of 6.

Table D.1. Bond distances (Å) of **6**.

Bond	Length (Å)	Bond	Length (Å)
Pt(1)-C(1)	2.158(11)	C(51)-C(59)	1.58(2)
Pt(1)-P(1)	2.262(3)	C(52)-C(53)	1.62(2)
Pt(1)-P(2)	2.290(3)	C(53)-C(54)	1.51(2)
Pt(1)-P(3)	2.290(3)	C(54)-O(55)	1.40(2)
P(1)-C(18)	1.819(12)	C(54)-C(58)	1.43(2)
P(1)-C(12)	1.827(11)	C(54)-C(60)	1.61(3)
P(1)-C(24)	1.838(10)	O(55)-C(56)	1.412(18)
P(2)-C(26)	1.787(13)	C(56)-C(57)	1.58(2)
P(2)-C(33)	1.825(11)	C(57)-C(58)	1.55(2)
P(2)-C(25)	1.827(10)	C(57)-C(61)	1.59(3)
C(1)-C(9)	1.467(17)	C(58)-C(59)	1.56(2)
C(1)-C(2)	1.522(16)	C(62)-C(67)	1.34(3)
C(2)-C(3)	1.553(18)	C(62)-C(63)	1.45(2)
C(3)-C(4)	1.43(2)	C(63)-C(64)	1.40(2)
C(4)-C(8)	1.423(17)	C(64)-C(65)	1.33(3)
C(4)-O(5)	1.460(15)	C(65)-C(66)	1.32(3)
C(4)-C(10)	1.61(3)	C(66)-C(67)	1.46(3)
O(5)-C(6)	1.374(19)	C(68)-C(73)	1.33(2)
P(5)-C(76)	1.788(17)	C(68)-C(69)	1.45(2)
P(5)-C(75)	1.831(13)	C(69)-C(70)	1.33(2)
P(5)-C821	1.850(5)	C(70)-C(71)	1.48(2)
P(5)-C822	1.850(5)	C(71)-C(72)	1.35(2)
P(5)-Pt(2)	2.281(4)	C(72)-C(73)	1.59(2)
C(6)-C(7)	1.56(2)	C(74)-C(75)	1.28(2)
C(7)-C(8)	1.479(19)	C(76)-C(81)	1.37(2)
C(7)-C(11)	1.50(2)	C(76)-C(77)	1.39(2)
C(8)-C(9)	1.546(16)	C(77)-C(78)	1.37(3)
C(12)-C(13)	1.367(15)	C(78)-C(79)	1.37(3)
C(12)-C(17)	1.412(14)	C(79)-C(80)	1.38(3)
C(13)-C(14)	1.390(16)	C(80)-C(81)	1.38(2)
C(14)-C(15)	1.423(17)	P61-C841	1.802(15)
C(15)-C(16)	1.338(17)	P61-C901	1.841(15)
C(16)-C(17)	1.378(16)	P61-C831	1.90(3)
C(18)-C(23)	1.368(15)	C821-C831	1.49(6)
C(18)-C(19)	1.411(14)	C841-C851	1.3900
C(19)-C(20)	1.375(17)	C841-C891	1.3900
C(20)-C(21)	1.372(19)	C851-C861	1.3900
C(21)-C(22)	1.379(17)	C861-C871	1.3900
C(22)-C(23)	1.377(16)	C871-C881	1.3900
C(24)-C(25)	1.540(14)	C881-C891	1.3900
C(26)-C(27)	1.388(17)	C901-C911	1.3900
C(26)-C(32)	1.393(16)	C901-C951	1.3900
C(27)-C(28)	1.37(2)	C911-C921	1.3900
C(28)-C(29)	1.36(2)	C921-C931	1.3900
C(29)-C(30)	1.39(2)	C931-C941	1.3900
C(30)-C(32)	1.395(18)	C941-C951	1.3900
C(33)-C(34)	1.551(16)	P62-C842	1.786(15)
C(34)-P(3)	1.828(14)	P62-C902	1.786(15)
C(35)-C(36)	1.36(2)	P62-C832	1.93(3)
C(35)-C(40)	1.41(2)	C822-C832	1.53(5)
C(35)-P(3)	1.794(16)	C842-C852	1.3900
C(36)-C(37)	1.40(2)	C842-C892	1.3900
C(37)-C(38)	1.46(3)	C852-C862	1.3900

C(38)-C(39)	1.36(3)	C862-C872	1.3900
C(39)-C(40)	1.32(2)	C872-C882	1.3900
C(41)-C(46)	1.40(2)	C882-C892	1.3900
C(41)-C(42)	1.440(19)	C902-C912	1.3900
C(41)-P(3)	1.825(13)	C902-C952	1.3900
C(42)-C(43)	1.41(2)	C912-C922	1.3900
C(43)-C(44)	1.37(2)	C922-C932	1.3900
C(44)-C(45)	1.37(2)	C932-C942	1.3900
C(45)-C(46)	1.34(2)	C942-C952	1.3900
Pt(2)-C(51)	2.144(17)	B(1)-F(3)	1.29(2)
Pt(2)-P(4)	2.267(4)	B(1)-F(2)	1.36(2)
Pt(2)-P61	2.301(8)	B(1)-F(1)	1.37(3)
Pt(2)-P62	2.311(8)	B(1)-F(4)	1.37(2)
P(4)-C(68)	1.701(17)	B(2)-F(5)	1.232(18)
P(4)-C(74)	1.82(2)	B(2)-F(8)	1.331(18)
P(4)-C(62)	1.845(16)	B(2)-F(7)	1.385(16)
C(51)-C(52)	1.40(2)	B(2)-F(6)	1.417(19)

Table D.2. Bond angles (°) of **6**.

Bonds	Angle (°)	Bonds	Angle (°)
C(1)-Pt(1)-P(1)	90.6(4)	C(74)-P(4)-C(62)	106.0(12)
C(1)-Pt(1)-P(2)	175.2(4)	C(68)-P(4)-Pt(2)	122.4(6)
P(1)-Pt(1)-P(2)	84.80(10)	C(74)-P(4)-Pt(2)	103.8(8)
C(1)-Pt(1)-P(3)	101.7(4)	C(62)-P(4)-Pt(2)	120.9(4)
P(1)-Pt(1)-P(3)	163.75(11)	C(52)-C(51)-C(59)	114.9(14)
P(2)-Pt(1)-P(3)	83.15(10)	C(52)-C(51)-Pt(2)	117.8(13)
C(18)-P(1)-C(12)	106.3(5)	C(59)-C(51)-Pt(2)	113.5(11)
C(18)-P(1)-C(24)	104.8(5)	C(51)-C(52)-C(53)	113.3(16)
C(12)-P(1)-C(24)	104.6(5)	C(54)-C(53)-C(52)	110.1(15)
C(18)-P(1)-Pt(1)	119.5(4)	O(55)-C(54)-C(58)	105.2(16)
C(12)-P(1)-Pt(1)	112.0(4)	O(55)-C(54)-C(53)	112.0(15)
C(24)-P(1)-Pt(1)	108.5(4)	C(58)-C(54)-C(53)	107.3(15)
C(26)-P(2)-C(33)	106.2(6)	O(55)-C(54)-C(60)	109.6(15)
C(26)-P(2)-C(25)	105.1(5)	C(58)-C(54)-C(60)	109.9(18)
C(33)-P(2)-C(25)	112.2(5)	C(53)-C(54)-C(60)	112.6(18)
C(26)-P(2)-Pt(1)	118.6(4)	C(54)-O(55)-C(56)	104.5(13)
C(33)-P(2)-Pt(1)	109.9(4)	O(55)-C(56)-C(57)	107.4(13)
C(25)-P(2)-Pt(1)	104.8(3)	C(58)-C(57)-C(56)	98.4(13)
C(9)-C(1)-C(2)	114.4(11)	C(58)-C(57)-C(61)	113.3(17)
C(9)-C(1)-Pt(1)	116.0(8)	C(56)-C(57)-C(61)	107.2(16)
C(2)-C(1)-Pt(1)	112.2(8)	C(54)-C(58)-C(57)	100.6(14)
C(1)-C(2)-C(3)	111.3(11)	C(54)-C(58)-C(59)	116.3(16)
C(4)-C(3)-C(2)	110.7(13)	C(57)-C(58)-C(59)	117.8(14)
C(8)-C(4)-C(3)	118.3(14)	C(58)-C(59)-C(51)	107.3(13)
C(8)-C(4)-O(5)	105.0(12)	C(67)-C(62)-C(63)	123.4(18)
C(3)-C(4)-O(5)	115.3(14)	C(67)-C(62)-P(4)	120.9(17)
C(8)-C(4)-C(10)	113.6(16)	C(63)-C(62)-P(4)	115.5(15)
C(3)-C(4)-C(10)	103.0(15)	C(64)-C(63)-C(62)	117.8(19)
O(5)-C(4)-C(10)	100.4(13)	C(65)-C(64)-C(63)	118(2)
C(6)-O(5)-C(4)	110.8(11)	C(66)-C(65)-C(64)	124(2)
C(76)-P(5)-C(75)	105.5(8)	C(65)-C(66)-C(67)	122(2)
C(76)-P(5)-C821	101.4(13)	C(62)-C(67)-C(66)	114(2)

C(75)-P(5)-C821	110.2(17)	C(73)-C(68)-C(69)	123.5(16)
C(76)-P(5)-C822	109.4(12)	C(73)-C(68)-P(4)	113.3(13)
C(75)-P(5)-C822	108.8(18)	C(69)-C(68)-P(4)	122.8(14)
C821-P(5)-C822	8(2)	C(70)-C(69)-C(68)	120.6(19)
C(76)-P(5)-Pt(2)	119.9(5)	C(69)-C(70)-C(71)	120.8(18)
C(75)-P(5)-Pt(2)	108.8(6)	C(72)-C(71)-C(70)	120.3(17)
C821-P(5)-Pt(2)	110.7(16)	C(71)-C(72)-C(73)	119(2)
C822-P(5)-Pt(2)	104.2(15)	C(68)-C(73)-C(72)	116.0(16)
O(5)-C(6)-C(7)	105.3(12)	C(75)-C(74)-P(4)	122.6(17)
C(8)-C(7)-C(11)	121.6(13)	C(74)-C(75)-P(5)	113.1(13)
C(8)-C(7)-C(6)	100.6(14)	C(81)-C(76)-C(77)	116.1(16)
C(11)-C(7)-C(6)	112.1(15)	C(81)-C(76)-P(5)	121.3(12)
C(4)-C(8)-C(7)	106.1(11)	C(77)-C(76)-P(5)	122.3(13)
C(4)-C(8)-C(9)	113.3(11)	C(78)-C(77)-C(76)	123.3(18)
C(7)-C(8)-C(9)	128.3(12)	C(79)-C(78)-C(77)	118.5(18)
C(1)-C(9)-C(8)	108.3(10)	C(78)-C(79)-C(80)	120(2)
C(13)-C(12)-C(17)	119.8(10)	C(81)-C(80)-C(79)	119(2)
C(13)-C(12)-P(1)	117.5(8)	C(76)-C(81)-C(80)	122.7(18)
C(17)-C(12)-P(1)	122.5(9)	C841-P61-C901	106.2(10)
C(12)-C(13)-C(14)	121.6(10)	C841-P61-C831	105.1(12)
C(13)-C(14)-C(15)	117.0(11)	C901-P61-C831	102.7(12)
C(16)-C(15)-C(14)	121.4(11)	C841-P61-Pt(2)	121.6(8)
C(15)-C(16)-C(17)	121.4(11)	C901-P61-Pt(2)	111.2(8)
C(16)-C(17)-C(12)	118.7(11)	C831-P61-Pt(2)	108.3(8)
C(23)-C(18)-C(19)	119.5(11)	C831-C821-P(5)	103(2)
C(23)-C(18)-P(1)	121.5(8)	C821-C831-P61	116.5(19)
C(19)-C(18)-P(1)	119.0(9)	C851-C841-C891	120.0
C(20)-C(19)-C(18)	119.4(12)	C851-C841-P61	120.8(12)
C(21)-C(20)-C(19)	121.4(12)	C891-C841-P61	119.1(11)
C(20)-C(21)-C(22)	118.2(12)	C861-C851-C841	120.0
C(23)-C(22)-C(21)	122.1(13)	C851-C861-C871	120.0
C(18)-C(23)-C(22)	119.5(11)	C881-C871-C861	120.0
C(25)-C(24)-P(1)	112.3(7)	C891-C881-C871	120.0
C(24)-C(25)-P(2)	106.9(7)	C881-C891-C841	120.0
C(27)-C(26)-C(32)	116.4(12)	C911-C901-C951	120.0
C(27)-C(26)-P(2)	121.6(10)	C911-C901-P61	120.0(11)
C(32)-C(26)-P(2)	121.9(9)	C951-C901-P61	120.0(11)
C(28)-C(27)-C(26)	122.1(14)	C901-C911-C921	120.0
C(29)-C(28)-C(27)	121.7(15)	C911-C921-C931	120.0
C(28)-C(29)-C(30)	117.6(14)	C941-C931-C921	120.0
C(29)-C(30)-C(32)	121.1(13)	C931-C941-C951	120.0
C(26)-C(32)-C(30)	120.9(12)	C941-C951-C901	120.0
C(34)-C(33)-P(2)	111.0(8)	C842-P62-C902	104.0(10)
C(33)-C(34)-P(3)	109.4(9)	C842-P62-C832	107.7(12)
C(36)-C(35)-C(40)	118.6(17)	C902-P62-C832	101.4(11)
C(36)-C(35)-P(3)	120.2(12)	C842-P62-Pt(2)	113.4(8)
C(40)-C(35)-P(3)	121.2(17)	C902-P62-Pt(2)	126.4(8)
C(35)-C(36)-C(37)	124(2)	C832-P62-Pt(2)	102.0(8)
C(36)-C(37)-C(38)	113(2)	C832-C822-P(5)	120(3)
C(39)-C(38)-C(37)	124(2)	C822-C832-P62	106(2)
C(40)-C(39)-C(38)	119(2)	C852-C842-C892	120.0
C(39)-C(40)-C(35)	122(2)	C852-C842-P62	117.9(12)
C(46)-C(41)-C(42)	121.6(13)	C892-C842-P62	122.1(12)
C(46)-C(41)-P(3)	121.2(11)	C862-C852-C842	120.0
C(42)-C(41)-P(3)	117.1(13)	C852-C862-C872	120.0
C(43)-C(42)-C(41)	115.6(17)	C882-C872-C862	120.0

C(44)-C(43)-C(42)	121.2(15)	C872-C882-C892	120.0
C(45)-C(44)-C(43)	120.1(16)	C882-C892-C842	120.0
C(46)-C(45)-C(44)	123.1(18)	C912-C902-C952	120.0
C(45)-C(46)-C(41)	118.3(15)	C912-C902-P62	121.0(11)
C(51)-Pt(2)-P(4)	93.1(5)	C952-C902-P62	118.9(11)
C(51)-Pt(2)-P(5)	175.8(5)	C922-C912-C902	120.0
P(4)-Pt(2)-P(5)	82.86(13)	C932-C922-C912	120.0
C(51)-Pt(2)-P61	103.1(6)	C922-C932-C942	120.0
P(4)-Pt(2)-P61	163.3(2)	C952-C942-C932	120.0
P(5)-Pt(2)-P61	80.8(2)	C942-C952-C902	120.0
C(51)-Pt(2)-P62	96.2(6)	F(3)-B(1)-F(2)	111(2)
P(4)-Pt(2)-P62	155.3(2)	F(3)-B(1)-F(1)	111.7(16)
P(5)-Pt(2)-P62	87.0(2)	F(2)-B(1)-F(1)	103.1(18)
P61-Pt(2)-P62	19.9(2)	F(3)-B(1)-F(4)	112.7(18)
C(35)-P(3)-C(41)	106.6(7)	F(2)-B(1)-F(4)	107.5(15)
C(35)-P(3)-C(34)	106.2(7)	F(1)-B(1)-F(4)	110(2)
C(41)-P(3)-C(34)	102.0(7)	F(5)-B(2)-F(8)	119.5(16)
C(35)-P(3)-Pt(1)	112.7(6)	F(5)-B(2)-F(7)	112.7(13)
C(41)-P(3)-Pt(1)	123.7(4)	F(8)-B(2)-F(7)	110.8(14)
C(34)-P(3)-Pt(1)	103.8(4)	F(5)-B(2)-F(6)	107.1(17)
C(68)-P(4)-C(74)	97.0(15)	F(8)-B(2)-F(6)	94.7(12)
C(68)-P(4)-C(62)	103.1(8)	F(7)-B(2)-F(6)	110.3(12)

Table D.3. Torsion angles ($^{\circ}$) of **6**.

Bonds	Angle ($^{\circ}$)	Bonds	Angle ($^{\circ}$)
C(1)-Pt(1)-P(1)-C(18)	67.9(5)	P61-Pt(2)-C(51)-C(59)	-90.3(13)
P(2)-Pt(1)-P(1)-C(18)	-110.6(4)	P62-Pt(2)-C(51)-C(59)	-71.4(13)
P(3)-Pt(1)-P(1)-C(18)	-152.9(5)	C(59)-C(51)-C(52)-C(53)	-49(2)
C(1)-Pt(1)-P(1)-C(12)	-57.2(5)	Pt(2)-C(51)-C(52)-C(53)	172.9(12)
P(2)-Pt(1)-P(1)-C(12)	124.2(4)	C(51)-C(52)-C(53)-C(54)	55(2)
P(3)-Pt(1)-P(1)-C(12)	81.9(6)	C(52)-C(53)-C(54)-O(55)	-172.5(14)
C(1)-Pt(1)-P(1)-C(24)	-172.2(5)	C(52)-C(53)-C(54)-C(58)	-58(2)
P(2)-Pt(1)-P(1)-C(24)	9.3(4)	C(52)-C(53)-C(54)-C(60)	63(2)
P(3)-Pt(1)-P(1)-C(24)	-33.0(6)	C(58)-C(54)-O(55)-C(56)	44.1(18)
C(1)-Pt(1)-P(2)-C(26)	68(4)	C(53)-C(54)-O(55)-C(56)	160.3(15)
P(1)-Pt(1)-P(2)-C(26)	85.8(5)	C(60)-C(54)-O(55)-C(56)	-74.0(19)
P(3)-Pt(1)-P(2)-C(26)	-105.1(5)	C(54)-O(55)-C(56)-C(57)	-19.0(19)
C(1)-Pt(1)-P(2)-C(33)	-169(4)	O(55)-C(56)-C(57)-C(58)	-10(2)
P(1)-Pt(1)-P(2)-C(33)	-151.8(4)	O(55)-C(56)-C(57)-C(61)	-127.6(17)
P(3)-Pt(1)-P(2)-C(33)	17.3(4)	O(55)-C(54)-C(58)-C(57)	-50.0(19)
C(1)-Pt(1)-P(2)-C(25)	-49(4)	C(53)-C(54)-C(58)-C(57)	-169.4(17)
P(1)-Pt(1)-P(2)-C(25)	-31.1(4)	C(60)-C(54)-C(58)-C(57)	68(2)
P(3)-Pt(1)-P(2)-C(25)	138.0(4)	O(55)-C(54)-C(58)-C(59)	-178.4(14)
P(1)-Pt(1)-C(1)-C(9)	88.4(10)	C(53)-C(54)-C(58)-C(59)	62(2)
P(2)-Pt(1)-C(1)-C(9)	106(4)	C(60)-C(54)-C(58)-C(59)	-61(2)
P(3)-Pt(1)-C(1)-C(9)	-80.9(10)	C(56)-C(57)-C(58)-C(54)	34(2)
P(1)-Pt(1)-C(1)-C(2)	-137.6(11)	C(61)-C(57)-C(58)-C(54)	147.4(18)
P(2)-Pt(1)-C(1)-C(2)	-120(4)	C(56)-C(57)-C(58)-C(59)	161.9(16)
P(3)-Pt(1)-C(1)-C(2)	53.1(11)	C(61)-C(57)-C(58)-C(59)	-85(2)
C(9)-C(1)-C(2)-C(3)	-52.6(19)	C(54)-C(58)-C(59)-C(51)	-55(2)
Pt(1)-C(1)-C(2)-C(3)	172.7(12)	C(57)-C(58)-C(59)-C(51)	-174.3(16)
C(1)-C(2)-C(3)-C(4)	46(2)	C(52)-C(51)-C(59)-C(58)	47(2)

C(2)-C(3)-C(4)-C(8)	-49(2)	Pt(2)-C(51)-C(59)-C(58)	-173.4(12)
C(2)-C(3)-C(4)-O(5)	-174.5(14)	C(68)-P(4)-C(62)-C(67)	143.9(17)
C(2)-C(3)-C(4)-C(10)	77.2(15)	C(74)-P(4)-C(62)-C(67)	43(2)
C(8)-C(4)-O(5)-C(6)	14(2)	Pt(2)-P(4)-C(62)-C(67)	-75.0(18)
C(3)-C(4)-O(5)-C(6)	146.0(17)	C(68)-P(4)-C(62)-C(63)	-40.8(15)
C(10)-C(4)-O(5)-C(6)	-104.1(16)	C(74)-P(4)-C(62)-C(63)	-142.1(17)
C(4)-O(5)-C(6)-C(7)	8(2)	Pt(2)-P(4)-C(62)-C(63)	100.4(12)
O(5)-C(6)-C(7)-C(8)	-25.7(18)	C(67)-C(62)-C(63)-C(64)	-2(3)
O(5)-C(6)-C(7)-C(11)	-156.4(14)	P(4)-C(62)-C(63)-C(64)	-177.4(15)
C(3)-C(4)-C(8)-C(7)	-161.4(16)	C(62)-C(63)-C(64)-C(65)	-4(3)
O(5)-C(4)-C(8)-C(7)	-31.1(19)	C(63)-C(64)-C(65)-C(66)	6(4)
C(10)-C(4)-C(8)-C(7)	77.6(16)	C(64)-C(65)-C(66)-C(67)	-2(4)
C(3)-C(4)-C(8)-C(9)	53(2)	C(63)-C(62)-C(67)-C(66)	5(3)
O(5)-C(4)-C(8)-C(9)	-176.9(13)	P(4)-C(62)-C(67)-C(66)	-179.5(14)
C(10)-C(4)-C(8)-C(9)	-68.2(17)	C(65)-C(66)-C(67)-C(62)	-4(3)
C(11)-C(7)-C(8)-C(4)	159.1(17)	C(74)-P(4)-C(68)-C(73)	-140.6(15)
C(6)-C(7)-C(8)-C(4)	34.7(18)	C(62)-P(4)-C(68)-C(73)	111.1(14)
C(11)-C(7)-C(8)-C(9)	-62(2)	Pt(2)-P(4)-C(68)-C(73)	-29.4(16)
C(6)-C(7)-C(8)-C(9)	173.6(14)	C(74)-P(4)-C(68)-C(69)	45.9(17)
C(2)-C(1)-C(9)-C(8)	53.4(16)	C(62)-P(4)-C(68)-C(69)	-62.4(16)
Pt(1)-C(1)-C(9)-C(8)	-173.6(9)	Pt(2)-P(4)-C(68)-C(69)	157.2(11)
C(4)-C(8)-C(9)-C(1)	-51.7(18)	C(73)-C(68)-C(69)-C(70)	2(3)
C(7)-C(8)-C(9)-C(1)	171.7(14)	P(4)-C(68)-C(69)-C(70)	174.8(14)
C(18)-P(1)-C(12)-C(13)	172.8(8)	C(68)-C(69)-C(70)-C(71)	-2(3)
C(24)-P(1)-C(12)-C(13)	62.3(9)	C(69)-C(70)-C(71)-C(72)	0(3)
Pt(1)-P(1)-C(12)-C(13)	-55.0(9)	C(70)-C(71)-C(72)-C(73)	2(3)
C(18)-P(1)-C(12)-C(17)	-13.5(10)	C(69)-C(68)-C(73)-C(72)	0(2)
C(24)-P(1)-C(12)-C(17)	-124.0(9)	P(4)-C(68)-C(73)-C(72)	-173.7(12)
Pt(1)-P(1)-C(12)-C(17)	118.7(8)	C(71)-C(72)-C(73)-C(68)	-2(2)
C(17)-C(12)-C(13)-C(14)	2.4(16)	C(68)-P(4)-C(74)-C(75)	95(3)
P(1)-C(12)-C(13)-C(14)	176.2(8)	C(62)-P(4)-C(74)-C(75)	-160(3)
C(12)-C(13)-C(14)-C(15)	-0.8(16)	Pt(2)-P(4)-C(74)-C(75)	-31(4)
C(13)-C(14)-C(15)-C(16)	-0.7(17)	P(4)-C(74)-C(75)-P(5)	16(4)
C(14)-C(15)-C(16)-C(17)	0.6(18)	C(76)-P(5)-C(75)-C(74)	-122(2)
C(15)-C(16)-C(17)-C(12)	0.9(16)	C821-P(5)-C(75)-C(74)	129(3)
C(13)-C(12)-C(17)-C(16)	-2.4(15)	C822-P(5)-C(75)-C(74)	121(3)
P(1)-C(12)-C(17)-C(16)	-176.0(8)	Pt(2)-P(5)-C(75)-C(74)	8(3)
C(12)-P(1)-C(18)-C(23)	-58.8(10)	C(75)-P(5)-C(76)-C(81)	139.4(13)
C(24)-P(1)-C(18)-C(23)	51.6(11)	C821-P(5)-C(76)-C(81)	-106(2)
Pt(1)-P(1)-C(18)-C(23)	173.3(8)	C822-P(5)-C(76)-C(81)	-104(2)
C(12)-P(1)-C(18)-C(19)	120.3(9)	Pt(2)-P(5)-C(76)-C(81)	16.4(15)
C(24)-P(1)-C(18)-C(19)	-129.2(9)	C(75)-P(5)-C(76)-C(77)	-47.8(14)
Pt(1)-P(1)-C(18)-C(19)	-7.5(11)	C821-P(5)-C(76)-C(77)	67(2)
C(23)-C(18)-C(19)-C(20)	0.0(18)	C822-P(5)-C(76)-C(77)	69(2)
P(1)-C(18)-C(19)-C(20)	-179.2(10)	Pt(2)-P(5)-C(76)-C(77)	-170.8(10)
C(18)-C(19)-C(20)-C(21)	-1(2)	C(81)-C(76)-C(77)-C(78)	-3(2)
C(19)-C(20)-C(21)-C(22)	1(2)	P(5)-C(76)-C(77)-C(78)	-176.7(14)
C(20)-C(21)-C(22)-C(23)	0.9(19)	C(76)-C(77)-C(78)-C(79)	0(3)
C(19)-C(18)-C(23)-C(22)	1.7(17)	C(77)-C(78)-C(79)-C(80)	6(3)
P(1)-C(18)-C(23)-C(22)	-179.1(9)	C(78)-C(79)-C(80)-C(81)	-7(3)
C(21)-C(22)-C(23)-C(18)	-2.2(18)	C(77)-C(76)-C(81)-C(80)	2(3)
C(18)-P(1)-C(24)-C(25)	148.3(8)	P(5)-C(76)-C(81)-C(80)	175.3(16)
C(12)-P(1)-C(24)-C(25)	-100.0(8)	C(79)-C(80)-C(81)-C(76)	3(3)
Pt(1)-P(1)-C(24)-C(25)	19.7(9)	C(51)-Pt(2)-P61-C841	-75.4(10)
P(1)-C(24)-C(25)-P(2)	-45.2(10)	P(4)-Pt(2)-P61-C841	118.5(11)
C(26)-P(2)-C(25)-C(24)	-75.0(8)	P(5)-Pt(2)-P61-C841	106.1(9)

C(33)-P(2)-C(25)-C(24)	170.0(7)	P62-Pt(2)-P61-C841	-146.9(15)
Pt(1)-P(2)-C(25)-C(24)	50.7(8)	C(51)-Pt(2)-P61-C901	50.7(9)
C(33)-P(2)-C(26)-C(27)	-111.9(12)	P(4)-Pt(2)-P61-C901	-115.3(10)
C(25)-P(2)-C(26)-C(27)	129.1(11)	P(5)-Pt(2)-P61-C901	-127.8(8)
Pt(1)-P(2)-C(26)-C(27)	12.4(13)	P62-Pt(2)-P61-C901	-20.8(10)
C(33)-P(2)-C(26)-C(32)	64.6(12)	C(51)-Pt(2)-P61-C831	162.9(10)
C(25)-P(2)-C(26)-C(32)	-54.4(12)	P(4)-Pt(2)-P61-C831	-3.2(14)
Pt(1)-P(2)-C(26)-C(32)	-171.1(9)	P(5)-Pt(2)-P61-C831	-15.6(9)
C(32)-C(26)-C(27)-C(28)	-1(2)	P62-Pt(2)-P61-C831	91.4(13)
P(2)-C(26)-C(27)-C(28)	176.1(13)	C(76)-P(5)-C821-C831	79(2)
C(26)-C(27)-C(28)-C(29)	4(3)	C(75)-P(5)-C821-C831	-169.6(19)
C(27)-C(28)-C(29)-C(30)	-4(3)	C822-P(5)-C821-C831	-88(24)
C(28)-C(29)-C(30)-C(32)	2(2)	Pt(2)-P(5)-C821-C831	-49(2)
C(27)-C(26)-C(32)-C(30)	-2(2)	P(5)-C821-C831-P61	36(3)
P(2)-C(26)-C(32)-C(30)	-178.2(10)	C841-P61-C831-C821	-142(2)
C(29)-C(30)-C(32)-C(26)	1(2)	C901-P61-C831-C821	107(2)
C(26)-P(2)-C(33)-C(34)	138.8(9)	Pt(2)-P61-C831-C821	-11(2)
C(25)-P(2)-C(33)-C(34)	-107.0(10)	C901-P61-C841-C851	-113.1(13)
Pt(1)-P(2)-C(33)-C(34)	9.3(10)	C831-P61-C841-C851	138.5(13)
P(2)-C(33)-C(34)-P(3)	-39.2(11)	Pt(2)-P61-C841-C851	15.2(15)
C(40)-C(35)-C(36)-C(37)	0(2)	C901-P61-C841-C891	63.0(14)
P(3)-C(35)-C(36)-C(37)	-177.2(13)	C831-P61-C841-C891	-45.4(15)
C(35)-C(36)-C(37)-C(38)	1(3)	Pt(2)-P61-C841-C891	-168.6(9)
C(36)-C(37)-C(38)-C(39)	-1(3)	C891-C841-C851-C861	0.0
C(37)-C(38)-C(39)-C(40)	1(3)	P61-C841-C851-C861	176.1(16)
C(38)-C(39)-C(40)-C(35)	0(3)	C841-C851-C861-C871	0.0
C(36)-C(35)-C(40)-C(39)	-1(2)	C851-C861-C871-C881	0.0
P(3)-C(35)-C(40)-C(39)	177.0(13)	C861-C871-C881-C891	0.0
C(46)-C(41)-C(42)-C(43)	1.5(17)	C871-C881-C891-C841	0.0
P(3)-C(41)-C(42)-C(43)	179.5(9)	C851-C841-C891-C881	0.0
C(41)-C(42)-C(43)-C(44)	-0.7(19)	P61-C841-C891-C881	-176.2(16)
C(42)-C(43)-C(44)-C(45)	1(2)	C841-P61-C901-C911	23.2(15)
C(43)-C(44)-C(45)-C(46)	-1(2)	C831-P61-C901-C911	133.3(13)
C(44)-C(45)-C(46)-C(41)	2(2)	Pt(2)-P61-C901-C911	-111.0(11)
C(42)-C(41)-C(46)-C(45)	-2.2(19)	C841-P61-C901-C951	-158.3(13)
P(3)-C(41)-C(46)-C(45)	179.8(10)	C831-P61-C901-C951	-48.2(15)
C(76)-P(5)-Pt(2)-C(51)	118(7)	Pt(2)-P61-C901-C951	67.5(13)
C(75)-P(5)-Pt(2)-C(51)	-3(7)	C951-C901-C911-C921	0.0
C821-P(5)-Pt(2)-C(51)	-124(7)	P61-C901-C911-C921	178.5(16)
C822-P(5)-Pt(2)-C(51)	-119(7)	C901-C911-C921-C931	0.0
C(76)-P(5)-Pt(2)-P(4)	101.4(5)	C911-C921-C931-C941	0.0
C(75)-P(5)-Pt(2)-P(4)	-20.0(6)	C921-C931-C941-C951	0.0
C821-P(5)-Pt(2)-P(4)	-141.2(15)	C931-C941-C951-C901	0.0
C822-P(5)-Pt(2)-P(4)	-135.9(16)	C911-C901-C951-C941	0.0
C(76)-P(5)-Pt(2)-P61	-82.2(5)	P61-C901-C951-C941	-178.5(16)
C(75)-P(5)-Pt(2)-P61	156.5(6)	C(51)-Pt(2)-P62-C842	-104.3(9)
C821-P(5)-Pt(2)-P61	35.2(15)	P(4)-Pt(2)-P62-C842	144.2(8)
C822-P(5)-Pt(2)-P61	40.5(16)	P(5)-Pt(2)-P62-C842	78.4(8)
C(76)-P(5)-Pt(2)-P62	-101.3(5)	P61-Pt(2)-P62-C842	7.4(10)
C(75)-P(5)-Pt(2)-P62	137.4(6)	C(51)-Pt(2)-P62-C902	26.1(10)
C821-P(5)-Pt(2)-P62	16.2(15)	P(4)-Pt(2)-P62-C902	-85.4(11)
C822-P(5)-Pt(2)-P62	21.4(16)	P(5)-Pt(2)-P62-C902	-151.2(10)
C(36)-C(35)-P(3)-C(41)	-115.7(12)	P61-Pt(2)-P62-C902	137.8(15)
C(40)-C(35)-P(3)-C(41)	66.8(12)	C(51)-Pt(2)-P62-C832	140.2(10)
C(36)-C(35)-P(3)-C(34)	136.1(12)	P(4)-Pt(2)-P62-C832	28.7(12)
C(40)-C(35)-P(3)-C(34)	-41.4(13)	P(5)-Pt(2)-P62-C832	-37.1(9)

C(36)-C(35)-P(3)-Pt(1)	23.1(13)	P61-Pt(2)-P62-C832	-108.1(14)
C(40)-C(35)-P(3)-Pt(1)	-154.4(10)	C(76)-P(5)-C822-C832	134(3)
C(46)-C(41)-P(3)-C(35)	-155.1(11)	C(75)-P(5)-C822-C832	-112(3)
C(42)-C(41)-P(3)-C(35)	26.9(11)	C821-P(5)-C822-C832	147(27)
C(46)-C(41)-P(3)-C(34)	-43.9(11)	Pt(2)-P(5)-C822-C832	4(4)
C(42)-C(41)-P(3)-C(34)	138.0(10)	P(5)-C822-C832-P62	-34(4)
C(46)-C(41)-P(3)-Pt(1)	71.8(12)	C842-P62-C832-C822	-73(2)
C(42)-C(41)-P(3)-Pt(1)	-106.2(9)	C902-P62-C832-C822	178(2)
C(33)-C(34)-P(3)-C(35)	-67.1(11)	Pt(2)-P62-C832-C822	47(2)
C(33)-C(34)-P(3)-C(41)	-178.5(9)	C902-P62-C842-C852	-85.9(13)
C(33)-C(34)-P(3)-Pt(1)	52.0(9)	C832-P62-C842-C852	167.1(12)
C(1)-Pt(1)-P(3)-C(35)	-100.5(6)	Pt(2)-P62-C842-C852	55.0(12)
P(1)-Pt(1)-P(3)-C(35)	121.4(6)	C902-P62-C842-C892	92.2(14)
P(2)-Pt(1)-P(3)-C(35)	78.9(5)	C832-P62-C842-C892	-14.9(16)
C(1)-Pt(1)-P(3)-C(41)	30.1(7)	Pt(2)-P62-C842-C892	-127.0(10)
P(1)-Pt(1)-P(3)-C(41)	-108.0(7)	C892-C842-C852-C862	0.0
P(2)-Pt(1)-P(3)-C(41)	-150.4(7)	P62-C842-C852-C862	178.1(15)
C(1)-Pt(1)-P(3)-C(34)	145.0(6)	C842-C852-C862-C872	0.0
P(1)-Pt(1)-P(3)-C(34)	6.9(7)	C852-C862-C872-C882	0.0
P(2)-Pt(1)-P(3)-C(34)	-35.5(5)	C862-C872-C882-C892	0.0
C(51)-Pt(2)-P(4)-C(68)	98.0(9)	C872-C882-C892-C842	0.0
P(5)-Pt(2)-P(4)-C(68)	-83.2(8)	C852-C842-C892-C882	0.0
P61-Pt(2)-P(4)-C(68)	-95.6(11)	P62-C842-C892-C882	-178.0(16)
P62-Pt(2)-P(4)-C(68)	-149.9(9)	C842-P62-C902-C912	11.7(15)
C(51)-Pt(2)-P(4)-C(74)	-154.3(15)	C832-P62-C902-C912	123.4(14)
P(5)-Pt(2)-P(4)-C(74)	24.5(14)	Pt(2)-P62-C902-C912	-122.3(11)
P61-Pt(2)-P(4)-C(74)	12.2(17)	C842-P62-C902-C952	-164.2(13)
P62-Pt(2)-P(4)-C(74)	-42.1(15)	C832-P62-C902-C952	-52.5(16)
C(51)-Pt(2)-P(4)-C(62)	-35.7(9)	Pt(2)-P62-C902-C952	61.8(16)
P(5)-Pt(2)-P(4)-C(62)	143.1(8)	C952-C902-C912-C922	0.0
P61-Pt(2)-P(4)-C(62)	130.7(11)	P62-C902-C912-C922	-175.8(17)
P62-Pt(2)-P(4)-C(62)	76.4(10)	C902-C912-C922-C932	0.0
P(4)-Pt(2)-C(51)-C(52)	-136.0(15)	C912-C922-C932-C942	0.0
P(5)-Pt(2)-C(51)-C(52)	-153(6)	C922-C932-C942-C952	0.0
P61-Pt(2)-C(51)-C(52)	48.0(16)	C932-C942-C952-C902	0.0
P62-Pt(2)-C(51)-C(52)	67.0(16)	C912-C902-C952-C942	0.0
P(4)-Pt(2)-C(51)-C(59)	85.7(13)	P62-C902-C952-C942	175.9(17)
P(5)-Pt(2)-C(51)-C(59)	69(7)		

Appendix E

X-Ray Structure of [(dppm)(PMe₃)PtI][I] (Chapter 4)

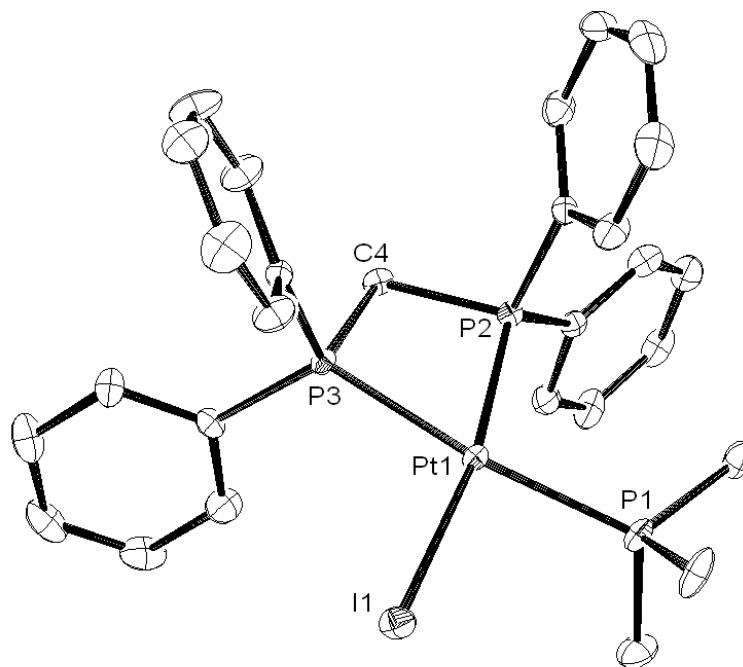


Figure E.1. ORTEP representation of [(dppm)(PMe₃)PtI][I].

Table E.1. Bond distances (Å) of [(dppm)(PMe₃)PtI][I].

Bond	Length (Å)	Bond	Length (Å)
Pt(1)-P(2)	2.2410(13)	C(11)-C(12)	1.398(8)
Pt(1)-P(1)	2.3172(13)	C(11)-C(16)	1.405(8)
Pt(1)-P(3)	2.3242(12)	C(12)-C(13)	1.375(9)
Pt(1)-I(1)	2.6329(4)	C(12)-H(12)	0.70(7)
P(1)-C(3)	1.805(5)	C(13)-C(14)	1.389(10)
P(1)-C(1)	1.805(6)	C(13)-H(13)	0.87(8)
P(1)-C(2)	1.807(6)	C(14)-C(15)	1.366(11)
P(2)-C(11)	1.801(5)	C(14)-H(14)	0.90(7)
P(2)-C(5)	1.809(5)	C(15)-C(16)	1.392(9)
P(2)-C(4)	1.839(5)	C(15)-H(15)	0.67(7)
P(2)-P(3)	2.6883(19)	C(16)-H(16)	0.83(6)
P(3)-C(23)	1.801(5)	C(17)-C(22)	1.390(8)
P(3)-C(17)	1.807(5)	C(17)-C(18)	1.392(8)
P(3)-C(4)	1.845(5)	C(18)-C(19)	1.391(8)
C(1)-H(1A)	1.06(8)	C(18)-H(18)	0.86(8)
C(1)-H(1B)	0.89(8)	C(19)-C(20)	1.378(10)
C(1)-H(1C)	0.93(10)	C(19)-H(19)	0.96(12)
C(2)-H(2A)	0.94(6)	C(20)-C(21)	1.376(10)
C(2)-H(2B)	0.93(7)	C(20)-H(20)	0.76(8)
C(2)-H(2C)	0.90(10)	C(21)-C(22)	1.387(9)
C(3)-H(3A)	1.06(9)	C(21)-H(21)	0.82(8)
C(3)-H(3B)	0.91(8)	C(22)-H(22)	1.09(10)
C(3)-H(3C)	1.01(10)	C(23)-C(24)	1.388(8)
C(4)-H(4A)	0.78(8)	C(23)-C(28)	1.405(8)
C(4)-H(4B)	0.93(6)	C(24)-C(25)	1.381(9)
C(5)-C(6)	1.376(9)	C(24)-H(24)	0.86(7)
C(5)-C(10)	1.400(8)	C(25)-C(26)	1.382(10)
C(6)-C(7)	1.392(8)	C(25)-H(25)	0.94(8)
C(6)-H(6)	0.96(8)	C(26)-C(27)	1.397(9)
C(7)-C(8)	1.394(9)	C(26)-H(26)	0.90(8)
C(7)-H(7)	0.86(7)	C(27)-C(28)	1.391(8)
C(8)-C(9)	1.386(10)	C(27)-H(27)	1.02(8)
C(8)-H(8)	0.91(7)	C(28)-H(28)	0.84(7)
C(9)-C(10)	1.377(9)	C(31)-Cl(33)	1.751(8)
C(9)-H(9)	0.92(7)	C(31)-Cl(32)	1.777(8)
C(10)-H(10)	0.74(10)	C(31)-H(31A)	1.09(7)
		C(31)-H(31B)	0.92(11)

Table E.2. Bond angles (°) of [(dppm)(PMe₃)PtI][I].

Bonds	Angle (°)	Bonds	Angle (°)
P(2)-Pt(1)-P(1)	99.16(5)	C(7)-C(8)-H(8)	122(4)
P(2)-Pt(1)-P(3)	72.13(5)	C(10)-C(9)-C(8)	120.0(6)
P(1)-Pt(1)-P(3)	171.17(5)	C(10)-C(9)-H(9)	120(4)
P(2)-Pt(1)-I(1)	169.85(3)	C(8)-C(9)-H(9)	120(4)
P(1)-Pt(1)-I(1)	90.98(4)	C(9)-C(10)-C(5)	120.5(6)
P(3)-Pt(1)-I(1)	97.73(3)	C(9)-C(10)-H(10)	114(7)
C(3)-P(1)-C(1)	105.5(3)	C(5)-C(10)-H(10)	125(7)
C(3)-P(1)-C(2)	104.2(3)	C(12)-C(11)-C(16)	119.2(5)
C(1)-P(1)-C(2)	103.1(3)	C(12)-C(11)-P(2)	122.0(4)
C(3)-P(1)-Pt(1)	112.7(2)	C(16)-C(11)-P(2)	118.7(4)
C(1)-P(1)-Pt(1)	113.4(2)	C(13)-C(12)-C(11)	120.3(6)
C(2)-P(1)-Pt(1)	116.8(2)	C(13)-C(12)-H(12)	120(5)
C(11)-P(2)-C(5)	110.2(2)	C(11)-C(12)-H(12)	120(5)
C(11)-P(2)-C(4)	107.5(2)	C(12)-C(13)-C(14)	120.2(6)
C(5)-P(2)-C(4)	107.9(2)	C(12)-C(13)-H(13)	114(5)
C(11)-P(2)-Pt(1)	113.34(18)	C(14)-C(13)-H(13)	125(5)
C(5)-P(2)-Pt(1)	120.14(17)	C(15)-C(14)-C(13)	120.4(6)
C(4)-P(2)-Pt(1)	96.06(18)	C(15)-C(14)-H(14)	119(4)
C(11)-P(2)-P(3)	108.12(18)	C(13)-C(14)-H(14)	121(4)
C(5)-P(2)-P(3)	138.13(18)	C(14)-C(15)-C(16)	120.5(6)
C(4)-P(2)-P(3)	43.23(17)	C(14)-C(15)-H(15)	121(7)
Pt(1)-P(2)-P(3)	55.37(4)	C(16)-C(15)-H(15)	118(7)
C(23)-P(3)-C(17)	106.6(2)	C(15)-C(16)-C(11)	119.5(6)
C(23)-P(3)-C(4)	108.8(2)	C(15)-C(16)-H(16)	124(4)
C(17)-P(3)-C(4)	107.5(3)	C(11)-C(16)-H(16)	116(4)
C(23)-P(3)-Pt(1)	119.60(18)	C(22)-C(17)-C(18)	120.5(5)
C(17)-P(3)-Pt(1)	119.36(17)	C(22)-C(17)-P(3)	121.0(4)
C(4)-P(3)-Pt(1)	93.13(17)	C(18)-C(17)-P(3)	118.3(4)
C(23)-P(3)-P(2)	137.35(18)	C(19)-C(18)-C(17)	119.6(6)
C(17)-P(3)-P(2)	112.32(18)	C(19)-C(18)-H(18)	110(5)
C(4)-P(3)-P(2)	43.05(16)	C(17)-C(18)-H(18)	130(5)
Pt(1)-P(3)-P(2)	52.50(4)	C(20)-C(19)-C(18)	119.8(6)
P(1)-C(1)-H(1A)	106(4)	C(20)-C(19)-H(19)	119(7)
P(1)-C(1)-H(1B)	111(5)	C(18)-C(19)-H(19)	120(7)
H(1A)-C(1)-H(1B)	108(6)	C(21)-C(20)-C(19)	120.5(6)
P(1)-C(1)-H(1C)	113(5)	C(21)-C(20)-H(20)	117(5)
H(1A)-C(1)-H(1C)	107(7)	C(19)-C(20)-H(20)	122(5)
H(1B)-C(1)-H(1C)	112(7)	C(20)-C(21)-C(22)	120.7(6)
P(1)-C(2)-H(2A)	105(4)	C(20)-C(21)-H(21)	119(6)
P(1)-C(2)-H(2B)	112(4)	C(22)-C(21)-H(21)	120(6)
H(2A)-C(2)-H(2B)	109(5)	C(21)-C(22)-C(17)	119.0(6)
P(1)-C(2)-H(2C)	106(6)	C(21)-C(22)-H(22)	119(5)
H(2A)-C(2)-H(2C)	109(7)	C(17)-C(22)-H(22)	122(5)
H(2B)-C(2)-H(2C)	116(7)	C(24)-C(23)-C(28)	119.1(5)
P(1)-C(3)-H(3A)	116(5)	C(24)-C(23)-P(3)	118.9(4)
P(1)-C(3)-H(3B)	111(4)	C(28)-C(23)-P(3)	122.0(4)
H(3A)-C(3)-H(3B)	104(6)	C(25)-C(24)-C(23)	121.3(6)
P(1)-C(3)-H(3C)	106(5)	C(25)-C(24)-H(24)	124(4)
H(3A)-C(3)-H(3C)	111(7)	C(23)-C(24)-H(24)	115(4)
H(3B)-C(3)-H(3C)	108(7)	C(24)-C(25)-C(26)	119.5(6)
P(2)-C(4)-P(3)	93.7(2)	C(24)-C(25)-H(25)	117(5)

P(2)-C(4)-H(4A)	104(5)	C(26)-C(25)-H(25)	124(5)
P(3)-C(4)-H(4A)	105(5)	C(25)-C(26)-C(27)	120.5(6)
P(3)-C(4)-H(4B)	120(3)	C(25)-C(26)-H(26)	121(5)
H(4A)-C(4)-H(4B)	114(6)	C(27)-C(26)-H(26)	118(5)
C(6)-C(5)-C(10)	119.5(5)	C(28)-C(27)-C(26)	119.8(6)
C(6)-C(5)-P(2)	122.9(4)	C(28)-C(27)-H(27)	120(4)
C(10)-C(5)-P(2)	117.6(4)	C(26)-C(27)-H(27)	120(4)
C(5)-C(6)-C(7)	120.3(6)	C(27)-C(28)-C(23)	119.8(6)
C(5)-C(6)-H(6)	121(5)	C(27)-C(28)-H(28)	120(4)
C(7)-C(6)-H(6)	119(5)	C(23)-C(28)-H(28)	120(4)
C(6)-C(7)-C(8)	119.9(6)	Cl(33)-C(31)-Cl(32)	111.0(5)
C(6)-C(7)-H(7)	117(5)	Cl(33)-C(31)-H(31A)	111(4)
C(8)-C(7)-H(7)	123(5)	Cl(32)-C(31)-H(31A)	109(4)
C(9)-C(8)-C(7)	119.8(6)	Cl(33)-C(31)-H(31B)	99(7)
C(9)-C(8)-H(8)	118(4)	Cl(32)-C(31)-H(31B)	114(7)
P(2)-C(4)-H(4B)	117(3)	H(31A)-C(31)-H(31B)	112(8)

Table E.3. Torsion angles (°) of [(dppm)(PMe₃)PtI][I].

Bonds	Angle (°)	Bonds	Angle (°)
P(2)-Pt(1)-P(1)-C(3)	124.5(3)	Pt(1)-P(2)-C(5)-C(10)	41.3(5)
P(3)-Pt(1)-P(1)-C(3)	133.7(4)	P(3)-P(2)-C(5)-C(10)	-29.0(5)
I(1)-Pt(1)-P(1)-C(3)	-55.7(3)	C(10)-C(5)-C(6)-C(7)	0.2(8)
P(2)-Pt(1)-P(1)-C(1)	-115.7(3)	P(2)-C(5)-C(6)-C(7)	179.6(4)
P(3)-Pt(1)-P(1)-C(1)	-106.5(4)	C(5)-C(6)-C(7)-C(8)	0.2(8)
I(1)-Pt(1)-P(1)-C(1)	64.1(3)	C(6)-C(7)-C(8)-C(9)	-0.4(8)
P(2)-Pt(1)-P(1)-C(2)	4.0(2)	C(7)-C(8)-C(9)-C(10)	0.4(8)
P(3)-Pt(1)-P(1)-C(2)	13.1(4)	C(8)-C(9)-C(10)-C(5)	0.0(8)
I(1)-Pt(1)-P(1)-C(2)	-176.3(2)	C(6)-C(5)-C(10)-C(9)	-0.2(8)
P(1)-Pt(1)-P(2)-C(11)	-84.94(19)	P(2)-C(5)-C(10)-C(9)	-179.7(4)
P(3)-Pt(1)-P(2)-C(11)	96.52(19)	C(5)-P(2)-C(11)-C(12)	64.5(5)
I(1)-Pt(1)-P(2)-C(11)	96.5(3)	C(4)-P(2)-C(11)-C(12)	-52.8(5)
P(1)-Pt(1)-P(2)-C(5)	48.3(2)	Pt(1)-P(2)-C(11)-C(12)	-157.7(4)
P(3)-Pt(1)-P(2)-C(5)	-130.2(2)	P(3)-P(2)-C(11)-C(12)	-98.3(5)
I(1)-Pt(1)-P(2)-C(5)	-130.2(2)	C(5)-P(2)-C(11)-C(16)	-119.5(4)
P(1)-Pt(1)-P(2)-C(4)	163.06(18)	C(4)-P(2)-C(11)-C(16)	123.2(5)
P(3)-Pt(1)-P(2)-C(4)	-15.47(18)	Pt(1)-P(2)-C(11)-C(16)	18.4(5)
I(1)-Pt(1)-P(2)-C(4)	-15.5(3)	P(3)-P(2)-C(11)-C(16)	77.7(4)
P(1)-Pt(1)-P(2)-P(3)	178.53(5)	C(16)-C(11)-C(12)-C(13)	1.4(9)
I(1)-Pt(1)-P(2)-P(3)	0.0(2)	P(2)-C(11)-C(12)-C(13)	177.4(5)
P(2)-Pt(1)-P(3)-C(23)	129.1(2)	C(11)-C(12)-C(13)-C(14)	-0.9(9)
P(1)-Pt(1)-P(3)-C(23)	119.6(3)	C(12)-C(13)-C(14)-C(15)	0.3(10)
I(1)-Pt(1)-P(3)-C(23)	-50.9(2)	C(13)-C(14)-C(15)-C(16)	-0.2(10)
P(2)-Pt(1)-P(3)-C(17)	-96.7(2)	C(14)-C(15)-C(16)-C(11)	0.7(10)
P(1)-Pt(1)-P(3)-C(17)	-106.2(3)	C(12)-C(11)-C(16)-C(15)	-1.2(9)
I(1)-Pt(1)-P(3)-C(17)	83.3(2)	P(2)-C(11)-C(16)-C(15)	-177.4(5)
P(2)-Pt(1)-P(3)-C(4)	15.35(18)	C(23)-P(3)-C(17)-C(22)	-84.0(5)
P(1)-Pt(1)-P(3)-C(4)	5.9(4)	C(4)-P(3)-C(17)-C(22)	32.6(5)
I(1)-Pt(1)-P(3)-C(4)	-164.65(18)	Pt(1)-P(3)-C(17)-C(22)	136.6(4)
P(1)-Pt(1)-P(3)-P(2)	-9.5(3)	P(2)-P(3)-C(17)-C(22)	78.2(5)
I(1)-Pt(1)-P(3)-P(2)	180.00(3)	C(23)-P(3)-C(17)-C(18)	90.6(5)
C(11)-P(2)-P(3)-C(23)	158.8(3)	C(4)-P(3)-C(17)-C(18)	-152.9(5)

C(5)-P(2)-P(3)-C(23)	3.3(4)	Pt(1)-P(3)-C(17)-C(18)	-48.8(5)
C(4)-P(2)-P(3)-C(23)	62.3(4)	P(2)-P(3)-C(17)-C(18)	-107.2(4)
Pt(1)-P(2)-P(3)-C(23)	-94.9(3)	C(22)-C(17)-C(18)-C(19)	0.9(9)
C(11)-P(2)-P(3)-C(17)	4.4(3)	P(3)-C(17)-C(18)-C(19)	-173.6(5)
C(5)-P(2)-P(3)-C(17)	-151.1(3)	C(17)-C(18)-C(19)-C(20)	0.2(10)
C(4)-P(2)-P(3)-C(17)	-92.1(3)	C(18)-C(19)-C(20)-C(21)	-1.2(11)
Pt(1)-P(2)-P(3)-C(17)	110.68(19)	C(19)-C(20)-C(21)-C(22)	1.2(11)
C(11)-P(2)-P(3)-C(4)	96.5(3)	C(20)-C(21)-C(22)-C(17)	0.0(11)
C(5)-P(2)-P(3)-C(4)	-59.0(4)	C(18)-C(17)-C(22)-C(21)	-1.0(9)
Pt(1)-P(2)-P(3)-C(4)	-157.2(3)	P(3)-C(17)-C(22)-C(21)	173.4(5)
C(11)-P(2)-P(3)-Pt(1)	-106.30(18)	C(17)-P(3)-C(23)-C(24)	-165.1(4)
C(5)-P(2)-P(3)-Pt(1)	98.3(2)	C(4)-P(3)-C(23)-C(24)	79.3(5)
C(4)-P(2)-P(3)-Pt(1)	157.2(3)	Pt(1)-P(3)-C(23)-C(24)	-25.8(5)
C(11)-P(2)-C(4)-P(3)	-98.1(3)	P(2)-P(3)-C(23)-C(24)	39.6(6)
C(5)-P(2)-C(4)-P(3)	143.1(2)	C(17)-P(3)-C(23)-C(28)	14.9(5)
Pt(1)-P(2)-C(4)-P(3)	18.7(2)	C(4)-P(3)-C(23)-C(28)	-100.8(5)
C(23)-P(3)-C(4)-P(2)	-140.7(2)	Pt(1)-P(3)-C(23)-C(28)	154.2(4)
C(17)-P(3)-C(4)-P(2)	104.2(3)	P(2)-P(3)-C(23)-C(28)	-140.4(4)
Pt(1)-P(3)-C(4)-P(2)	-17.9(2)	C(28)-C(23)-C(24)-C(25)	-0.9(9)
C(11)-P(2)-C(5)-C(6)	-3.6(5)	P(3)-C(23)-C(24)-C(25)	179.1(5)
C(4)-P(2)-C(5)-C(6)	113.4(5)	C(23)-C(24)-C(25)-C(26)	0.3(9)
Pt(1)-P(2)-C(5)-C(6)	-138.2(4)	C(24)-C(25)-C(26)-C(27)	0.2(9)
P(3)-P(2)-C(5)-C(6)	151.5(3)	C(25)-C(26)-C(27)-C(28)	-0.1(9)
C(11)-P(2)-C(5)-C(10)	175.8(4)	C(26)-C(27)-C(28)-C(23)	-0.5(9)
C(4)-P(2)-C(5)-C(10)	-67.1(4)	C(24)-C(23)-C(28)-C(27)	1.0(8)
		P(3)-C(23)-C(28)-C(27)	-179.0(4)

REFERENCES

- Aizawa, S.; Sone, Y.; Kawamoto, T.; Yamada, G.; Nakamura, M.; *Inorg. Chim. Acta* **2002**, *338*, 235-239.
- Annibale, G.; Bergamini, P.; Bertolasi, V.; Besco, E.; Cattabriga, M.; Rossi, R. *Inorg. Chim. Acta* **2002**, *333*, 116-123.
- Annibale, G.; Bergamini, P.; Bertolasi, V.; Cattabriga, M.; Ferretti, V. *Inorg. Chem. Commun.* **2000**, *3*, 303-306.
- Annibale, G.; Bergamini, P.; Cattabriga, M. *Inorg. Chim. Acta* **2001**, *316*, 25-32.
- Aubert, C.; Buisine, O.; Malacria, M. *Chem. Rev.* **2002**, *102*, 813-834.
- Azam, K. A.; Ferguson, G.; Ling, S. S. M.; Puddephatt, R. J.; Srokowski, D. *Inorg. Chem.* **1985**, *24*, 2799-2802.
- Bartlett, P. A. In *Asymmetric Synthesis*; Morrison, J. D., Ed.; Academic Press: New York, 1984; Vol. 3, p 341-409.
- Bennett, B. L.; Hoerter, J. M.; Houlis, J. F.; Roddick, D. M. *Organometallics* **2000**, *19*, 615-621.
- Biosynthesis of Isoprenoid Compounds*; Porter, J. W.; Spurgeon, S. L., Eds.; John Wiley & Sons: New York, 1981; Vol. 1.
- Brookhart, M.; Liu, Y. *J. Am. Chem. Soc.* **1991**, 939-944.
- Butikofer, J. L.; Hoerter, J. M.; Peters, R. G.; Roddick, D. M. *Organometallics* **2004**, *23*, 400-408.
- Casey, C. P.; Smith-Vosejпка, L. J. *Organometallics* **1992**, *11*, 738-744.
- Casey, C. P.; Strotman, N. A. *J. Am. Chem. Soc.* **2004**, *126*, 1699-1704.
- Chuang, C. *Tetrahedron Lett.* **1992**, *33*, 6311-6314.
- Clark, H. C.; Manzer, L. E. *J. Organomet. Chem.* **1973**, *59*, 411-428.
- Colacot, T. J.; Qian, H.; Cea-Olivares, R.; Hernandez-Ortega, S. *J. Organomet. Chem.* **2001**, *637-639*, 691-697.
- Corey, E. J.; Wood, H. B. *J. Am. Chem. Soc.* **1996**, *118*, 11982-11983.
- Croteau, R. *Chem. Rev.* **1987**, *87*, 929-954.

- Croteau, R. In *Recent Developments in Flavor and Fragrance Chemistry: Proceedings of the 3rd International Harmann & Reimer Symposium*; VCH: Weinheim, 1993; p 263.
- Cucciolito, M. E.; D'Amora, A.; Vitagliano, A. *Organometallics* **2005**, *24*, 3359-3361.
- Davis, D. D.; Johnson, H. T. *J. Am. Chem. Soc.* **1974**, *96*, 7576-7577.
- Desai, L. V.; Hull, K. L.; Sanford, M. S. *J. Am. Chem. Soc.* **2004**, *126*, 9542-9543.
- Dick, A. R.; Hull, K. L.; Sanford, M. S. *J. Am. Chem. Soc.* **2004**, *126*, 2300-2301.
- Diver, S. T.; Giessert, A. J. *Chem. Rev.* **2004**, *104*, 1317-1382.
- Dockter, D. W.; Fanwick, P. E.; Kubiak, C. P. *J. Am. Chem. Soc.* **1996**, *118*, 4846-4852.
- DuBois, D. L.; Meek, D. W. *Inorg. Chem.* **1976**, *15*, 3076-3083.
- DuBois, D. L.; Miedaner, A. *Inorg. Chem.* **1986**, *25*, 4642-4650.
- DuBois, D. L.; Miedaner, A. *J. Am. Chem. Soc.* **1987**, *109*, 113-117.
- DuBois, D. L.; Miedaner, A.; Haltiwanger, R. C. *J. Am. Chem. Soc.* **1991**, *113*, 8753-8764.
- Echavarren, A. M.; Nevado, C. *Chem. Soc. Rev.* **2004**, *33*, 431-436.
- Eschenmoser, A.; Ruzika, L.; Jeger, O.; Arigoni, D. *Helv. Chim. Acta.* **1955**, *38*, 1890-1904.
- Fanizzi, F. P.; Intini, F. P.; Maresca, L.; Natile, G. *J. Chem. Soc., Dalton Trans.* **1992**, 309-312.
- Feducia, J. A.; Campbell, A. N.; Anthis, J. W.; Gagné, M. R. *Organometallics* **2006**, *25*, 3114-3117.
- Ferguson, G.; *et. al.* *J. Organomet. Chem.* **2001**, *617-618*, 671-680.
- Fernández, D.; Sevillano, P.; Garcia-Seijo, M. I.; Castiñeiras, A.; Jánosi, L.; Berente, Z.;
- Kollár, L.; García-Fernández, M. E. *Inorg. Chim. Acta* **2001**, *312*, 40-52.
- Fleming, I.; Urch, C. J. *Tetrahedron Lett.* **1983**, *24*, 4591-4594.
- Forschner, T. C.; Cutler, A. R. *Organometallics* **1985**, *4*, 1247-1257.
- Freixa, Z.; van Leeuwen, P. W. N. M. *J. Chem. Soc., Dalton Trans.* **2003**, 1890-1901.
- Gao, D.; Pan, Y. K.; Byun, K.; Gao, J. *J. Am. Chem. Soc.* **1998**, *120*, 4045-4046.

- Garrou, P. E. *Chem. Rev.* **1981**, *81*, 229-266.
- Hahn, C. *Chem. Eur. J.* **2004**, *10*, 5888-5899.
- Hahn, C.; Morvillo, P.; Herdtweck, E.; Vitagliano, A. *Organometallics* **2002**, *21*, 1807-1818.
- Hahn, C.; Morvillo, P.; Vitagliano, A. *Eur. J. Inorg. Chem.* **2001**, 419-429.
- Hahn, C.; Cucciolito, M. E.; Vitagliano, A. *J. Am. Chem. Soc.* **2002**, *124*, 9038-9039.
- Hegedus, L. S. In *Comprehensive Organic Synthesis*; Trost, B. M., Ed.; Pergamon Press: Elmsford, NY, 1991; Vol. 4, pp 551-569.
- Hegedus, L. S. In *Transition Metals in the Synthesis of Complex Organic Molecules*; University Science Books: Mill Valley, California, 1994; pp 199-236.
- Helfer, D. S.; Atwood, J. D. *Organometallics* **2004**, *23*, 2412-2420.
- Heyduk, A. F.; Labinger, J. A.; Bercaw, J. E. *J. Am. Chem. Soc.* **2003**, *125*, 6366-6367.
- Hill, G. S.; Rendina, L. M.; Puddephatt, R. J. *Organometallics* **1995**, *14*, 4966-4968.
- Ishibani, H.; Ishihara, K.; Yamamoto, H. *J. Am. Chem. Soc.* **2004**, *126*, 11122-11123.
- Ishihara, K.; Ishibashi, H.; Yamamoto, H. *J. Am. Chem. Soc.* **2002**, *124*, 3647-3655.
- Jawad, J. K.; Puddephatt, R. J.; Stalteri, M. A. *Inorg. Chem.* **1982**, *21*, 332-337.
- Johansson, L.; Tilset, M. *J. Am. Chem. Soc.* **2001**, *123*, 739-740.
- Johnson, W. S.; Bartlett, W. R.; Czeskis, B. A.; Gautier, A.; Lee, C. H.; Lemoine, R.; Leopold, E. J.; Luedtke, G. R.; Bancroft, K. J. *J. Org. Chem.* **1999**, *64*, 9587-9595.
- Julia, M.; Fourneron, J. D. *Tetrahedron* **1976**, *32*, 1113-1116.
- Kalberer, E. W.; Houlis, J. F.; Roddick, D. M. *Organometallics* **2004**, *23*, 4112-4115.
- Kannenbergh, E. L.; Poralla, K. *Naturwissenschaften* **1999**, *86*, 168-176.
- Kerber, W. D.; Gagné, M. R. *Org. Lett.* **2005**, *7*, 3379-3381.
- Kerber, W. D.; Koh, J. H.; Gagné, M. R. *Org. Lett.* **2004**, *6*, 3013-3015.
- Koh, J. H.; Gagné, M. R. *Angew. Chem. Int. Ed.* **2004**, *43*, 3459-3461.

- Koh, J. H.; Mascarenhas, C.; Gagné, M. R. *Tetrahedron* **2004**, *60*, 7405-7410.
- Lambert, J. B.; Salvador, L. A.; So, J. H. *Organometallics* **1993**, *12*, 697-703.
- Lansbury, P. T.; Briggs, P. C.; Demmin, T. R.; DuBois G. E. *J. Am. Chem. Soc.* **1971**, *93*, 1311-1313.
- Lansbury, P. T.; Demmin, T. R.; DuBois, G. E.; Haddon V. R. *J. Am. Chem. Soc.* **1975**, *97*, 394-403.
- Lansbury, P. T.; DuBois, G. E. *Chem. Commun.* **1971**, 1107-1108.
- Lee, A. S.; Lin, L. *Tetrahedron Lett.* **2000**, *41*, 8803-8806.
- Lersch, M.; Tilset, M. *Chem. Rev.* **2005**, *105*, 2471-2526.
- Ling, S. S. M.; Puddephatt, R. J. *Inorg. Chim. Acta* **1983**, *77*, L95-L96.
- Liu, C.; Han, X.; Wang, X.; Widenhoefer, R. A. *J. Am. Chem. Soc.* **2004**, *126*, 3700-3701.
- Lloyd-Jones, G. C. *Org. Biomol. Chem.* **2003**, *1*, 215-236.
- López-Torres, M.; Fernández, A.; Fernández, J. J.; Suárez, A.; Pereira, M. T.; Ortigueira, J. M.; Vila, J. M.; Adams, H. *Inorg. Chem.* **2001**, *40*, 4583-4587.
- Lucey, D. W.; Helfer, D. S.; Atwood, J. D. *Organometallics* **2003**, *22*, 826-833.
- Ma, S.; Yu, S.; Gu, Z. *Angew. Chem. Int. Ed.* **2006**, *45*, 200-203.
- Marinus B.; Groen, M. B.; Zeelen, F. J. *J. Org. Chem.* **1978**, *43*, 1961-1964.
- Matsunaga, P. T.; Hillhouse, G. L.; Rheingold, A. L. *J. Am. Chem. Soc.* **1993**, *115*, 2075-2077.
- Matsunaga, P. T.; Mavropoulos, J. C.; Hillhouse, G. L. *Polyhedron* **1995**, *14*, 175-185.
- McWilliam, D. C.; Balasubramanian, T. R.; Kuivila, H. G. *J. Am. Chem. Soc.* **1978**, *100*, 6407-6413.
- Méndez, M.; Mamane, V.; Fürstner, A. *Chemtracts* **2003**, *16*, 397-425.
- Merrifield, J. H.; Godschalx, J. P.; Stille, J. K. *Organometallics* **1984**, *3*, 1108-1112.
- Michael, F. E.; Cochran, B. M. *J. Am. Chem. Soc.* **2006**, *128*, 4246-4247.
- Muci, A. R.; Campos, K. R.; Evans, D. A. *J. Am. Chem. Soc.* **1995**, *117*, 4075-4076.

- Nishizawa, M.; Takenaka, H.; Hayashi, Y. *J. Org. Chem.* **1986**, *51*, 806-813.
- Oppolzer, W.; Ruiz-Montes, J. *Helv. Chim. Acta* **1993**, *76*, 1266-1274.
- Papish, E. T.; Rix, F. C.; Spetseris, N.; Norton, J. R.; Williams, R. D. *J. Am. Chem. Soc.* **2000**, *122*, 12235-12242.
- Parrett, F. W.; Sun, M. S. *J. Chem. Educ.* **1977**, *54*, 448-449.
- Peters, R. G.; White, S.; Roddick, D. M. *Organometallics* **1998**, *17*, 4493-4499.
- Petőcz, G.; Jánosi, L.; Wissensteiner, W.; Csók, H. E.; Man, Z.; Kollár, L. *Inorg. Chim. Acta* **2000**, *303*, 300-305.
- Procelewska, J.; Zahl, A.; van Eldik, R.; Zhong, H. A.; Labinger, J. A.; Bercaw, J. E. *Inorg. Chem.* **2002**, *41*, 2808-2810.
- Puddephatt, R. J. *Coord. Chem. Rev.* **2001**, *219-221*, 157-185.
- Qian, H.; Han, X.; Widenhoefer, R. A. *J. Am. Chem. Soc.* **2004**, *126*, 9536-9537.
- Raebiger, J. W.; Miedaner, A.; Curtis, C. J.; Miller, S. M.; Anderson, O. P.; DuBois, D. L. *J. Am. Chem. Soc.* **2004**, *126*, 5502-5514.
- Reinert, D. J.; Balliano, G.; Schulz, G. E. *Chem. Biol.* **2004**, *11*, 121-125.
- Sevillano, P.; Habtemariam, A.; Parsons, S.; Castiñeiras, A.; García, M. E.; Sadler, P. J. *J. Chem. Soc., Dalton Trans.* **1999**, 2861-2870.
- Siedle, A. R.; Newmark, R. A.; Pignolet, L. H. *J. Am. Chem. Soc.* **1981**, *103*, 4947-4948.
- Stahl, S. S.; Labinger, J. A.; Bercaw, J. E. *J. Am. Chem. Soc.* **1996**, *118*, 5961-5976.
- Stork, G.; Burgstahler, A. W. *J. Am. Chem. Soc.* **1955**, *77*, 5068-5077.
- Stull, D. R.; Westrum, E. F., Jr.; Sinke, G. C. In *The Chemical Thermodynamics of Organic Compounds*; Wiley: New York, 1969.
- Tau, K. D.; Uriarte, R.; Mazanec, T. J.; Meek, D. W. *J. Am. Chem. Soc.* **1979**, *101*, 6614-6619.
- Terada, Y.; Arisawa, M.; Nishida, A. *Angew. Chem. Int. Ed.* **2004**, *43*, 4063-4067.
- Thorn, D. L. *Organometallics* **1998**, *17*, 348-352.
- Tolman, C. A. *Chem. Rev.* **1977**, *77*, 313-348.

- Tong-Shuang, L.; Ji-Tai, L.; Hui-Zhang, L. *J. Chrom. A.* **1995**, *715*, 372-375.
- Trost, B. M. *Acc. Chem. Res.* **1990**, *23*, 34-42.
- Trost, B. M.; Krische, M. J. *Synlett* **1998**, 1-16.
- Uyanik, M.; Ishihara, K.; Yamamoto, K. *Bioorg. Med. Chem.* **2005**, *13*, 5055-5065.
- van Leeuwen, P. W. N. M.; Kamer, P. C. J.; Reek, J. N. H.; Dierkes, P. *Chem. Rev.* **2000**, *100*, 2741-2770.
- Weiner, M. A.; Pasternack, G. *J. Org. Chem.* **1967**, *32*, 3707-3709.
- Wendt, K. U.; Poralla, K.; Schulz, G. E. *Science* **1997**, *277*, 1811-1815.
- Widenhoefer, R. A. *Acc. Chem. Res.* **2002**, *35*, 905-913.
- Wik, B. J.; Lersch, M.; Tilset, M. *J. Am. Chem. Soc.* **2002**, *124*, 12116-12117.
- Xia, B.; Che, C.; Phillips, D. L.; Leung, K.; Cheung, K. *Inorg. Chem.* **2002**, *41*, 3866 -3875.
- Xia, B.; Zhang, H.; Che, C.; Leung, K.; Phillips, D. L.; Zhu, N.; Zhou, Z. *J. Am. Chem. Soc.* **2003**, *125*, 10362-10374.
- Yamanoi, Y.; Imamoto, T. *J. Org. Chem.* **1999**, *64*, 2988-2989.
- Yasutake, M.; Gridnev, I. D.; Higashi, N.; Imamoto, T. *Org. Lett.* **2001**, *3*, 1701 -1704.
- Yoder, R. A.; Johnston, J. N. *Chem. Rev.* **2005**, *105*, 4730-4756.